Outcrop of the Permian Park City Formation showing through-going fractures

Drill rig completing culinary water-supply well in the Jurassic Nugget Sandstone

Culinary water-supply spring in the Jurassic Twin Creek Limestone

Historic mine ruins in Thaynes Canyon

Low-angle normal fault in the Tertiary Keetley Volcanics

Fractures in the Jurassic Nugget Sandstone

ISBN 1-55791-652-7

Ashland, Bishop, Lowe, Mayes

GEOLOGY OF SNYDERVILLE BASIN, WESTERN SUMMIT COUNTY, UTAH, AND ITS RELATION TO GROUND-WATER CONDITIONS

UGS WRB 28

THE GEOLOGY OF THE SNYDERVILLE BASIN, WESTERN SUMMIT COUNTY, UTAH, AND ITS RELATION TO GROUND-WATER CONDITIONS

by

Francis X. Ashland, Charles E. Bishop, Mike Lowe, and Bea H. Mayes

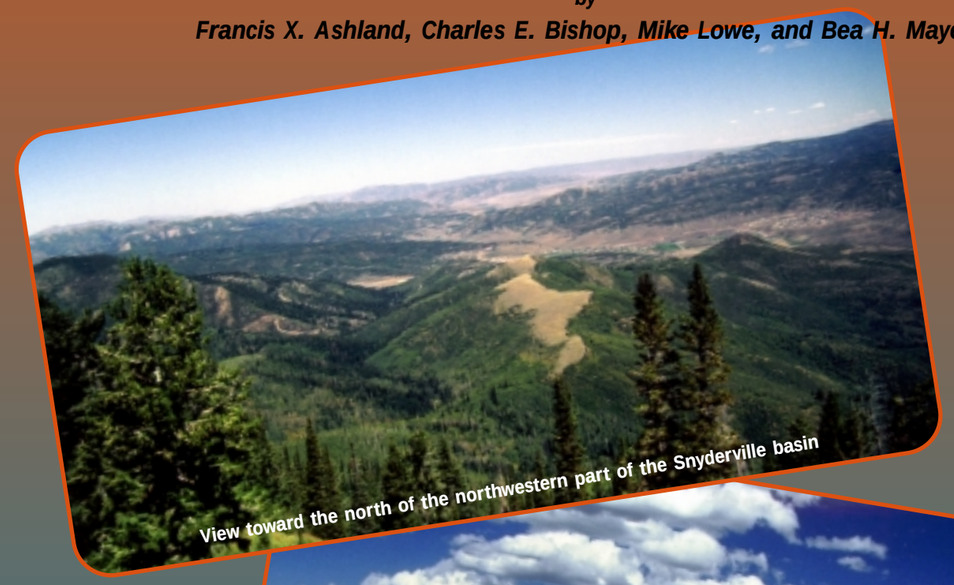

View toward the north of the northwestern part of the Snyderville basin

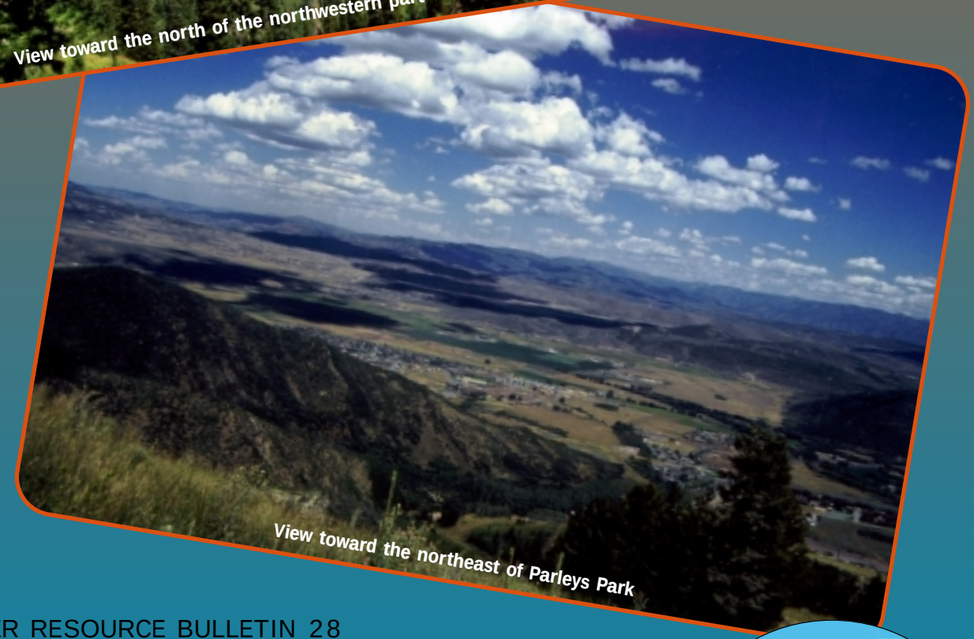

View toward the northeast of Parleys Park

WATER RESOURCE BULLETIN 28
UTAH GEOLOGICAL SURVEY
a division of
2001 **UTAH DEPARTMENT OF NATURAL RESOURCES**

UTAH GEOLOGICAL SURVEY

THE GEOLOGY OF THE SNYDERVILLE BASIN, WESTERN SUMMIT COUNTY, UTAH, AND ITS RELATION TO GROUND-WATER CONDITIONS

by
Francis X. Ashland, Charles E. Bishop, Mike Lowe, and Bea H. Mayes

ISBN 1-55791-652-7

WATER RESOURCE BULLETIN 28
UTAH GEOLOGICAL SURVEY
a division of
UTAH DEPARTMENT OF NATURAL RESOURCES
2001

UTAH GEOLOGICAL SURVEY

UTAH GEOLOGICAL SURVEY

The **UTAH GEOLOGICAL SURVEY** is organized into five geologic programs with Administration, Editorial, and Computer Resources providing necessary support to the programs. The **ECONOMIC GEOLOGY PROGRAM** undertakes studies to identify coal, geothermal, uranium, hydrocarbon, and industrial and metallic resources; initiates detailed studies of these resources including mining district and field studies; develops computerized resource data bases, to answer state, federal, and industry requests for information; and encourages the prudent development of Utah's geologic resources. The **APPLIED GEOLOGY PROGRAM** responds to requests from local and state governmental entities for engineering-geologic investigations; and identifies, documents, and interprets Utah's geologic hazards. The **GEOLOGIC MAPPING PROGRAM** maps the bedrock and surficial geology of the state at a regional scale by county and at a more detailed scale by quadrangle. The **GEOLOGIC EXTENSION SERVICE** answers inquiries from the public and provides information about Utah's geology in a non-technical format. The **ENVIRONMENTAL SCIENCES PROGRAM** maintains and publishes records of Utah's fossil resources, provides paleontological and archeological recovery services to state and local governments, conducts studies of environmental change to aid resource management, and evaluates the quantity and quality of Utah's ground-water resources.

The UGS Library is open to the public and contains many reference works on Utah geology and many unpublished documents on aspects of Utah geology by UGS staff and others. The UGS has several computer data bases with information on mineral and energy resources, geologic hazards, stratigraphic sections, and bibliographic references. Most files may be viewed by using the UGS Library. The UGS also manages a sample library which contains core, cuttings, and soil samples from mineral and petroleum drill holes and engineering geology investigations. Samples may be viewed at the Sample Library or requested as a loan for outside study.

The UGS publishes the results of its investigations in the form of maps, reports, and compilations of data that are accessible to the public. For information on UGS publications, contact the Natural Resources Map/Bookstore, 1594 W. North Temple, Salt Lake City, Utah 84116, (801) 537-3320 or 1-888-UTAH MAP. E-mail: nrugs.geostore@state.ut.us and visit our web site at http://www.ugs.state.ut.us.

UGS Editorial Staff

J. Stringfellow	Editor
Vicky Clarke, Sharon Hamre	Graphic Artists
Patricia H. Speranza, James W. Parker, Lori Douglas	Cartographers

TABLE OF CONTENTS

ILLUSTRATIONS

TABLES

PLATES

THE GEOLOGY OF THE SNYDERVILLE BASIN, WESTERN SUMMIT COUNTY, UTAH, AND ITS RELATION TO GROUND-WATER CONDITIONS

by
Francis X. Ashland, Charles E. Bishop, Mike Lowe, and Bea H. Mayes

ABSTRACT

Urbanization of parts of the Snyderville basin has been accompanied by an increasing demand to develop the area's ground-water resources. Ground water is present in shallow unconsolidated deposits and fractured rock. Because of the limited extent and thickness of the unconsolidated deposits, the ground-water resources in fractured rock have a greater potential for future development.

The unconsolidated deposits consist primarily of alluvium and glacial till and outwash. Glacial or colluvial deposits form only a thin veneer in most upland areas. In lowland areas, the thickness of the deposits generally exceeds 40 feet (12 m), and may be as much as 275 feet (84 m) in the southern part of Parleys Park. The combination of the exceptional thickness of unconsolidated deposits and shallow water table in the southern part of Parleys Park suggests that the unconsolidated aquifer is more substantial here than elsewhere in the study area. However, the deposits are typically fine-grained and unlikely to produce high-yielding wells.

Fractured sedimentary and volcanic rocks consist of limestone, sandstone, quartzite, siltstone, shale, tuff, and volcanic breccia. Permeability in these rocks is primarily a result of fracturing which may be locally enhanced by solution widening in limestone and other calcareous units. Primary permeability in Cretaceous sedimentary rocks and locally in the lower part of the Keetley Volcanics may be sufficiently high to yield small quantities of water to wells. However, primary permeability in Jurassic or older limestones and sandstones is probably negligible.

Fracture characteristics, excluding attitude, are generally controlled by lithology and therefore do not vary significantly in a lithologically homogeneous formation or member. Joints, bedding joints, and cleavage fractures likely enhance rock permeability but the overall increase in rock-mass permeability because of their presence may locally be negligible. Faults may act as conduits, increasing permeability parallel to the fault but generally inhibiting ground-water flow perpendicular to the fault. In general, fractures in limestone and sandstone are more persistent than fractures in shale, allowing ground water to flow perpendicular to beds. High-angle-to-bedding fractures in shale generally have very low persistence, terminate against shale partings or ductile beds, and are tight or clay-infilled. Whereas persistent bedding fractures in shale may act as ground-water conduits parallel to bedding, high-angle-to-bedding fractures likely have a negligible influence on the ability of ground water to flow perpendicular to bedding. Hydraulic conductivities of fracture-poor shale beds, such as the gypsiferous shale bed in the lower part of the Woodside Shale, likely approach that of intact (unfractured) shale.

Fractured limestone and sandstone beds form stratigraphic ground-water compartments (SGWCs) that are separated by shale confining beds that have very low hydraulic conductivity perpendicular to bedding. Aquifer-test results indicate a lack of hydraulic communication between wells completed in fractured limestone and sandstone SGWCs separated by intervening shale confining beds. Stratigraphic control of ground-water flow is also indicated by historical accounts from mine workings. Water accumulation above fracture-poor shale beds likely reflects the inability of ground water to flow perpendicular to these beds.

Macroscopic faults act in a complex manner as ground-water conduit-barrier systems and also sever the continuity of SGWCs. Fault-zone cores commonly consist of gouge zones that likely act as barriers to ground-water flow. Gouge-zone width is a function of wall-rock type and the amount of displacement on the fault. Zones of interconnected subsidiary fractures in brittle wall rock may act as conduits parallel to the fault, but may terminate along strike at contacts with ductile rock types.

Severing of SGWCs by faults has resulted in the formation of at least sixteen discrete ground-water compartments (GWCs). Several GWCs, including those in the Twin Creek Limestone and Thaynes Formation, may be subdividable on the basis that they contain an intraformational confining bed. All GWCs vary considerably in extent, thickness, physiography, and hydrology. Some GWCs have small recharge areas and thus have low safe yields.

Although fracture trends vary across the study area, distinct fracture domains with different fracture trends are recognizable. Whereas major structures or geologic contacts in many cases are fracture-domain boundaries, in some cases, such as in the Keetley Volcanics, fracture-domain boundaries are less well defined and transitional. Fracture patterns presented on rose diagrams may be useful in predicting hydraulic communication between wells in a single GWC and help predict the shape of drawdown cones. Fracture-trend data determined from outcrops correlate well with subsurface fracture data, but correlate poorly with linear-trace data.

Other factors may affect the production history or yields of wells completed in fractured rock. Reduction in pore pressure during continuous pumping may close fractures. Fracture aperture may not recover as a result of seasonal spring recharge, causing diminishing well yields over time. Solution widening in limestone and calcareous rocks may gradually increase fracture permeability and may favor specific structural settings such as the crests of anticlines. As a result of the steep dip of most fractures, vertical wells are less likely to intercept transmissive fracture zones. Higher well yields may be achieved using inclined drilling methods, particularly in formations such as the Nugget Sandstone and Weber Quartzite, where moderate- to low-angle bedding fractures are rare. Water-well-production-history data reveal seasonal fluctuations in well yields that suggest fracture-storage characteristics may preclude long-term storage of recharge.

INTRODUCTION

Background

The Snyderville basin is in the Wasatch Range section of the Middle Rocky Mountains physiographic province in north-central Utah (Stokes, 1977). The basin is about 20 miles (32 km) east of Salt Lake City on the eastern slope of the Wasatch Range in western Summit County (figure 1, plate 1). Park City, with an estimated population in 2000 of 6,750, is the largest urban area in the basin. Park City began as a silver-mining community in the late 1860s and mining was the primary industry in the area for more than 100 years. All mines are currently idle. The first ski resort, Park City Ski Resort, was developed in 1963. Skiing surpassed mining as the major industry in the area in the 1970s as additional winter recreational facilities such as The Canyons (originally Park West) and Deer Valley ski resorts were developed. The Snyderville basin is experiencing rapid growth due to its recreation facilities, mild summer climate, spectacular mountain scenery, and proximity to the Wasatch Front metropolitan area. Park City's population increased by 58 percent between 1980 and 1990, and 38 percent between 1990 and 1994. The peak-season population for the entire basin is estimated to reach 47,180 by the year 2000 (Economics Research Associates, 1981).

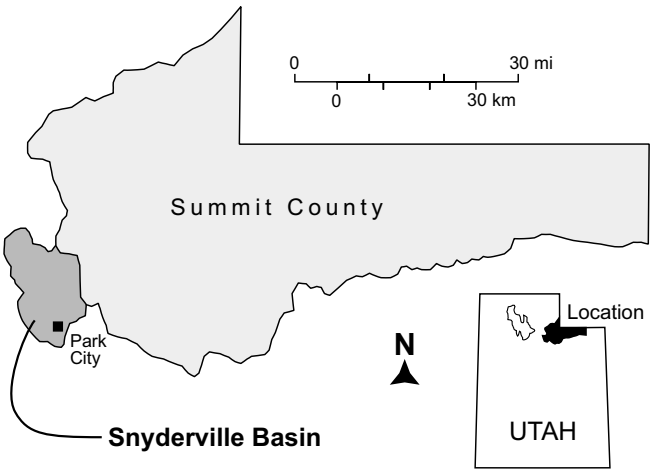

Figure 1. *Location map.*

As a result of this growth, the demand to develop the area's ground-water resources is increasing. Presently ground water is withdrawn from wells completed in unconsolidated deposits or fractured rock and from tunnels in rock in the Park City mining district. Most new residential developments outside the Park City corporate boundary rely on springs and wells that are completed in fractured rock for their water supplies.

Physiography

Terrain in the Snyderville basin area ranges from steep, rugged mountains cut by deep canyons in the south, to broad valley bottoms in the center of the basin and low hills in the north. The Wasatch Range portion of the Snyderville basin includes high alpine terrain with peaks above 10,000 feet (3,050 m). The mountain ridges consist primarily of erosion-resistant sedimentary and igneous rock. Areas at higher elevations were glaciated during the Pleistocene and glaciated canyons contain cirques and moraines. The broad valley bottoms in the central Snyderville basin were formed by deposition of alluvium and glacial outwash by streams flowing out of the Wasatch Range. The low, rounded hills in the north have gentle slopes and low relief because they are underlain by less-resistant bedrock (shale, mudstone, and siltstone).

The two major drainages in the Snyderville basin area are Silver Creek and East Canyon-Kimball Creek. Silver Creek, which heads in Empire Canyon, is the principal drainage on the eastern side of the basin. East Canyon-Kimball Creek, which heads in Thaynes Canyon where it is called McLeod Creek, is the principal drainage on the western side of the basin. Both flow from the southern boundary of the basin northward and eventually join the Weber River. The lowest elevations are along East Canyon-Kimball Creek and Silver Creek where they exit the basin at about 6,280 feet (1,910 m) in the northwestern and northeastern parts of the study area, respectively.

The Snyderville basin has a sub-humid climate. Annual precipitation ranges from 20 to 25 inches (51-64 cm) in the lower parts of the basin to 25 to 30 inches (64-76 cm) in the mountains (Baker, 1970). Most of the precipitation falls as snow during November through April. May through September is generally the driest period, with less than 8 inches (20 cm) of precipitation (Baker, 1970).

Purpose and Scope

The purpose of this study is to provide geologic information important in assessing ground-water resources and siting water wells in the Snyderville basin. This geologic study was one phase of a cooperative and more comprehensive water-resource investigation. Subsequent phases conducted by the U.S. Geological Survey Water Resources Division (USGS WRD), focused on the hydrology of the Snyderville basin. The information presented in this report is generalized and is not intended to substitute for site-specific investigations. Future detailed studies will add to the understanding of the geology and ground-water resources of the study area and supplement the information presented herein.

The scope of work for this study included producing maps and cross sections to help determine the relationship

between geology and ground water. To accomplish this we did the following:

1. Reviewed available geologic data, including: published geologic maps, unpublished geologic information such as university theses and data from mines, and drillers' logs of water wells.
2. Modified geologic mapping compiled from published maps by the U.S. Geological Survey (USGS).
3. Mapped linear traces (possibly representing faults and major fractures) using aerial photos.
4. Measured fracture characteristics (orientation, aperture width, fracture filling, spacing) at outcrops and mining-related exposures (adits, drain tunnels, quarries) and transferred appropriate parameters onto compiled geologic maps. These data were augmented with fracture information from unpublished data from mines. We analyzed fracture-trend data and plotted rose diagrams to determine domains.
5. Compiled cross sections in valley-fill deposits using drillers' logs of water wells and seismic-refraction soundings to show depth to bedrock and, where possible, stratigraphy in the unconsolidated sediments. We constructed a map delineating the unconsolidated aquifer in the basin.
6. Constructed geologic cross sections based on the compiled geologic mapping.
7. Constructed structure-contour and isochore maps for the principal aquifer-forming formations in the basin.
8. Analyzed data and prepared maps and this final report.

The study was performed from July 1994 through October 1995. Principal field work was completed from July to September 1994. Additional data gathering and analysis was conducted between September 1996 and February 1998.

Organization of the Report

This report is divided into several parts. The first part introduces the general stratigraphy and structure that provides an overall geologic framework for understanding the ground-water resources of the study area. The second part discusses the characteristics of unconsolidated deposits in the study area. The last part of the report discusses the characteristics of fractured rocks. It also introduces a conceptual hydrostratigraphic model for these rock units that incorporates the variable fracture characteristics and demonstrates how major faults sever the continuity of the hydrostratigraphic units. Plates in this report include cross sections and maps showing the general geology, structure, and thickness of important fractured-rock units. Appendix A discusses the methods used to collect and analyze data presented in the report. Appendix B explains how to use plates 4 through 11. Appendices C through F contain a variety of technical information that may be useful to some readers. A glossary is attached to assist in understanding technical terms. Unit measurements are given using standard conventions and are followed by a conversion.

Previous Work

The first extensive geologic study of the Park City mining district, by Boutwell (1912), remains the standard reference for the area and contains useful accounts of ground-water conditions encountered in mine workings. Wilson (1959), Eardley (1968), and Bromfield (1968, 1989) also discuss the geology of the Park City mining district. Geologic maps in the Snyderville basin include Baker and others (1966), Crittenden and others (1966), Bromfield and others (1970), Bromfield and Crittenden (1971), and Bryant (1990, 1992). Crittenden (1974) discussed the regional extent and age of thrusts in the northern Utah area. The U.S. Department of Agriculture Soil Conservation Service [now Natural Resources Conservation Service] (1977) mapped soils in the area. Gill and Lund (1984) discussed the engineering geology of the Park City area. Much of the unpublished geologic and hydrologic information has been gathered by various mining companies; United Park City Mines Company provided some of this information for use in this study. Hydrologic reports pertaining to the study area include Baker (1970) and Holmes and others (1986). Jarvis and Yonkee (1993), Weston Engineering, Inc. (1996a), and Jarvis and Loughlin (1996) discuss the hydrogeology in the Summit Park area. Weston Engineering, Inc. (1996b) studied the hydrogeology of the Pinebrook area. The USGS WRD (Downhour and Brooks, 1996) studied surface and ground-water hydrology in the Park City area. This study was originally published as Utah Geological Survey Open-File Report 337 and, as presented herein, is slightly modified from that report.

GEOLOGIC FRAMEWORK

Water-yielding geologic units in the study area consist of unconsolidated deposits and fractured rock. The majority of rock units are sedimentary rocks that have been folded and faulted and are locally overlain by unconsolidated deposits. The following sections describe the geologic units and major structures that deform the sedimentary rocks to provide a geologic framework for understanding the hydrostratigraphy.

Stratigraphy

Geologic units in the Snyderville basin range in age from Pennsylvanian to Holocene (figure 2). Sedimentary rocks consist of Pennsylvanian to Tertiary quartzite, limestone, sandstone, siltstone, mudstone, conglomerate, and shale. Tertiary igneous rocks consist of andesite breccia and tuff (volcanic) and quartz monzonite and granodiorite porphyry (intrusive). Pennsylvanian to Jurassic sedimentary rocks crop out primarily in the southern and western parts of the basin, Cretaceous sedimentary rocks crop out in the northwestern part, and Tertiary rocks crop out primarily in the northern and eastern parts (plate 2). Unconsolidated deposits consist of Tertiary gravel and Quaternary glacial deposits, landslide deposits, alluvium, and colluvium.

Paleozoic

Pennsylvanian: The oldest rock unit that crops out in the

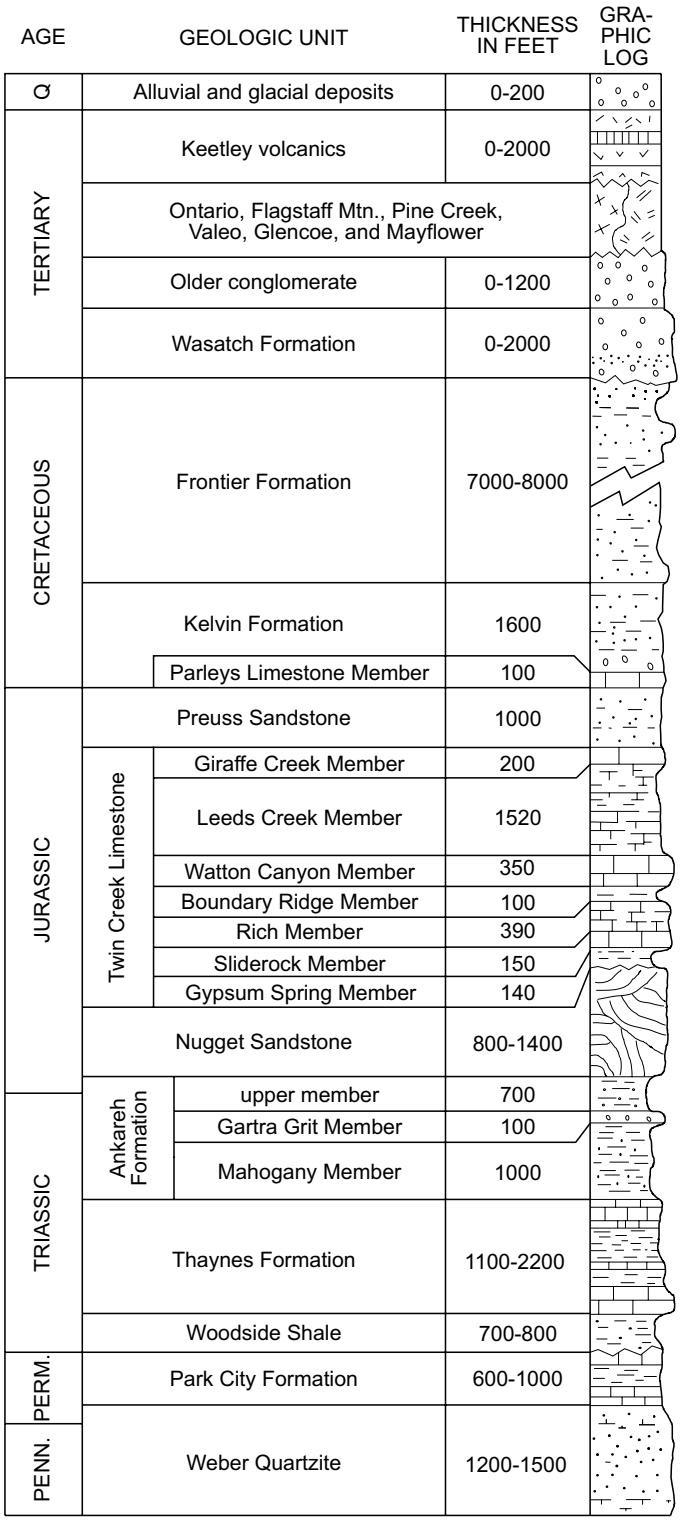

Figure 2. *Summary of stratigraphic units in the Snyderville basin area. Modified from Hintze (1988). Thickness as reported by Hintze.*

Snyderville basin is the Weber Quartzite (IPw). It consists of medium- to thick-bedded, pale-gray, tan-weathering, fine-grained quartzite and sandstone containing some thin, light gray to white limestone and dolostone interbeds (Crittenden and others, 1966; Barnes and Simos, 1968; Bromfield, 1968). Barnes and Simos (1968) tentatively subdivided the Weber Quartzite into three informal units, the lower, middle, and upper members. The lower member consists of interbedded quartzite and sandstone; the middle member is mostly massive quartzite; and upper member consists of interbedded quartzite, limestone, and dolostone. Overall, limestone and dolostone make up about 15 to 20 percent of the stratigraphic section (Bromfield, 1968). In the Park City mining district, the Weber Quartzite is estimated to be between 1,215 and 1,350 feet (370-411 m) thick by Barnes and Simos (1968) and between 1,300 and 1,500 feet (396-457 m) thick by Bromfield (1968).

Permian: The Park City Formation (Ppc) is a lithologically heterogeneous unit (Barnes and Simos, 1968) that consists of interbedded limestone, dolostone, sandstone, siltstone, and shale. Limestones range from "massive, gray, and finely crystalline to thin-bedded, black, and fossiliferous with very thin shaly partings" (Barnes and Simos, 1968). The formation contains a middle phosphatic shale member (Bromfield and Crittenden, 1971). In the Park City mining district, the Park City Formation is estimated to be approximately 670 feet (204 m) thick by Barnes and Simos (1968) and between 550 and 650 feet (168-198 m) thick by Bromfield (1968).

Mesozoic

Triassic: The Woodside Shale (Ŧw) consists of interbedded dark- and purplish-red shale, siltstone, and very fine-grained sandstone (Bromfield, 1968; Bromfield and Crittenden 1971). Shale becomes more dominant toward the bottom of the formation. A gypsiferous shale bed in the lower part of the formation is exposed in the Spiro Tunnel. In the Park City mining district, the Woodside Shale is estimated to be between 680 and 700 feet (207-213 m) thick by Barnes and Simos (1968) and between 700 and 800 feet (213-244 m) thick by Bromfield (1968).

The Thaynes Formation (Ŧt) consists of brown-weathering, fine-grained, limy sandstone and siltstone interbedded with olive-green to dull-red shale and gray, fine-grained, fossiliferous limestone (Crittenden and others, 1966; Bromfield and Crittenden, 1971). A shale unit, known as the “mid-red shale” (of Boutwell, 1912; and Barnes and Simos, 1968), divides the formation into an upper and lower section of nearly equal thickness. The upper section is more calcareous than the lower. In the Park City mining district, the Thaynes Formation is estimated to be about 1,150 feet (351 m) thick by Barnes and Simos (1968) and between 1,100 and 1,300 feet (335-396 m) thick by Bromfield (1968).

The Ankareh Formation (Ŧa) comprises three members; the lower Mahogany Member (Ŧam), the middle Gartra Grit Member (Ŧag), and the upper member (Ŧau). The Mahogany Member consists of about 960 feet (293 m) of purplish-gray and pale-red, ripple-laminated, fine-grained sandstone, purplish mudstone, and a few thin limestone beds (Bromfield, 1968; Bromfield and Crittenden, 1971). The middle Gartra Grit Member consists of between 40 and 100 feet (12-30 m) of white to pale-purple, massive, cross-bedded, coarse-grained to pebbly quartzite (Bromfield, 1968; Bromfield and Crittenden, 1971). The upper member consists of moderate-red, grayish-red, and grayish-purple mudstone and fine-grained sandstone (Bromfield, 1968; Bromfield and Crittenden, 1971). The contact between the Gartra Grit Member and the upper member is gradational.

Jurassic: The Nugget Sandstone (Jn) consists of pale-red to

pale-orange, fine- to medium grained, cross-bedded sandstone (Bromfield, 1968; Bromfield and Crittenden, 1971). The thickness of the Nugget Sandstone is estimated to be about 800 feet (244 m) in the Park City area by Bromfield (1968) and about 1,400 feet (427 m) in the Summit Park area by Jarvis and Yonkee (1993).

The Twin Creek Limestone (Jt; Jtc of Crittenden and others, 1966) comprises seven members: the Gypsum Spring, Sliderock, Rich, Boundary Ridge, Watton Canyon, Leeds Creek, and Giraffe Creek Members (Imlay, 1967; Hintze, 1988). The Gypsum Spring Member at the base of the unit is a gypsiferous, red to red-brown clayey siltstone and silty claystone containing local blocks of gray to pink limestone (Imlay, 1967; Jarvis and Yonkee, 1993). The upper members of the Twin Creek Limestone in the Snyderville basin area consist primarily of olive drab-weathering, gray, oolitic, finely crystalline, and clayey to silty (micritic) limestone (Crittenden and others, 1966; Jarvis and Yonkee, 1993). However, the Boundary Ridge Member also contains a red mudstone layer. The Twin Creek is estimated to be about 1,400 feet (427 m) thick near the eastern boundary of the study area by Bromfield and Crittenden (1971) and about 2,600 feet (792 m) thick in the Summit Park area by Jarvis and Yonkee (1993).

The Preuss Sandstone (Jp) consists mainly of pale-red, interbedded, silty sandstone and shale (Granger, 1953). The middle to upper part of the formation is mostly shale. The Preuss Sandstone is estimated to be about 1,000 feet (305 m) thick (Granger, 1953; Bromfield and Crittenden, 1971).

Cretaceous: The Kelvin Formation (Kk) comprises a lower Parleys Limestone Member (Kkp) and an unnamed upper member (Hintze, 1988). The Parleys Limestone Member (Morrison [?] Formation of Granger, 1953) consists of very light-gray, algal limestone and pale red siltstone, sandstone, and conglomerate and is about 100 feet (30 m) thick. The upper member (Kk) consists of red siltstone, purplish-red sandstone, and sandy conglomerate and is about 1,500 feet (457 m) thick (Granger, 1953).

The Frontier Formation (Kf) consists of pale yellowish-brown sandstone interbedded with pale yellowish-brown to pale red tuffaceous clay and some conglomerate and is about 8,700 feet (2,653 m) thick (Granger, 1953). Conglomerate, belonging to the conglomerate facies (Kfcg) of Bryant (1990), becomes dominant in the upper part of the Frontier Formation.

Cenozoic

Tertiary: The Wasatch Formation (Twc) in the Snyderville basin area consists of a conglomerate containing well-rounded, mostly sandstone and quartzite pebbles and boulders (Granger, 1953; Gill and Lund, 1984; Bryant, 1990). The deposits are localized and very thin in some areas (Gill and Lund, 1984).

An Oligocene and Eocene(?) conglomerate (Toc) consists of boulder, cobble, and pebble conglomerate derived primarily from upper Paleozoic and Mesozoic sandstones, but also contains a few lahars and beds of tuff and volcanic gravel (Bryant, 1990). The conglomerate unconformably overlies Jurassic and Cretaceous rocks and underlies the Keetley Volcanics north and east of Kimball Junction (Crittenden and others, 1966).

Oligocene intrusive rocks (Ti; Tgp and Tm of Bryant, 1990), consisting mostly of monzonite, quartz monzonite, and granodiorite porphyry and small dikes of intermediate composition (Boutwell, 1912; Baker and others, 1966; Bryant, 1990), are found in the southernmost part of the Snyderville basin.

The Oligocene Keetley Volcanics (Tk; Tkb of Bryant, 1990) consist mostly of flows, tuffs, and volcanic breccias of andesitic to rhyodacitic composition (Kildale, 1956; Crittenden and others, 1966; Bromfield and Crittenden, 1971). The Silver Creek Breccia Member (Tksc of Bromfield and Crittenden, 1971) is the primary member of the Keetley Volcanics that crops out in the study area.

Quaternary: Quaternary unconsolidated deposits in the Snyderville basin include Pleistocene glacial till and outwash (Qtp of Bryant, 1990), and alluvium, alluvial-fan deposits, colluvium, and landslides of Pleistocene to Holocene age (Qop and Qoa of Bryant, 1990). Glacial till, landslides, and colluvium are of limited areal extent and/or thickness. Glacial outwash, alluvial-fan deposits, and Pleistocene to Holocene alluvial sediments are found over much of the Snyderville basin. The alluvial deposits consist chiefly of gravel, sand, silt, and clay. These alluvial sediments are generally finer grained where derived primarily from limestone, shale, siltstone, and mudstone rock units.

Structure

The sedimentary rocks in the study area have been complexly folded and fractured by multiple episodes of deformation (plate 2) and to a lesser extent by intrusion of Tertiary igneous rocks (Boutwell, 1912). Most rocks in the northwestern part of the study area are in the hanging wall of the Mount Raymond-Medicine Butte thrust (Bryant, 1990). The thrust is part of a series of thrust faults that make up the Cordilleran thrust belt and that transported hanging-wall rocks eastward during the Cretaceous to early Tertiary Sevier orogeny. The hanging-wall rocks experienced at least two episodes of folding (Bradley and Bruhn, 1988; Bryant 1990; Yonkee and others, 1992) and related deformation. Most rocks in the southeastern part of the study area are below (in the footwall of) the Mount Raymond-Medicine Butte thrust. These footwall rocks also experienced at least two distinct episodes of folding, in addition to Tertiary extensional deformation and intrusion. Tertiary high-angle normal faults and related wall-rock deformation become increasingly dominant to the south.

Thrust Faults

Mount Raymond-Medicine Butte thrust: The Mount Raymond-Medicine Butte thrust is the only major thrust fault in the Cordilleran thrust belt that crosses the study area. Rocks in the hanging wall were transported eastward by the thrust and were folded and fractured. Enough transport occurred that the isopach thicknesses of some formations are significantly different on opposite sides of the fault (table 1). In addition, and probably most importantly to the overall hydrogeologic framework of the study area, the thrust severs the entire stratigraphic sequence of sedimentary rocks. Southwest of Kimball Junction (plate 2; sections 23, 24, 25, 26, 35, and 36, T. 1. S., R. 3. E.), for instance, the thrust juxtaposes

Table 1.
Summary of formation isopach thicknesses.

Formation	Hanging-Wall Thickness (ft)	Footwall Thickness (ft)
Twin Creek Ls.	2,640[1]	1,500[2]
Nugget Ss.	1,400[1]	1,150[2]
Thaynes Fm.	2,200[3]	1,150[4]
Park City Fm.	970[5]	670[6]

[1] *Jarvis and Yonkee (1993).*
[2] *This report based on Mount (1952), Bromfield and Crittenden (1971), and Hintze (1988).*
[3] *This report based on mapping of Crittenden and others (1966).*
[4] *Barnes and Simos (1968) and Hintze (1988).*
[5] *Granger (1953).*
[6] *Barnes and Simos (1968).*

the Park City Formation against the Nugget and Twin Creek Formations.

As mapped by Crittenden and others (1966), the thrust trace is sinuous across the study area as a result of folding but also, to a lesser extent, topography (figure 3). The thrust strikes east-northeast where it enters the study area in the west. However, the thrust curves northeast where it is apparently folded by two gently plunging to horizontal folds. The Willow Draw anticline is the westernmost of the two folds. On the northwest limb of this fold the thrust juxtaposes the Park City Formation against the Twin Creek Limestone and Nugget Sandstone. The trace continues northeast to Kimball Junction where it curves across the nose of the fold. Crittenden and others (1966) show the thrust trace on the southeast limb of the anticline to continuing southwest parallel to its trace on the northwest limb. The easternmost fold, the Dutch Draw syncline, folds the thrust so that its trace curves back to the northeast near Iron Hill.

The exact location of the thrust trace along the southeast limb of the Dutch Draw syncline and the position where the thrust merges with other imbricate strands are unknown because it is covered by Tertiary and younger deposits. Crittenden and others (1966) mapped only a single trace that extended northeast across Parleys Park. A later interpretation by Crittenden (1974) shows two strands that diverge somewhere beneath the unconsolidated deposits in Parleys Park. In the Rockport Reservoir area northeast of the study area, Crittenden (1974) named the northwestern strand the Dry Canyon thrust and the southeastern strand the Crandall Canyon thrust. The southeastern strand has subsequently been referred to as the Mount Raymond-Absaroka thrust (Lamerson, 1982; Bradley and Bruhn, 1988; Yonkee and others, 1992). Bryant (1990) considers the northwestern strand to be the southwestern continuation of the Medicine Butte thrust.

Whereas many subsequent researchers (Crittenden, 1974; Bradley and Bruhn, 1988; Bryant, 1990; Yonkee and others, 1992) have adopted or slightly modified this interpretation, others (Lamerson, 1982; B. McBride, formerly with Mobil Oil, verbal communication, 1996) have reinterpreted the structural geology of the area and show the trace of the thrust as having a simpler map pattern (figure 3). Lamerson

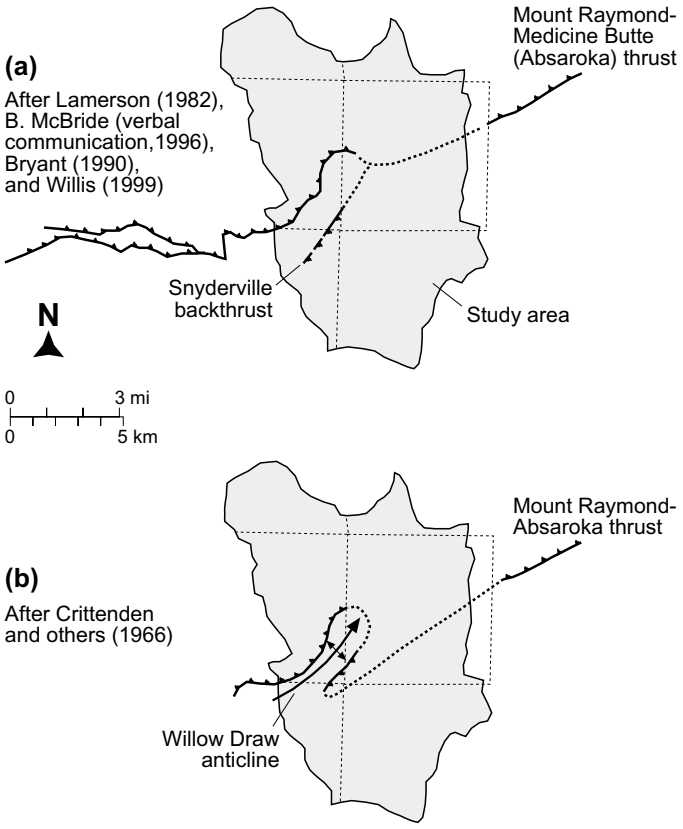

Figure 3. *Alternate interpretations of the Mount Raymond-Medicine Butte thrust trace. (a) Recent mapping by B. McBride for Mobil Oil indicates that the thrust exposed near Snyderville is a separate backthrust that we refer to as the Snyderville backthrust. (b) Crittenden and others (1966) mapped this as the Mount Raymond-Absaroka thrust and interpreted it to be folded by the Willow Draw anticline. Most later researchers adopted this interpretation. However, we favor the interpretation shown in (a). Bryant (1990) and Willis (1999) show the thrust trace to be in Medicine Butte and not the Absaroka.*

(1982) shows the thrust trace to trend roughly east from Kimball Junction. This interpretation is consistent with the folding of a high-angle fault that strikes oblique to the trend of the fold. We adopt the thrust trace of Lamerson (1982), but favor the interpretation of Bryant (1990) and others (Willis, 1999) that the thrust is the Medicine Butte rather than the Absaroka.

Although the presence of a thrust that places the Nugget Sandstone over the Twin Creek Limestone near Snyderville is unequivocal, this thrust may not be the Mount Raymond-Medicine Butte. Preliminary mapping by Mobil Oil (B. McBride, verbal communication, 1996) interprets the thrust near Snyderville as a high-angle out-of-syncline backthrust in the footwall of the Mount Raymond-Medicine Butte thrust. We interpret the thrust trace as mapped by Lamerson (1982) to be the Mount Raymond-Medicine Butte thrust.

Toll Canyon fault: The Toll Canyon fault (Crittenden and others, 1966; Yonkee and others, 1992) trends east-northeast between Summit Park and Ecker Hill (plates 1 and 2). The fault trace continues to the southwest, outside of the study area, where it appears to terminate south of Lambs Canyon. Jarvis and Yonkee (1993) recognized a second upper strand of the fault in the Summit Park area. The two strands bound

a complexly deformed zone in the Twin Creek Limestone. The upper strand splays from the main, lower strand just west of the study-area boundary. From that point, it trends roughly parallel to the main strand for about a quarter mile (0.4 km), and then curves to the north. The main strand continues east-northeast toward Ecker Hill. To the west-northwest of Ecker Hill (section 10, T. 1 S., R. 3 E.), the fault offsets the lower contact of the Nugget Sandstone about 2,300 feet (700 m). In this area, faulting juxtaposes the Nugget and Ankareh Formations on the north against the Twin Creek and Nugget Formations, respectively, on the south. Jarvis and Yonkee (1993) estimated the throw across the fault (zone) to be roughly 755 feet (230 m) in the Summit Park area (section 16, T. 1 S., R. 3 E.) with an apparent northwest side-up displacement. In this area, faulting juxtaposes Nugget Sandstone on the north against Twin Creek Limestone on the south in the subsurface. The fault is speculated to dip steeply north. The Toll Canyon fault may be a subsidiary hanging-wall imbricate thrust to the Mount Raymond-Medicine Butte thrust.

Frog Valley thrust: The Frog Valley thrust (Boutwell, 1912) is a roughly north-south-trending fault on the east side of the Park City mining district. The thrust apparently is truncated to the south by the east-northeast-trending Hawkeye-McHenry fault located just outside the southeast part of the study area. The thrust trends generally northward along the east side of Bald Eagle Mountain and Deer Valley and dips roughly 45 degrees to the west (Boutwell, 1912). The fault juxtaposes Weber Quartzite on the west against the Woodside Shale and Park City Formation on the east. Throw across the fault increases to the north with an apparent west-side-up displacement. North of Deer Valley, the fault trace continues north-northeast where it disappears beneath Quaternary and Tertiary deposits. The thrust may be equivalent to an unnamed east-northeast-trending thrust (Bryant, 1990) located approximately 3 miles (5 km) southeast of the Crandall Canyon thrust at Rockport Reservoir. In such a case, the Frog Valley thrust would represent a subsidiary frontal imbricate thrust to the Mount Raymond-Medicine Butte thrust. Some geomorphic evidence suggests that the Frog Valley thrust has been reactivated as a down-to-the-west normal fault (Sullivan and others, 1986).

High-Angle Faults in the Park City Mining District

The major faults in the Park City mining district are high-angle normal faults that generally strike east-west to east-northeast. These faults were sites of mineralization and subsequent mining activity, and include the Crescent and Ontario-Daly West faults. The faults postdate folds and thrusts, such as the Park City anticline and Frog Valley thrust, and are considered to be nearly contemporaneous with intrusion of the Tertiary igneous rocks (Barnes and Simos, 1968).

Folds

Multiple episodes of folding (plate 2; appendix C) deformed the layered sedimentary rocks in the study area. North- to northeast-plunging folds are rotated by younger, northeast(?)- to east-northeast-plunging folds (Bradley and Bruhn, 1988). Disharmonic folds (see glossary) formed mostly above the Mount Raymond-Medicine Butte thrust and are especially prominent in the Twin Creek Limestone (figure 4). Folds also occur in the footwall of the thrust that either postdate or initiated during the latest stage of thrusting, because northeast-plunging folds deform the Mount Raymond-Medicine Butte thrust. Disharmonic, northwest-plunging folds represent a distinct phase of folding in the footwall of the Mount Raymond-Medicine Butte thrust. Minor Tertiary folds and flexures related to high-angle normal faults are superimposed on older folds in the Park City mining district (Barnes and Simos, 1968).

Parleys Canyon syncline: The Parleys Canyon syncline is a broad, northeast-plunging fold that has a trough line northwest of the study area. It is important because all of the rocks in the hanging wall of the Mount Raymond-Medicine Butte thrust are folded by it. The rocks in the northern part of the study area dip to the north to form the southeast limb of the fold. Rocks underlying the Preuss Formation are folded by an older phase of north-northeast- and a few north-northwest-trending folds. The Preuss and younger formations do not appear to be deformed by these folds.

Willow Draw anticline: The Willow Draw anticline (Crittenden and others, 1966) is the westernmost of a pair of horizontal to moderately northeast-plunging folds that deform the Mount Raymond-Medicine Butte thrust. Due to the paucity of outcrops on the northwest limb of the fold, the fold geometry can only be approximated. The anticline is an upright, close to gentle (see "Fold Tightness" in glossary) fold that ranges from horizontal in the northeast to moderately northeast-plunging in the southwest. Crittenden and others (1966) show the fold becoming tighter to the southwest. Erosion has exposed the uppermost footwall rocks (Twin Creek, Nugget, and Ankareh Formations) beneath the thrust in the core of the fold. As a result of a combination of erosion and faulting, the Twin Creek Limestone and Nugget Sandstone are present only on the limbs of the southwestern half of the fold. Because of faulting, only the lower part of the Twin Creek Limestone is present on the limbs of the fold. The partial Twin Creek sequence is thickest on the southeast limb of the fold.

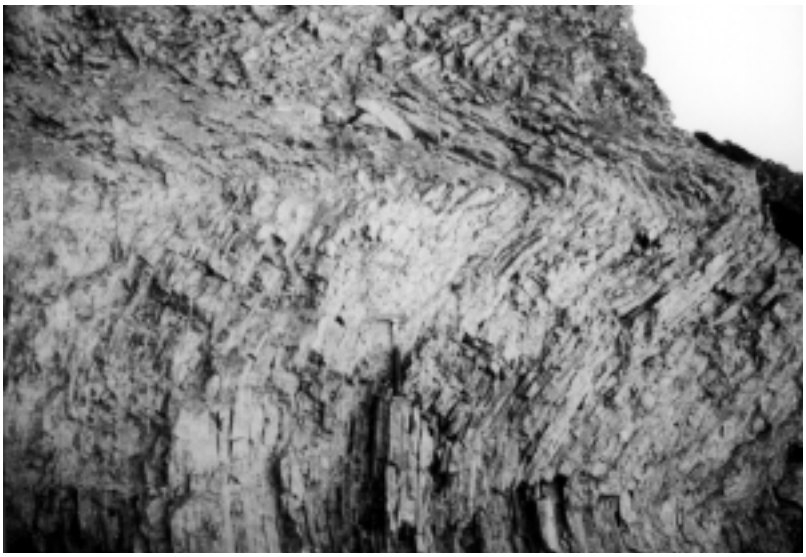

Figure 4. *Folding in the Twin Creek Limestone. View is to the west. Hammer shown for scale. Exposure located in foundation excavation in SE $^1/_4$ section 9, T. 1 S., R. 3 E.*

Dutch Draw syncline: The Dutch Draw syncline (Crittenden and others, 1966) is the eastern companion fold to the Willow Draw anticline. The fold geometry is less well constrained than that of the Willow Draw anticline due to a lack of outcrops on its southeast limb. The fold ranges from horizontal in the northeast to moderately plunging in the southwest, similar to the Willow Draw anticline. We estimate the fold axis attitude to range between upright and steeply plunging and the fold tightness to range between close and gentle. The series of northwest-plunging folds located to the southeast may deform the southeast limb of the Dutch Draw syncline. However, there is no evidence to either support or refute this speculation. If the northwest-plunging folds do not deform the southeast limb, they must die out rapidly beneath the Quaternary cover and are disharmonic folds. The Twin Creek and Nugget Formations are exposed in the up-plunge nose and along part of the northwest limb of the fold. Rocks folded by the syncline are buried by alluvium to the northeast. The Mount Raymond-Medicine Butte thrust may be folded by the syncline (Crittenden and others, 1966) or an out-of-syncline backthrust may offset formations on the fold's northwest limb (B. McBride, verbal communication, 1996).

Park City anticline: The Park City anticline has been described extensively in the geologic literature (Boutwell, 1912; Barnes and Simos, 1968; Bromfield, 1989) due to its prominence in the Park City mining district. The anticline is a gentle, north- to northwest-plunging fold that can be traced as far south as Bald Mountain, where it truncates against several igneous intrusions.

The fold is dissected by numerous high-angle normal faults described above that are roughly perpendicular to its axis (Barnes and Simos, 1968). The Frog Valley thrust severs the east limb of the anticline. Erosion has exposed the Weber Quartzite in the core of the fold and the Park City, Woodside, and Thaynes Formations on both limbs.

Discrepancy exists regarding the location of the northern portion of the crest line of the fold. Boutwell (1912) did not label the crest line of the fold on the geologic map included in his report. However, a cross section shows that the crest line crosses through the Rossi Hill area between Park City and Deer Valley. Later mapping by Bromfield and Crittenden (1971) shows the crest line to be farther to the west along the west side of Ontario Ridge. A later unpublished map (provided by K. Gee of United Park City Mines Co.) shows the crest line to trend roughly north-south in the position depicted in Boutwell's cross section. The discrepancy is likely a result of differences in the quality of data available to mappers. At the surface the anticline is defined by bedding in the poorly bedded Weber Quartzite. The recognition of bedding and the ability to differentiate it from sheeting at surface outcrops is a difficult task, whereas the recognition of apparent dips of bedding in mine workings is less so. Therefore, we favor the interpretation based on the subsurface data.

We speculate that the Park City anticline bifurcates and a branch continues farther northwest than previously mapped, although a second northeast-trending branch likely also is in the Deer Valley area (figure 5). Bromfield and Crittenden (1971) show the fold to die out near historic Park City and the later unpublished mine map shows it to die out in the Masonic Hill area. Both interpretations likely reflect the poor manifestation of the fold in the Park City Formation and immediately overlying formations farther to the north. Analysis of bedding orientation in the Park City Formation to determine the shape of the rock structure, however, validates the continuation of the fold in a northwest direction. The fold is very broad or gentle north of historic Park City, and plunges gently northwest to north-northwest. A similar fold geometry is recognized by analyzing bedding in both the overlying Ankareh Formation and Nugget Sandstone. The northwest-plunging fold was recognized by Bryant (1990), but was not considered to be continuous with the Park City anticline. We refer to this northwest branch as the Iron Mountain anticline (plate 2).

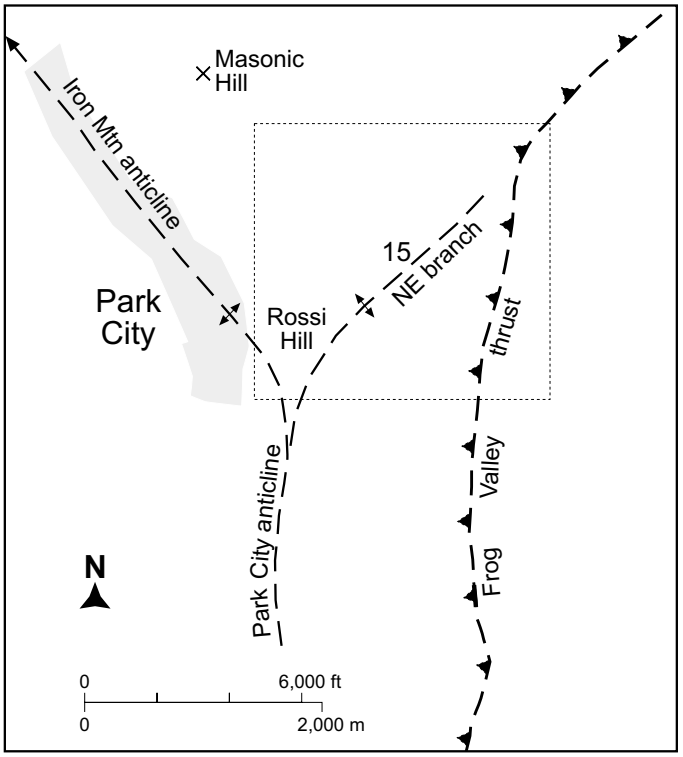

Figure 5. *Branches of the Park City anticline. Trace of the northwest branch is inferred to cross historic Park City and is referred to as the Iron Mountain anticline. Trace of northeast branch is inferred to cross the Deer Valley Meadow area in the SE¼ section 15, T. 2 S., R. 4 E. Crest of anticline is eroded northeast of its intersection with the Frog Valley thrust.*

Northwest-plunging folds: A series of steeply inclined to upright, gentle, northwest- to west-northwest-plunging folds deform the sedimentary rocks in the footwall of the Mount Raymond-Medicine Butte thrust north of Park City. We have informally named these folds, from east to west, the Round Valley anticline, the Quarry Mountain syncline, and the Iron Mountain anticline.

Igneous Intrusions

Tertiary stocks intrude the sedimentary strata along the southern boundary of the study area. Intrusion resulted in localized, and in some cases, distal deformation of the country rock (Boutwell, 1912). The four Tertiary stocks that crop out at the surface include the Alta, Clayton Peak, Flagstaff (Baker and others, 1966), and a small, unnamed intrusion on the west slope of Frog Valley (Bromfield and Crittenden,

1971). The intrusions are reported to be more extensive in the subsurface (Boutwell, 1912) where they extend as far north as the Silver King mine, located west-southwest of Park City. Extensive crushing and fracturing of the country rock adjacent to the intrusions was frequently observed in mine workings. Lack of evidence for extensive stoping (see glossary) suggests that more regional deformation must have accompanied the intrusion of the stocks. Boutwell (1912) speculated that the Frog Valley thrust may have been reactivated during intrusion; however, the majority of the displacement on the fault, particularly north of the Park City mining district, probably occurred during the Sevier orogeny.

HYDROGEOLOGY OF UNCONSOLIDATED DEPOSITS

Unconsolidated deposits (plate 2, figure 6), principally derived from erosion of the surrounding bedrock highlands by fluvial, glacial, and mass-wasting processes, cover 28 percent of the Snyderville basin. Composition, grain size, and sorting of unconsolidated deposits vary with method of deposition and proximity to source areas. Figure 6 is a map of major unconsolidated deposits in the Snyderville basin. These Quaternary deposits have a maximum thickness of about 275 feet (84 m). Where saturated and sufficiently permeable, the unconsolidated deposits are an aquifer.

Alluvium is of two ages in the Snyderville basin. The younger alluvium underlies the larger perennial streams in valley bottoms (Bryant, 1990). In general, the younger alluvium along all streams consists of poorly sorted gravel and cobbles in a matrix of silt, clay, and sand. Based on drillers' logs, these deposits probably reach a maximum thickness of 10 feet (3 m). Along East Canyon-Kimball Creek in Parleys Park, the younger alluvium consists of several types of materials. Upstream to the south, the younger alluvium consists of poorly sorted gravel and cobbles containing some sand beds and minor silt. Downstream to the north, the deposits become finer grained and better sorted, but even at the northern end of the basin they contain a large proportion of gravel.

Older alluvium (Bryant, 1990) exists along the margins of the lower Silver Creek and East Canyon Creek drainages, and in the northern Parleys Park area. These deposits consist of poorly sorted gravel, silty gravel, and sandy silt. In some areas, such as northern Parleys Park, the older alluvium consists of finer grained deposits (sandy silt) generally containing little gravel. The thickness of the older alluvium ranges from a feather edge along the outer margin of the alluvial plains to a maximum of 50 feet (15 m) along East Canyon Creek and 80 feet (24 m) along Silver Creek. A conservative estimate of the minimum average thickness of the older alluvial deposits that underlie the northern Parleys Park area is about 25 to 30 feet (7-9 m).

Glacial till is present in some areas at elevations above 7,000 feet (2134 m). During the Pleistocene, glaciers advanced and retreated in these areas, depositing till in ground, end, and lateral moraines along steep canyons and on some steep mountain slopes. Till is a poorly sorted, unstratified, heterogeneous mixture of boulders, cobbles, and gravel in a finer matrix of silt, sand, and clay. The permeability of silt- and clay-rich till is generally low (Freeze and Cherry, 1979). Till deposits are present on Ontario Ridge, at the mouth of Woodside Gulch, at the northwest end of Rossi Hill, and in the White Pine Lake area (Crittenden and others, 1966; Gill and Lund, 1984). The deposits range in thickness from a few feet to 100 feet (30 m) (Boutwell, 1912).

Glacial erosion supplied significant volumes of sediment to drainages. Glaciers in the Dutch Draw and Empire Canyon areas discharged sediment-laden meltwater into streams that carried outwash materials into the Parleys Park and Park City areas. Glacial-outwash deposits formed a relatively flat surface extending down valley. The advance and retreat of the glaciers in the mountains over time laid down successive layers of glacial sediments resulting in a complex stratigraphy. Coarse material was deposited closer to the ice margin, and finer material was carried farther down valley. The high variability of discharge from glacial sources produced highly heterogeneous materials. Outwash and related alluvial deposits consist of gravel, fine sand, and silt and are poorly to moderately sorted, but are better sorted and stratified than till.

Other unconsolidated deposits in the Snyderville basin include talus, colluvium, and alluvial-fan material. Mass-wasting processes, producing landslides and rock falls, are active on many slopes, but the area involved is relatively small.

Unconsolidated deposits along the major perennial streams generally contain water at shallow depths. Gill and Lund (1984) reported that shallow ground water occurs principally in valley-bottom alluvium and colluvium at the base of slopes, as is evident by the existence of large areas of marshy or boggy ground. Recharge to the unconsolidated deposits is from infiltration of precipitation and irrigation water, seepage from perennial and ephemeral streams, and upward crossflow from rock. Locally, some water-yielding unconsolidated deposits may be confined or semiconfined, but water-table conditions prevail in the unconsolidated aquifer.

Extent

The rock contact defines the lateral and lower boundaries of the unconsolidated deposits. To define the boundaries of the unconsolidated aquifer, we used ground-water levels from water wells completed in unconsolidated deposits. Figure 7 shows the location of unconsolidated deposits that yield water to wells and springs. Thin, saturated deposits outside the boundary shown in figure 7 may provide small quantities of water to low-flow-rate wells.

Thickness and Stratigraphy

We constructed four cross sections depicting stratigraphy in unconsolidated deposits and depth to rock. Figure 7 shows the locations of the cross sections. Stratigraphy in the cross sections is based primarily on water-well drillers' logs. It was necessary to project some data from drillers' logs onto the cross-section lines.

Figure 8 (line A-A') is a cross section across Parleys Park near Snyderville, oriented perpendicular to the axis of the valley. Parleys Park is a broad valley near the center of the basin. The thickness of the unconsolidated deposits is vari-

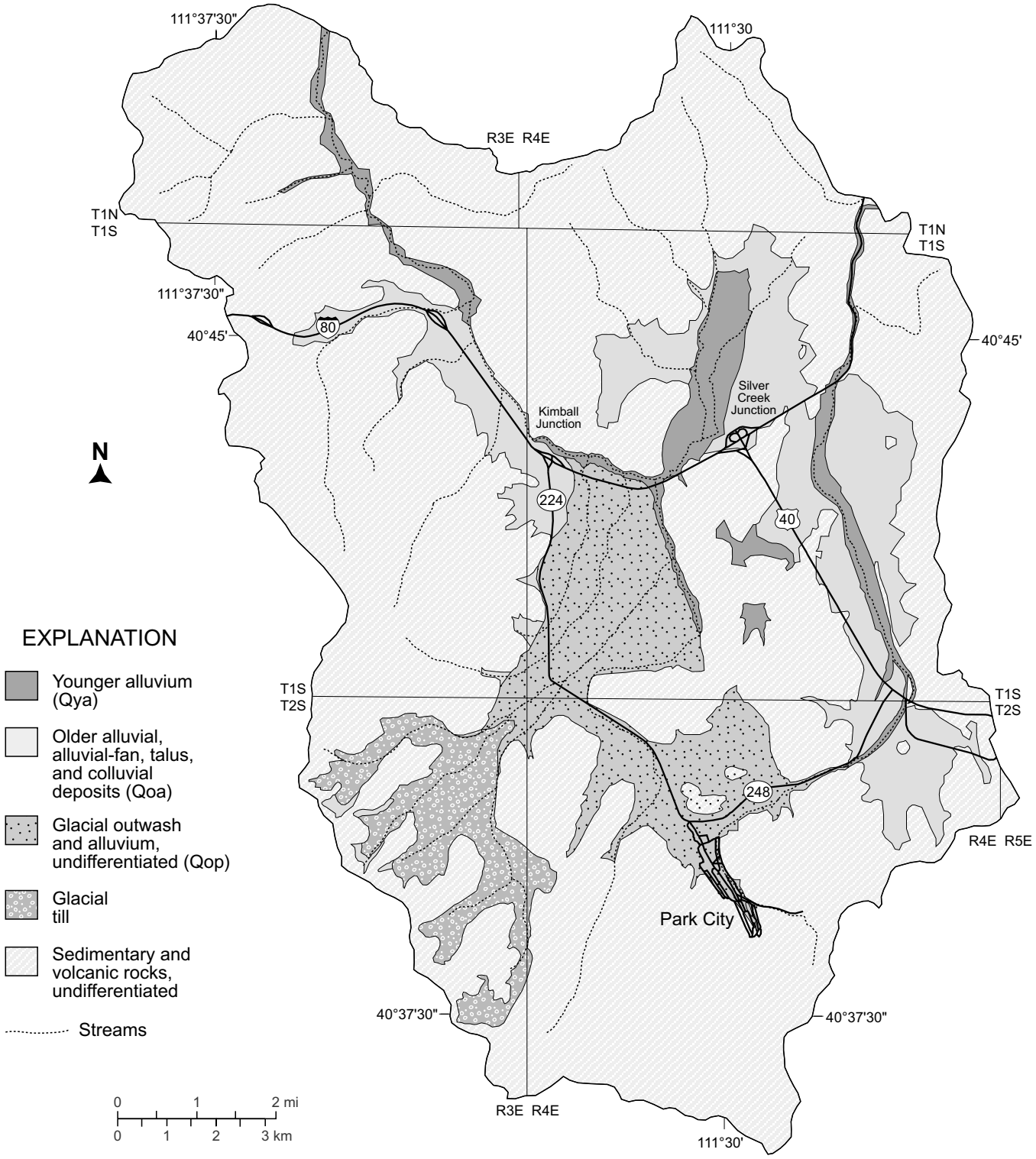

Figure 6. *Unconsolidated deposits in the Snyderville basin.*

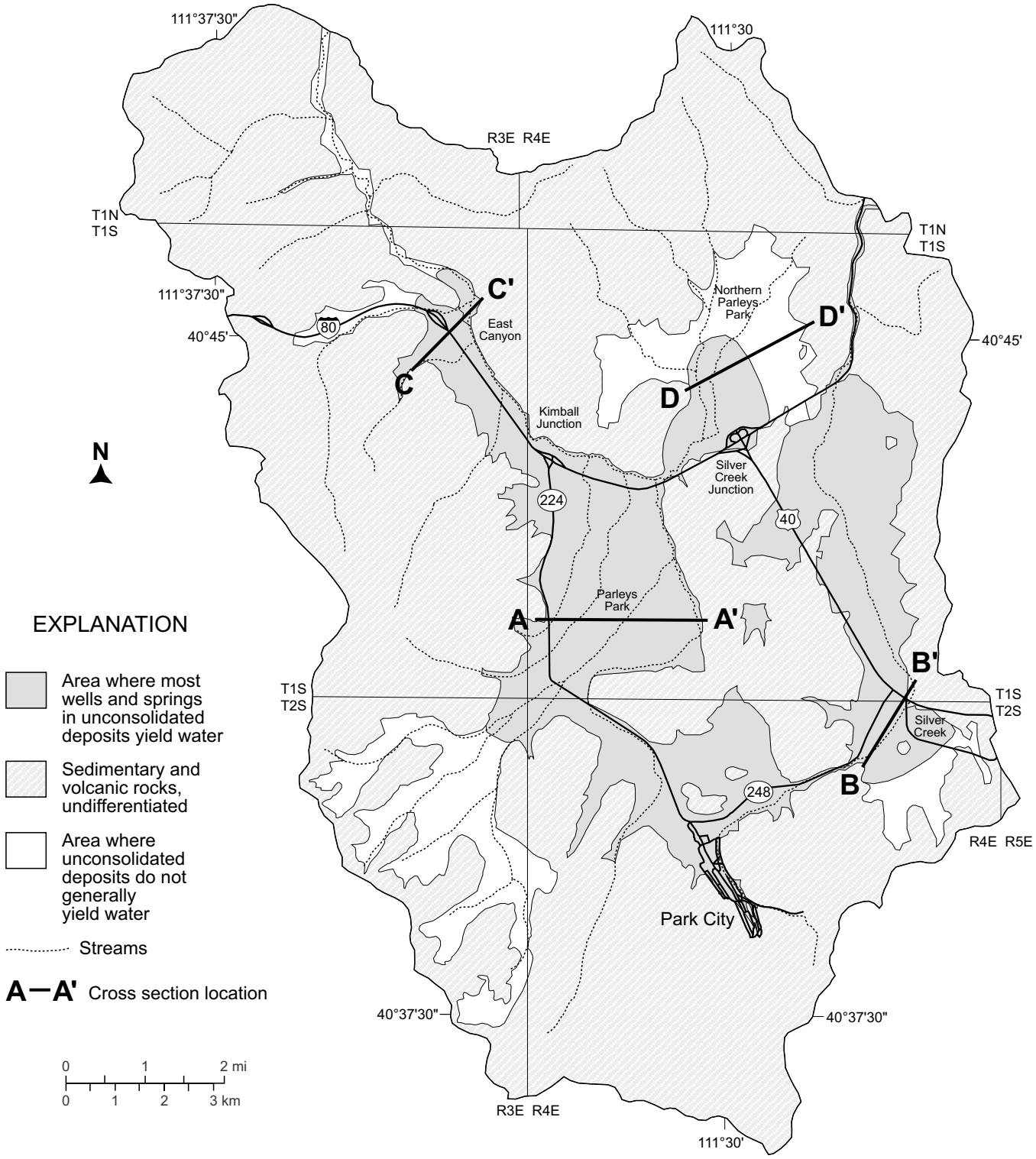

Figure 7. *Areal extent of unconsolidated deposits that yield water to wells and springs. Locations of cross sections are also shown.*

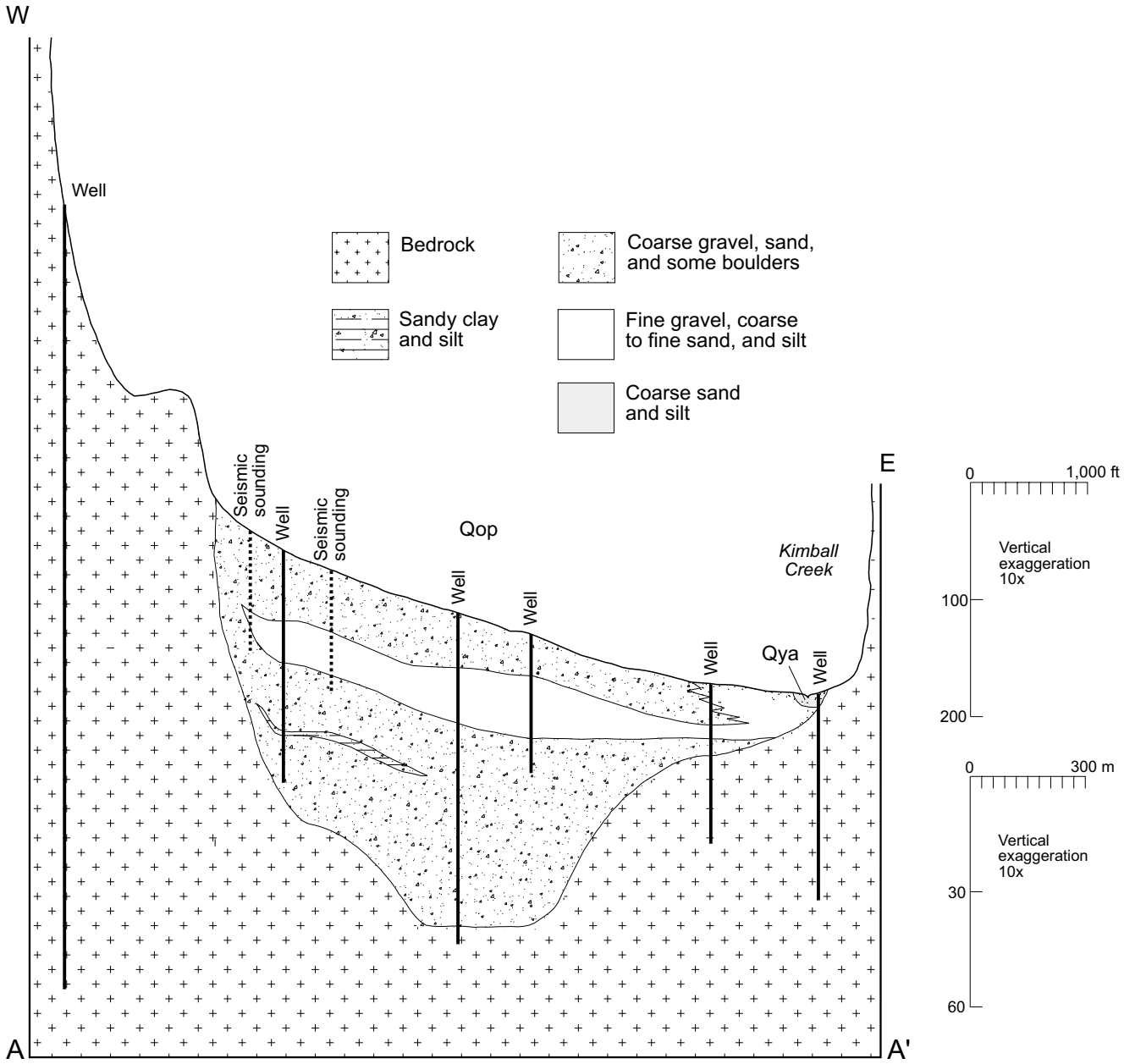

Figure 8. *Geologic cross section of unconsolidated deposits across Parleys Park near Snyderville. Location of cross section is shown in figure 7. Qop - outwash deposits, Qya - young alluvium.*

able as is the thickness and persistence of individual stratigraphic units. Of particular significance is the total thickness of the deposits, which is up to 275 feet (85 m). Depth to rock in this area exceeds the expected level of Pleistocene downcutting as indicated by shallow rock thresholds of both East Canyon and Silver Creek where they exit the basin, and is well below the present base level. The relatively great apparent thickness of unconsolidated deposits in Parleys Park may indicate a Quaternary-age subsiding structural (fault-bounded) basin or a deeply incised erosion feature inherited from a Tertiary-age landscape much different from the present. Alternatively, highly weathered bedrock with seismic velocities similar to unconsolidated deposits may underlie the area.

Figure 9 (line B-B') is a cross section across Silver Creek south of Keetley Junction. The cross section is oblique to the valley and cuts across the Silver Creek channel twice (see figure 7). Valley relief consists of low rolling hills within which the stream has become incised, forming steep-sided banks and gully-dissected abandoned flood plains. Unconsolidated deposits at this location consist of predominantly fine to coarse gravels containing some alternating layers of sandy clay up to 3 feet (1 m) thick. The lateral extent of these sandy clay layers is unknown, but is probably limited. In general, individual stratigraphic units could not be correlated between more than two wells. Young alluvium in this section contains coarse sand, silt, and reworked mine tailings. The thickness of unconsolidated deposits varies, but is inferred to be less than 90 feet (27 m).

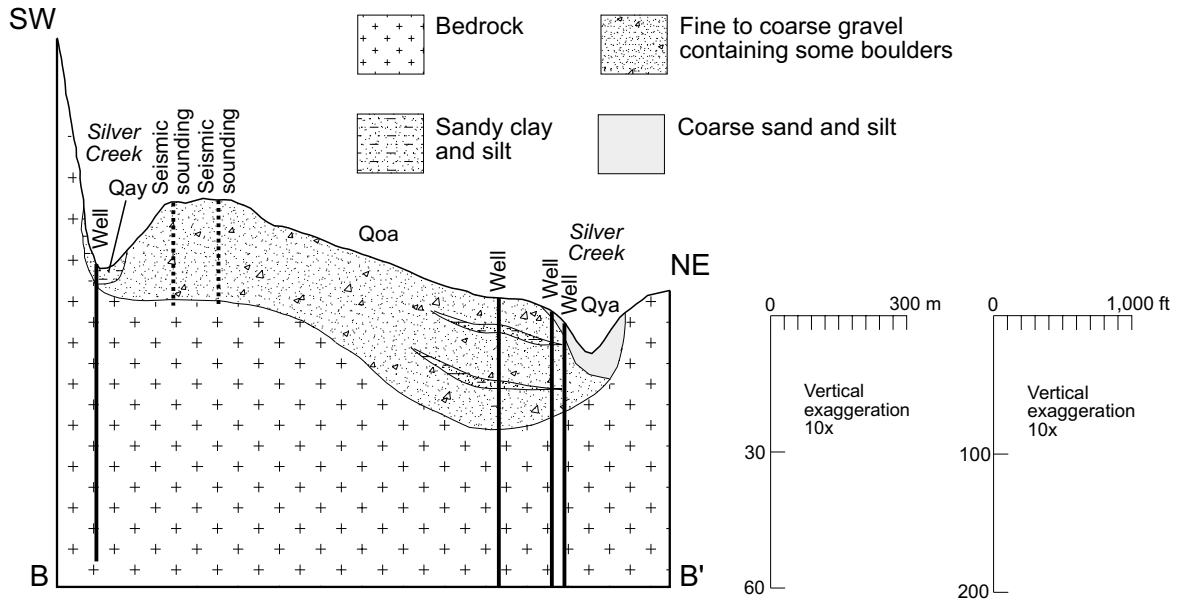

Figure 9. *Geologic cross section of unconsolidated deposits across Silver Creek south of Keetley Junction. Location of cross section is shown on figure 7. Qoa - alluvium, Qya - young alluvium.*

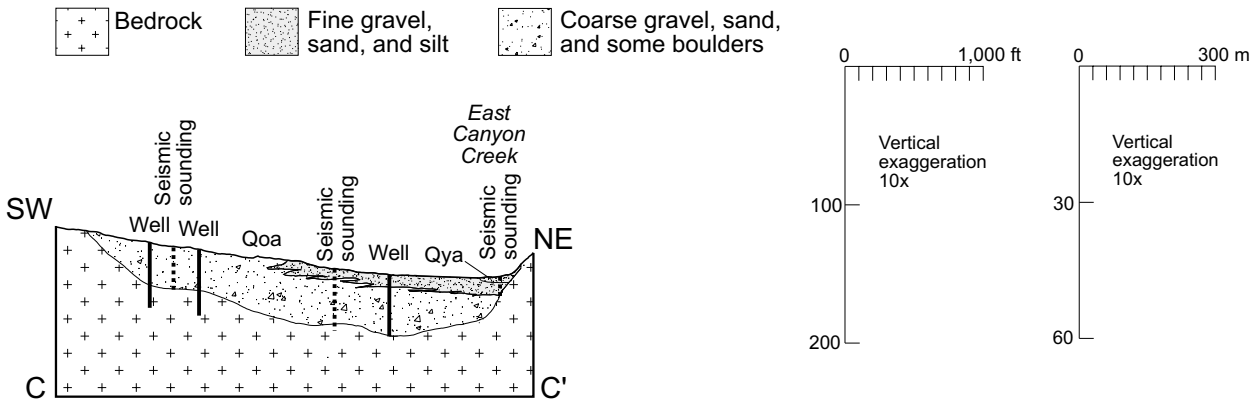

Figure 10. *Geologic cross section of unconsolidated deposits across East Canyon Creek in Toll Canyon near Pinebrook. Location of cross section is shown on figure 7. Qoa - old alluvium, Qya - young alluvium.*

Figure 10 (line C-C') is a cross section roughly perpendicular to East Canyon Creek near Pinebrook. Topographic relief in the drainage is moderate with only a narrow flood plain. The alluvial fan from Twomile Canyon produces moderate slopes west of East Canyon Creek. Unconsolidated deposits consist of older interbedded alluvium and alluvial-fan deposits of coarse gravel to fine gravel and sand. Younger alluvium deposited by East Canyon Creek consists of gravel- to silt-size materials. The thickness of alluvium varies, but is generally less than 50 feet (15 m).

Figure 11 (line D-D') is a cross section across northern Parleys Park north of Silver Creek Junction oriented perpendicular to the broad, gently rolling valley. Unconsolidated deposits range in thickness from 0 to 30 feet (0-10 m) and include younger alluvium, consisting primarily of sand and gravel, older alluvium containing coarser gravel and boulders, and colluvium on hillsides in volcanic rocks.

To provide information for estimating the volume of water in the unconsolidated deposits, we produced a map (figure 12) showing our best estimate of the thickness of these deposits (see appendix A for details on method of construction). The bedrock contact at the surface represents a zero-thickness line, and we chose 40 feet (12 m) as a contour interval. The thickness of unconsolidated deposits ranges from 20 to over 275 feet (9-84+ m). Of particular significance is the thickness of the unconsolidated deposits in the Parleys Park area.

Interaction with Underlying Saturated Fractured Rock

An aquifer test performed for Park City's Park Meadows and Middle School wells in 1991 (by J.M. Montgomery, 1991) provides important insight into the interaction between the unconsolidated aquifer and the underlying saturated fractured rock. Both wells are completed in the Thaynes Formation in areas where it is overlain by a relatively thick sequence of alluvium. Aquifer test results for these wells, which were both pumped at a discharge rate of about 1,100 gallons per minute (gal/min) (69 L/s) for several days, indicate that shallow monitoring wells completed in alluvium responded differently than deep monitoring wells. Whereas drops in water levels were recorded in all deep wells during pumping, no response was noted in any of the shallow wells. The water-level decline in the deep wells suggests that pumping from fractured rock reduces discharge to the deeper unconsolidated deposits (resulting from upward flow of ground water in the fractured rock) and possibly induces recharge of the fractured rock from the lower part of the overlying saturated deposits. The lack of response in overlying shallow wells suggests that local semiconfined or confined conditions may exist in the unconsolidated deposits in this area.

Implications for Ground-Water Management

The maps and cross sections (figures 6 through 12) can be used to determine areas and approximate thicknesses of unconsolidated materials that are potential aquifers. Although unconsolidated deposits are less than 90 feet (27 m) thick in most areas, they generally yield some water. Because these deposits are commonly thin, they do not store much ground water and therefore cannot yield large quantities of water to wells.

Aquifer-test results suggest that the saturated unconsolidated deposits may recharge the underlying fractured rock during continuous pumping from wells completed in rock. Such an interaction between the unconsolidated and rock aquifers may be important for high sustained yields to be attained from wells completed in rock. Both the Park Meadows and Middle School wells are capable of higher yields than other wells completed in the Thaynes Formation, such as wells in the Pinebrook area (see figure 2, Jarvis and Yonkee, 1993), and particularly those where thick, saturated unconsolidated deposits are absent above the rock.

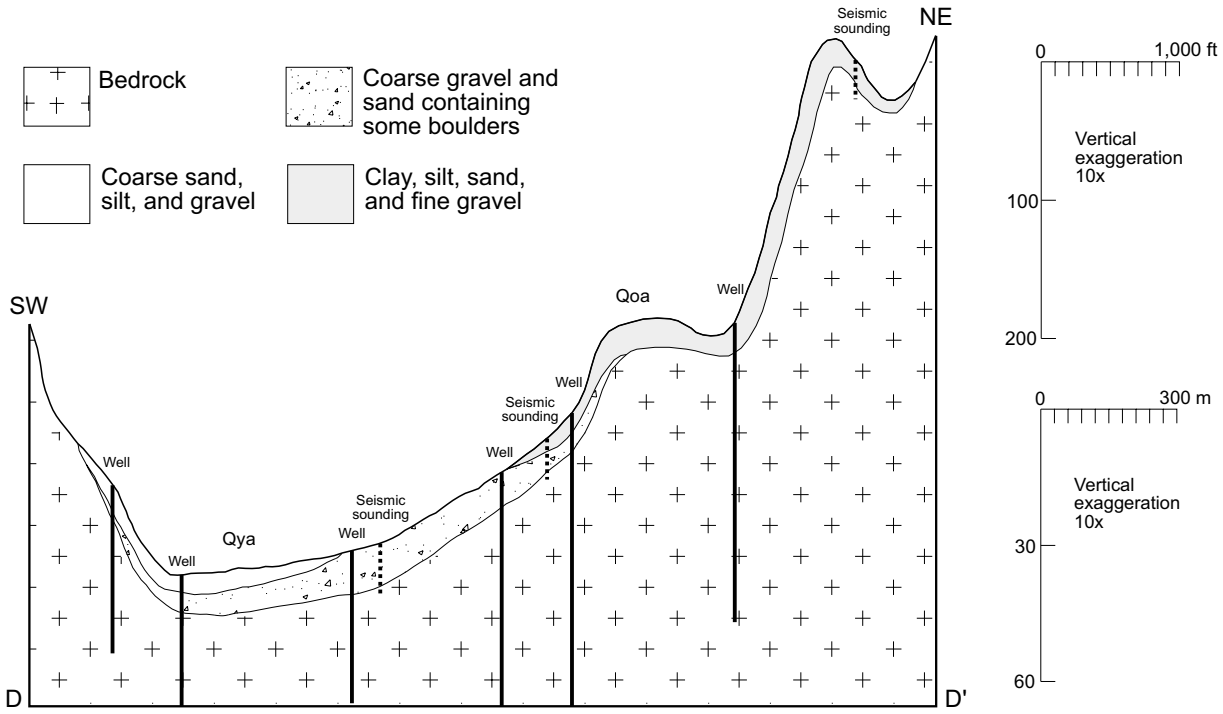

Figure 11. *Geologic cross section of unconsolidated deposits across northern Parleys Park north of Silver Creek Junction. Location of cross section is shown in figure 7. Qoa - old alluvium, Qya - young alluvium.*

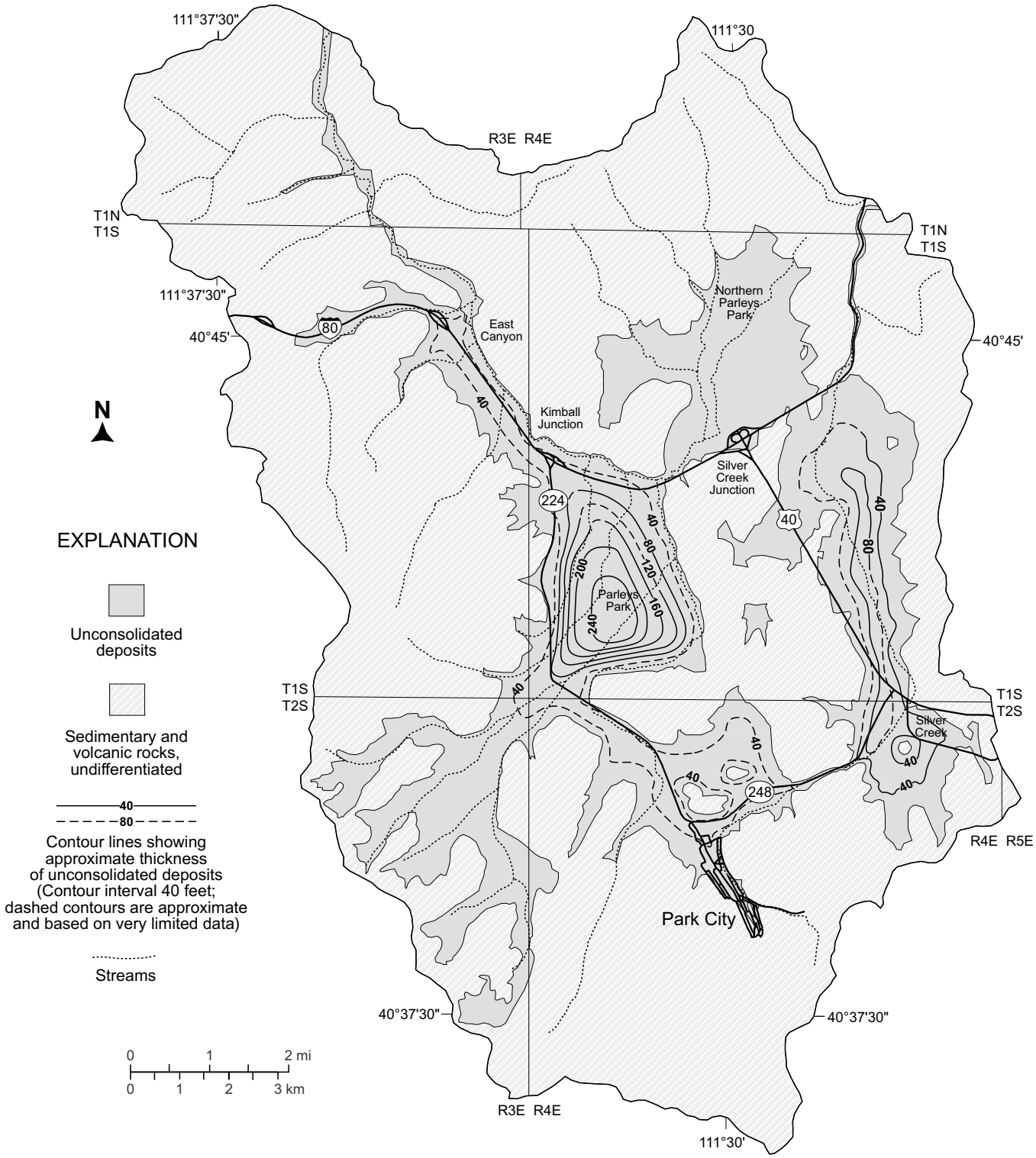

Figure 12. *Schematic map showing the possible thickness of unconsolidated deposits.*

HYDROGEOLOGY OF FRACTURED ROCK

Demand is increasing for ground-water resources in fractured rock as a result of ongoing growth in the Snyderville basin. Most water-supply wells in rock are completed in sedimentary rock formations such as the Twin Creek, Nugget, and Thaynes Formations. Ground-water inflows exceeding 100 gal/min (6.3 L/s) are reported in tunnels and mine workings penetrating the Thaynes, Park City, and Weber Formations (Gee, 1994). Rock types in the Twin Creek, Thaynes, and Park City Formations are primarily limestone or dolostone interbedded with shale and sandstone. The Nugget Sandstone and Weber Quartzite are primarily sandstone; however, the Weber Quartzite contains limestone interbeds. In general, fractured limestone and sandstone beds yield water to wells and tunnels whereas shale beds inhibit ground-water flow (Gee, 1994).

Primary Permeability Versus Secondary Permeability

Sandstones and limestones can have both primary and secondary permeability. We refer to the capacity of rock to transmit fluids through intergranular pore space (effective primary porosity) as primary permeability and through openings formed after consolidation (such as solution openings and fractures) as secondary permeability. Primary permeability in a sandstone is related to the interconnected void space between grains of sand that make up the rock. The amount of void space is a function of grain size, sorting, and degree of cementation. In some sandstones, primary permeability can be high enough to obtain significant water yields from wells (Freeze and Cherry, 1979). Primary permeability of sandstones in the Snyderville basin has, to date, not been studied in any detail. However, field observations suggest that some Cretaceous sandstones may have relatively high primary permeability (see Recommended Future Studies). In limestones, primary permeability decreases with the age of the rock (Freeze and Cherry, 1979). Typically, the primary permeability of intact, geologically "old" limestone, such as that present in the study area, is not significant enough to contribute to ground-water yields in wells (Freeze and Cherry, 1979). The hydraulic conductivity of "old" limestone is typically less than 10^{-7} feet/second (10^{-7} m/s).

Secondary permeability in both limestone and sandstone results from fracturing of the intact rock. In general, fracture intensities in these rocks are highly variable across the basin and may be dependent on proximity to major structures. In limestones, solution widening may enhance secondary permeability, but our conclusions regarding the extent of such a process in the study area are only preliminary (see Changes in Fracture Aperture).

Fracture Types and Characteristics

Ground-water flow along a single fracture is controlled primarily by the physical characteristics of the fracture, such as its aperture (width), persistence (length), planarity, roughness, and the presence or absence of minerals or other infilling material in the fracture. Fracture characteristics are, in turn, dependent on the origin of the fracture, rock properties, and the subsequent history of the fracture (reactivation, hydrothermal activity). Ground-water flow in fractured rock is controlled by additional factors such as fracture spacing (or intensity), attitude (trend and dip of fracture sets), and fracture connectivity.

Fracture types in the study area include joints, faults, bedding fractures (joints and faults that are parallel to bedding), and cleavage fractures. Joints are the predominant fracture type in the study area; however, faults dominate locally. Bedding fractures are prominent in some horizontally bedded formations. Cleavage is present in the Twin Creek Limestone and locally in the Thaynes Formation.

In general, fracture characteristics in a lithologically homogeneous unit (formation or member) do not vary by location, suggesting that rock properties dominantly control mesoscopic fracture characteristics and that local structural setting and deformational style (contractional versus extensional) are less important controls. For example, highly polished faults are the dominant type in the Nugget Sandstone in both the footwall and hanging wall of the Mount Raymond-Medicine Butte thrust. These faults are also ubiquitous where the Nugget Sandstone crops out along the Wasatch fault zone west of the study area, suggesting that the structural setting does not control the fracture characteristics. For this reason, mesoscopic fracture characteristics are described for each lithologically homogeneous unit in tables 2 and 3. In general, mesoscopic fractures are high angle, suggesting that the majority of fracturing occurred as a late phase of the regional deformation and/or many fracture sets were oriented such that later folding or tilting did not re-orient the fractures to low-angle dips.

Joints

Mesoscopic joint characteristics are summarized in table 2. Photographs showing typical joint characteristics in selected formations are included (appendix D). Most joints observed in outcrops range up to 5 meters (16 ft) in length (persistence) (see discussion in appendix A) and can be classified as common joints (Eberly, 1985) on the basis of their lengths. However, macrojoints (joints exceeding 5 meters [16 ft] in length) and microjoints (joints measuring only several centimeters in length) (Wise, 1964) were observed in some areas. Excluding bedding joints, most joints are both high-angle (dip exceeds 45 degrees) and are at a high angle to bedding. Subhorizontal sheeting is most common in the Keetley Volcanics and Weber Quartzite. Joints range from planar to undulating, smooth to rough, and fresh to mineralized (veins).

Faults

Scales of faulting range from microscopic to macroscopic, and faults range from normal to reverse, strike-slip to dip-slip, and high angle to low angle. The majority of our observations are related to mesoscopic faults, however, and their characteristics are summarized in tables 3 and 4. Photographs showing typical mesoscopic fault characteristics in selected formations are presented (appendix E). Macroscopic fault characteristics are generally more complex and will be discussed in a later section of this report.

The wide variety of faults are the result of both local

contractional and extensional deformation. Many mesoscopic faults are subsidiary faults adjacent to major thrust faults such as the Mount Raymond-Medicine Butte thrust, or to macroscopic, high-angle faults in the Park City mining district. Several prominent, distinct fault types are recognized in the study area as shown in table 4. In general, fault surfaces are mineralized, most commonly with calcite, quartz, or epidote, or stained with oxides and hydroxides of iron and/or manganese. Mesoscopic fault surfaces range from planar to highly curviplanar, and typically exhibit surface asperities (irregularities). In general, fault surface roughness, although variable, appears to be proportional to fault length.

Breccia and gouge zones: Breccia and gouge zones of various types are associated with more than one-third of all faults. Breccia and gouge represent incohesive material that is formed by fracturing and crushing of wall rock adjacent to a fault. Breccia contains more than 30 percent visible fragments of wall rock, whereas gouge is fine-grained material that contains less than 30 percent visible fragments. We used the term breccia-gouge when the percentage of visible fragments was either highly variable or indeterminable. Some breccias are partly to wholly relithified or healed, particularly in the Nugget, Park City, and Weber Formations.

The wide variety of breccia and gouge types owe their origins to differences in wall-rock types along faults. Variably thick, clay-bearing gouge or breccia is most common in the Twin Creek Limestone, but is also associated with some faults that offset limestone beds in the Thaynes Formation. Clay zones range from thin smears to over a meter (3 ft) in width. Non-clay-bearing breccia zones are typically wider than non-clay gouge zones and both are common in the Keetley Volcanics and Nugget Sandstone.

The permeability of breccia-gouge zones likely varies over a wide range. Breccia zones in sandstones may be highly permeable, particularly where the majority of the breccia is relatively coarse grained. Clay- and non-clay gouge likely have low permeability or are relatively impermeable dependent mostly on grain-size distribution (Morrow and others, 1984). Clay gouge zones likely have permeabilities ranging between 10^{-19} and 10^{-21} m^2 (10^{-18} and 10^{-20} ft^2) (Morrow and others, 1984). Finely pulverized, non-clay gouge may have similar to slightly higher permeability (Morrow and others, 1984; Jarvis, T., Weston Engineering, Inc., personal communication, 1996).

Subsidiary fault zones: Zones consisting of numerous closely or very closely spaced, interconnected faults are common adjacent to major faults. The subsidiary fault zones range up to several meters in width in the Preuss Sandstone and Nugget Sandstone, but are more typically less than 0.5 meter (1.6 ft) in width. Because of the enhanced connectivity of such fault zones, they would likely be relatively transmissive.

Bedding Fractures

Bedding fractures (figure 13) are common in most outcrops of sedimentary rock, and are prominent in layered rocks such as the Preuss, Twin Creek, Ankareh, Thaynes, Woodside, and Park City Formations. In these rocks, bedding fractures may be important in transmitting ground water parallel to bedding (Lachmar, 1993). Bedding fractures are common only near the top-of-rock in the Nugget Sandstone, and are rare to absent in the Keetley Volcanics and the Weber Quartzite. Outcrops are insufficient to assess the frequency of bedding fractures in Cretaceous formations. Fracture-spacing data suggest that the average bedding-fracture spacing in the Nugget Sandstone is slightly greater than in either the Twin Creek Limestone or Preuss Sandstone.

Bedding joints: Bedding joints are, in most cases, likely the result of unloading, and are best developed where bedding is roughly parallel to topography. Some evidence suggests that bedding-joint frequency decreases with depth. Differentiation between bedding joints and faults is essential prior to evaluating bedding-fracture spacing. Most bedding joints likely developed as lateral and vertical loads were removed during erosion. If bedding joints are mostly related to unloading then conceivably their average frequency may decrease (average spacing increase) with depth. However, because bedding faults are the result of tectonic processes (thrusting, flexural slip) their frequency is unrelated to depth.

We evaluated the relationship of bedding-joint spacing with depth in the Twin Creek and Nugget Formations at two separate sites. Factors not related to unloading may influence bedding-joint spacing near the top-of-rock, including variable bed thickness and rock types and the proximity to faults. The inclusion of random bedding faults in a sample also poses a problem. To reduce the influence of these factors we plotted average bedding-joint spacing. The average spacing appears to increase with depth in the Twin Creek Limestone (table 5 and figure 14). The correlation co-efficient for the simple linear regression shown in figure 14 approaches 0.9 and supports an assumption that a linear trend may exist between depth and spacing (Mendenhall and Sincich, 1992). However, extrapolating this trend to depths typical of water wells should be used with caution. Using the regression, we estimate the average bedding-joint spacing to be approximately 12 m (40 feet) at a depth of 650 feet (200 m). Although this may be a reasonable value, other factors as described above contribute to the spacing of bedding joints.

Average bedding-joint spacing in the Nugget Sandstone also appears to increase with depth (figure 15 and table 6). The spacing values are much more scattered than for the Twin Creek Limestone, and the simple linear regression has a low correlation coefficient. Most bedding joints in the Nugget Sandstone are likely a result of unloading, and thus it is reasonable to assume that bedding-joint spacing would increase with depth, except near faults. Bedding faults appear to be rare in the Nugget Sandstone.

Bedding faults: Bedding faults are present in most layered formations in the study area, but are notably prominent in the Twin Creek Limestone. Excluding their occurrence in the Twin Creek, bedding faults become more numerous to the south in the Park City mining district. Most bedding faults likely developed during thrusting or during flexural folding. Bedding faults are common in shale beds and, to a lesser degree, in limestone beds. Thin to thick clay gouge zones are commonly associated with bedding faults in limestone. Highly polished shale smears are typically associated with bedding faults in shale-rich units such as the Preuss Sandstone and the Mahogany Member of the Ankareh Formation.

Cleavage Fractures

Disjunctive, stylolitic cleavage (figure 16) is present in

Table 2.
Summary of mesoscopic joint characteristics.

Formation - Rock Type	Dip[1]	Aperture[1,2]	Persistence[1,3]	Planarity	Minerals	Other Infilling	Other
Tertiary intrusives	high angle	tight	low to very low	planar to curviplanar (?)	Fe- and Mn-oxides[4]; rare epidote-hematite	—	bleached wall rock
Keetley Vol.	high angle	tight	low to very low	planar	—	—	—
Undiff. Creataceous conglomerates	low to high angle	tight	very low	planar	—	—	micro-joints; confined to clasts
Undiff. Creatceous rocks	high angle	moderately open to tight	—	planar	Fe- and Mn-oxides[4]; calcite	—	common joints
Preuss Ss.	high angle	slightly open	very low except for bedding joints	planar	—	thin clay	—
Twin Creek Ls.	high angle	open to moderately open; typically <1 cm	very low except for bedding joints	planar	Fe-oxides[4]; calcite	clay	—
Nugget Ss.	high angle	open to moderately open; typically < 0.5 cm	generally low, but local medium or higher persistence joints present	planar	Fe- and Mn-oxides[4]; rare quartz and calcite[5]	—	—
Ankareh Fm. upper mbr.	high angle	tight	low to very low	planar	rare calcite and Fe-oxides[4]	—	bleached wall rock
Ankareh Fm. Garta Grit Mbr.	high angle	tight	generally low, but medium or higher persistence joints present	planar	—	—	—
Ankareh Fm. Mahogany Mbr.	high angle	moderately open	low to very low	planar	rare calcite and Fe-oxides[4]	—	bleached wall rock
Thaynes Fm. limestones and calcareous sandstones	high angle	moderately open to tight; typically <0.5 cm	varies, but greater than in Jt; bedding joint persistence generally medium or higher	planar	Fe- and Mn-oxides[4]; calcite	—	—

(*table 2 continued*)

Formation - Rock Type	Dip[1]	Aperture[1,2]	Persistence[1,3]	Planarity	Minerals	Other Infilling	Other
Woodside Shale mostly sandstone and siltstone	high angle	tight	very low	planar	calcite	—	slight oxidation
Park City Fm.	high angle	moderately open to tight; typically <0.5 cm	—	planar	Fe- and Mn-oxides[4]; calcite; quartz	—	—
Weber Qtz.	high angle	moderately open to tight	second only to Jn	planar to curviplanar	Fe- and Mn-oxides[4]; rare quartz	—	surface asperities common

[1] *Refer to glossary for explanation of dip, aperture, and persistence terms.*
[2] *Surface processes such as freeze-thaw and root wedging may be reflected in observations possibly resulting in a wider aperture than encountered in subsurface.*
[3] *Outcrop dimensions restrict maximum observed persistence.*
[4] *Also includes hydroxides such as goethite (Fe) and possibly manganite and psilomelane (Mn).*
[5] *Reported by Todd Jarvis of Weston Engineering, Inc. (verbal communication, 1996).*

Table 3.
Summary of mesoscopic fault characteristics.

Formation - Rock Type	**Dip[1]**	**Aperture or Infilling Width[1,2]**	**Persistence[1,3]**	**Planarity**	**Minerals**	**Gouge/Breccia Types[1]**	**Fault Type Classification[4]**	**Other**
Tertiary intrusives	—	—	—	—	—	—	—	none observed, but mapped by others
Keetley Volcanics	high-angle	moderately wide to wide	medium or higher	generally planar	epidote	undiff. gouge and breccia; zones range up to 10 cm	types 3 and 6	mostly normal faults
Undiff. Cretaceous conglomerates	—	up to 8 cm	—	—	calcite	undiff. gouge	—	very few observed
Preuss Ss.	high-angle	slightly open to tight	very low	—	—	shale smears	type 2	—
Twin Creek Ls.	high-angle	wide to open	generally low to moderate; many exceed 5 meters	planar to curviplanar	calcite	clay gouge and breccia zones	types 3 and 6	folds associated with faults with meter-scale offset
Nugget Ss.	high-angle	tight	low to very low	planar	quartz	breccia zones up to 2 m; sandy gouge and breccia zones; rare clay-size gouge	type 1 predominates	bleaching of wall rock; fault zones near major faults; intensely fractured fault zones
Ankareh Fm. upper mbr.	high-angle	varies	low	planar	—	some breccia and gouge zones, and shale smears	some type 2 and 3	—
Ankareh Fm. Gartra Grit Mbr.	high- to low-angle; most >30°	moderately open to tight	very low	—	Fe-oxides[5]	—	type 1	—
Ankareh Fm. Mahogany Mbr.	—	open	—	—	—	shale smears more common than in upper mbr.	some types 2 and 3	otherwise similar to upper mbr.

(*table 3 continued*)

Formation - Rock Type	Dip[1]	Aperture or Infilling Width[1,2]	Persistence[1,3]	Planarity	Minerals	Gouge/Breccia Types[1]	Fault Type Classification[4]	Other
Thaynes Fm. limestones and calcareous sandstones	high-angle	open to wide	generally low, but one-third are medium or higher	planar	calcite; Fe- and Mn-oxides[5]	clay gouge and breccia zones up to 1 m	types 3,4, and 6	—
Woodside Shale mostly sandstone and siltstone	high-angle	wide	medium or higher	planar	calcite	some clay-rich breccia and gouge zones; shale smears	some types 2 and 3	most observations from hanging-wall fold above thrust and likely anomalous
Park City Fm.	high-angle	wide	low	planar	calcite; quartz; Fe- and Mn-oxides[5]	partially to wholly relithified breccia zones	type 5 common	—
Weber Qtz.	high-angle	moderately open to tight	very low to medium	curviplanar	Fe- and Mn-oxides[5]; euhedral and massive quartz	some sandy gouge and breccia zones; wholly relithified breccia zones	types 1,4, 5 and 6, but 1 and 6 are predominant types	some intensely fractured fault zones

[1] Refer to glossary for explanation of dip, aperture, persistence, and other geologic terms.
[2] Aperture is defined as the distance between the adjacent wall rock and where infilling is present and is equivalent to the infilling width.
[3] Outcrop dimensions restrict maximum observed persistence.
[4] Refer to table 4 for descriptions of fault types.
[5] Also includes hydroxides such as goethite (Fe) and possibly manganite and psilomelane (Mn).

Table 4.
Summary of distinct fault types.

Fault Type	Formation
Type 1: highly polished, tight, striated	Nugget Ss., Ankareh Fm. (Gartra Grit Mbr.), Weber Qtz.
Type 2: highly polished shale smears	Preuss Ss., Ankareh Fm. (Mahogany Mbr.), Woodside Shale
Type 3: clay gouge zones	Twin Creek Ls., Thaynes Fm.
Type 4: non-clay breccia-gouge zones	Keetley Vol., Nugget Ss., Park City Fm., Weber Qtz.
Type 5: partially or wholly healed breccias	Nugget Ss., Park City Fm., Weber Qtz.
Type 6: mineralized	Keetley Vol., Twin Creek Ls.,Thaynes Fm., Park City Fm., Weber Qtz.

Table 5.

Simple linear regression of average bedding-joint spacing versus distance to top-of-rock in the Twin Creek Limestone.

Bedding-Joint Data	
Average Spacing cm	Distance to top-of-rock cm
6.6	50
9.8	100
11.2	135
16.6	160
12.2	185
15.8	210

Regression Information	
Standard Error of Y Estimate	2.154
Coeff. of Determination (r^2)	0.77
Coeff. of Correlation (r)	0.88
Number of Field Observations	30
Number of Average Values Input	6

Table 6.

Simple linear regression of average bedding-joint spacing versus distance to top-of-rock in Nugget Sandstone.

Bedding-Joint Data	
Average Spacing cm	Distance to top-of-rock cm
29	46
23	112
27	178
31	246
27	312
36	356

Regression Output	
Standard Error of Y Estimate	3.97
Coeff. of Determination (r^2)	0.35
Coeff. of Correlation (r)	0.59
Number of Field Observations	19
Number of Average Values Input	6

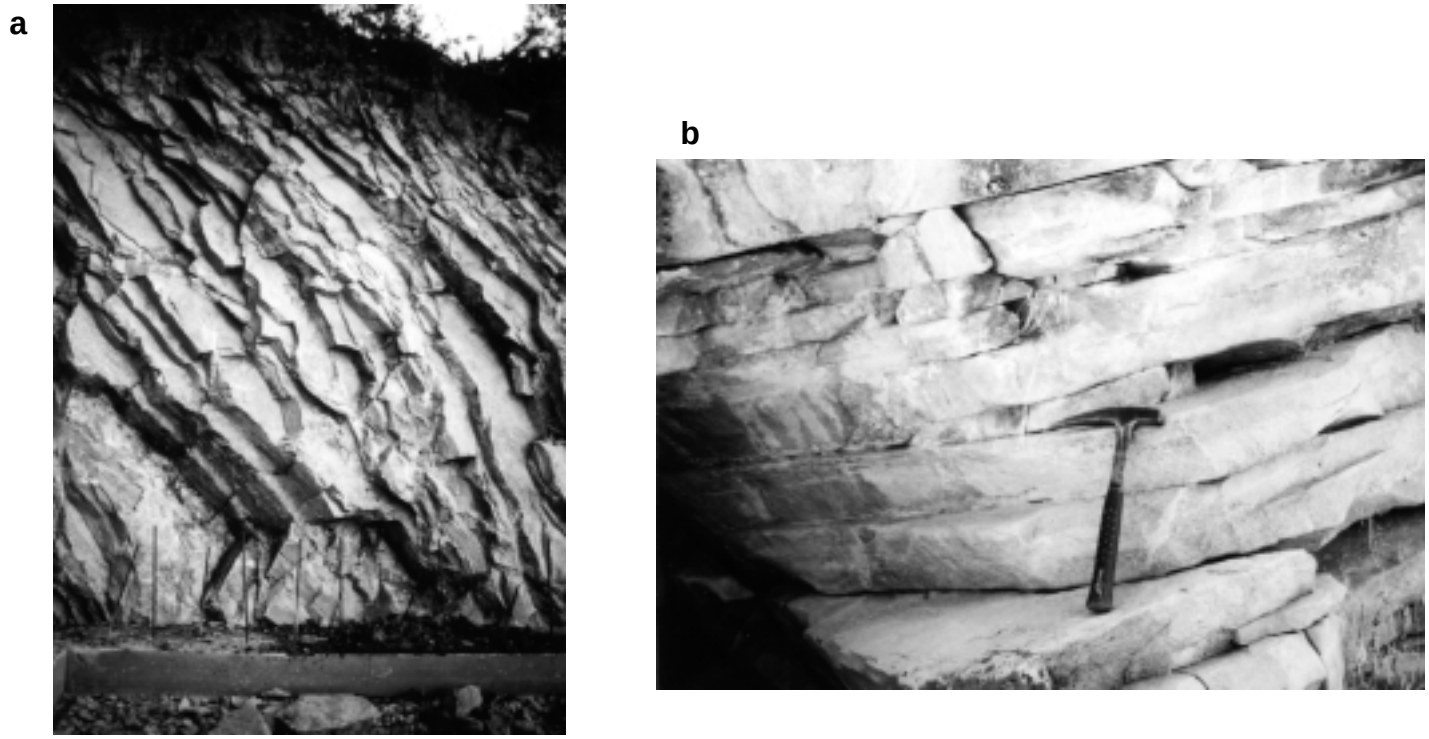

***Figure 13**. Bedding fractures. (a) Bedding joints and faults in the Twin Creek Limestone exhibiting medium persistence. Note that bedding-fracture spacing increases from top to bottom of the exposture. Also note very low to low persistence high-angle-to-bedding joints cut only single beds. Exposure located in foundation excavation in SE¼ section 9, T. 1 S., R. 3 E. (b) Bedding joints in the Nugget Sandstone. Exposure located in abandoned quarry in NE¼NE¼ section 6, T. 2 S., R. 4 E.*

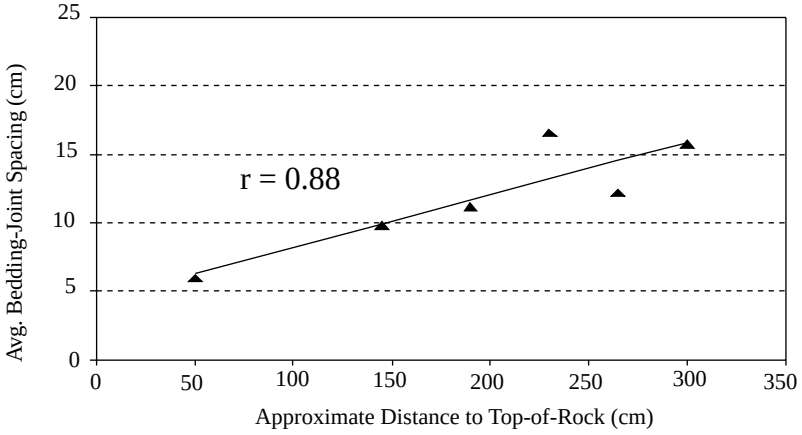

***Figure 14.** Average bedding-joint spacing in the Twin Creek Limestone. Plot shows that the spacing of bedding joints, inferred to be mostly the results of unloading, increases with depth. Data collected from exposure in figure 13A.*

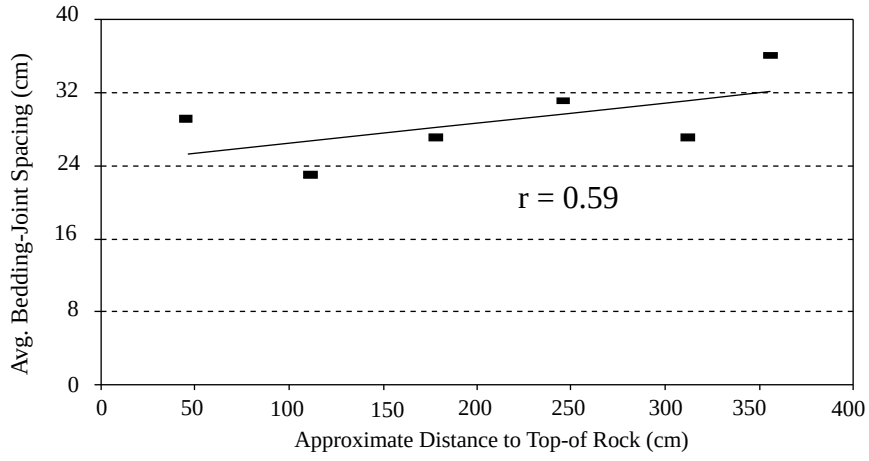

***Figure 15.** Average bedding-joint spacing in the Nugget Sandstone. Plot shows that although average spacing values are scattered, spacing generally increases with depth. Low correlation coefficient implies that other factors, such as variable bed thickness and rock composition, influence fracture spacing at this site. Data collected in abandoned quarry in NE¼ section 11, T. 1 S., R. 3 E.*

Figure 16. *Stylolitic cleavage in the Twin Creek Limestone. Note the characteristically irregular trace of the cleavage. View is to the north. Outcrop located in NW¼SW¼ section 28, T. 1 S., R. 4 E.*

the Rich and Leed Creek Members of the Twin Creek Limestone (Yonkee and others, 1992; Jarvis and Yonkee, 1993) and locally in the Thaynes Formation. The stylolitic cleavage is generally a continuous but highly irregular surface that has a distinct toothlike geometry in cross section. Very thin clay-rich, dissolution residual seams have been described along many stylolitic cleavage surfaces (Twiss and Moores, 1992). Cleavage ranges from closely to widely spaced in the Twin Creek. Fractures along the cleavage have been reported by Jarvis and Yonkee (1993) and observed at the top-of-rock as part of this study, but may not be present in the subsurface. Except where these surfaces are open as a result of subsequent extension (such as the "sprung" stylolites of Huntoon, 1993) or unloading (near the ground surface), cleavage planes are likely secondary to other fractures with respect to their ability to transmit ground water.

Fracture Characteristics in Subsurface Exposures

Although descriptions of underground fracture characteristics are scarce in the literature and on available maps, observations made during our visit to the Spiro Tunnel suggest that fracture characteristics at depth are similar to those at the surface. We observed numerous fractures in the Thaynes, Woodside, Park City, and Weber Formations at various locations along an approximately 13,500-foot-long (4,115 m) section of the Spiro Tunnel. In general, faults are the most persistent fracture type. In contrast, joints typically are relatively tight, and in thinly bedded formations (such as the Woodside Shale) cut only single competent beds. Bedding fractures appeared to be less common in the tunnel than in typical surface exposures, and are generally tight. Curviplanar surfaces and surface asperities are more typical of faults than joints, which tend to be mostly planar. Fracture intensity is highly variable within each of the four formations exposed in the tunnel. Fractures are rare or absent in some beds, whereas in others fractures are common and very closely spaced. In the lower part of the Woodside Shale, fractures are least common where gypsum seams and lenses are present, but ductile folds are prominent. Intensely sheared and fractured zones are almost always associated with faults.

Joints in Shales Versus Limestones and Sandstones

Based on observations at outcrops and in the Spiro Tunnel, some comparisons of overall joint characteristics can be made between shales and limestones and sandstones (including the Weber Quartzite). Such a comparison is partly the basis for the proposed hydrostratigraphy presented in the following section. Our ability to assess joint characteristics of shale units in outcrops was impeded by the paucity of outcrops or cuts in shale-dominated units. The entire sequence of the Woodside Shale was exposed in the Spiro Tunnel; however, other shale units, such as the mid-red shale of the Thaynes or shale sequences in the Preuss, Twin Creek, and Ankareh Formations, are poorly exposed and are not represented in the fracture data in tables 2 and 3.

In general, shales occur in horizontally bedded sequences in the Preuss, Twin Creek (Boundary Ridge and Gypsum Spring Members), Ankareh (upper and Mahogany members), Thaynes (mid-red shale member), Woodside, and Park City (middle phosphatic member) Formations. Joints in these rocks consist of bedding joints (dominantly near the ground surface) of medium or higher persistence and high-angle-to-bedding joints that have low to very low persistence normal to bedding (figure 17). Joints in shales commonly have thin clay infilling. In gypsiferous, ductile shale beds (lower part of Woodside Shale, Gypsum Spring Member, and possibly parts of Preuss Sandstone), joints may be absent or extremely rare.

We infer from these observations that parts of the shale-rich units may act as confining beds and be moderately to very impermeable. Whereas ground water may flow along persistent bedding joints, flow normal to bedding may be inhibited by the low joint persistence normal to beds, thus indicating a distinct anisotropy. Ductile, gypsiferous, joint-poor beds may have hydraulic conductivities approaching those of intact shale, as measured normal to bedding, and

Figure 17. *Very low-persistence high-angle-to-bedding joints in the Preuss Sandstone. Photograph shows that most high-angle-to-bedding joints (HATBJ) cut only single beds. Note that persistence of north-dipping, low-angle bedding fractures is much higher. View is to the southwest. Eraser pencil in foreground (arrow) shown for scale. Exposure in foundation excavation in SE¼ section 2, T. 1 S., R. 3 E.*

ranging between 10^{-12} and 10^{-10} feet/second (10^{-12} and 10^{-10} m/sec) (Freeze and Cherry, 1979). To place such a hydraulic conductivity in perspective, using a steep hydraulic gradient of 0.5 and a hydraulic conductivity of 10^{-11}, about 20,000 years would be required for ground water to flow through a 3-foot (1 m) thick gypsiferous shale bed.

In contrast, joints in limestones and sandstones are generally more through-going (figure 18). However, the persistence of high-angle-to-bedding joints commonly varies with bed thickness, particularly in limestone members in the Twin Creek Limestone. High-angle, persistent joints are common in the Nugget, Thaynes, Park City, and Weber Formations. These fractures likely transmit ground water across the stratigraphic sequence between shale confining beds.

Hydrostratigraphy

On the basis of these joint characteristics, we have established a preliminary concept of the hydrostratigraphy of the layered rock units in the study area (figure 19). We propose that stratigraphic ground-water compartments (SGWCs) consisting of fractured limestone and sandstone are separated by confining beds of dominantly shale which may have local hydraulic conductivities normal to bedding approaching those of intact rock. We refer to this separation of the generally permeable fractured-rock units by low permeability confining beds as stratigraphic compartmentalization. In the following section we present additional data that support this concept.

We recognize several important confining beds or units that likely inhibit ground-water flow normal to bedding. These include the phosphatic shale bed in the middle part of the Park City Formation, the lowermost Woodside Shale, the lower part of the Mahogany Member of the Ankareh Formation, the upper member of the Ankareh Formation, the Gypsum Spring Member of the Twin Creek Limestone, the Boundary Ridge Member of the Twin Creek Limestone, and shale beds in the Preuss Sandstone.

The intervening limestone and sandstone beds are SGWCs. These SGWCs may be part of one or more formations. For instance, the stratigraphically lowest SGWC in the study area consists of the Weber Quartzite and lower part of the Park City Formation beneath the phosphatic shale confining bed, whereas another SGWC is solely intraformational, consisting of the intervening limestone members of the Twin Creek Limestone (Sliderock and Rich) between the Boundary Ridge and Gypsum Spring confining beds.

Evidence for Stratigraphic Compartmentalization

Evidence that supports local stratigraphic compartmentalization as described above includes inflow data from the Spiro Tunnel and aquifer-test data for the Middle School and Park Meadows wells (J. M. Montgomery, 1991) and Summit Park No. 7 well (Weston Engineering, Inc., 1996a). Other researchers have recognized stratigraphic compartmentalization in fractured sedimentary rocks elsewhere in the Rocky Mountain area (Stone, 1967; Bruce, 1988; Huntoon, 1993; Al-Raisi and others, 1996). Stone (1967) observed that Triassic-Jurassic shales, evaporites, and siltstones in the Big Horn Basin serve as a regional confining layer even where sharply folded, thus isolating ground-water circulation in underlying limestones and sandstones from rocks above. Bruce (1988) described evidence that the Gypsum Spring Member acts as an effective confining bed even where overlying members of the Twin Creek Limestone are fractured.

Historical Ground-Water Conditions in Mine Workings

Historical accounts from mine workings suggest stratigraphic control on ground-water flow and illustrate the inability of ground water to flow through shale units. Both examples below illustrate that the basal Woodside Shale acts as a regional confining bed.

a

b

Figure 18. *Persistent joints in sandstone and quartzite beds. (a) Highly persistent joint in Nugget Sandstone exhibiting plumose structure (see glossary). View is to the north. Hammer shown for scale. Outcrop is located in SW¼ section 24, T. 1 S., R. 3 E. (b) High-angle, planar joints in Weber Quartzite. Outcrop is located in NE¼NE¼ section 21, T. 2 S., R. 4 E.*

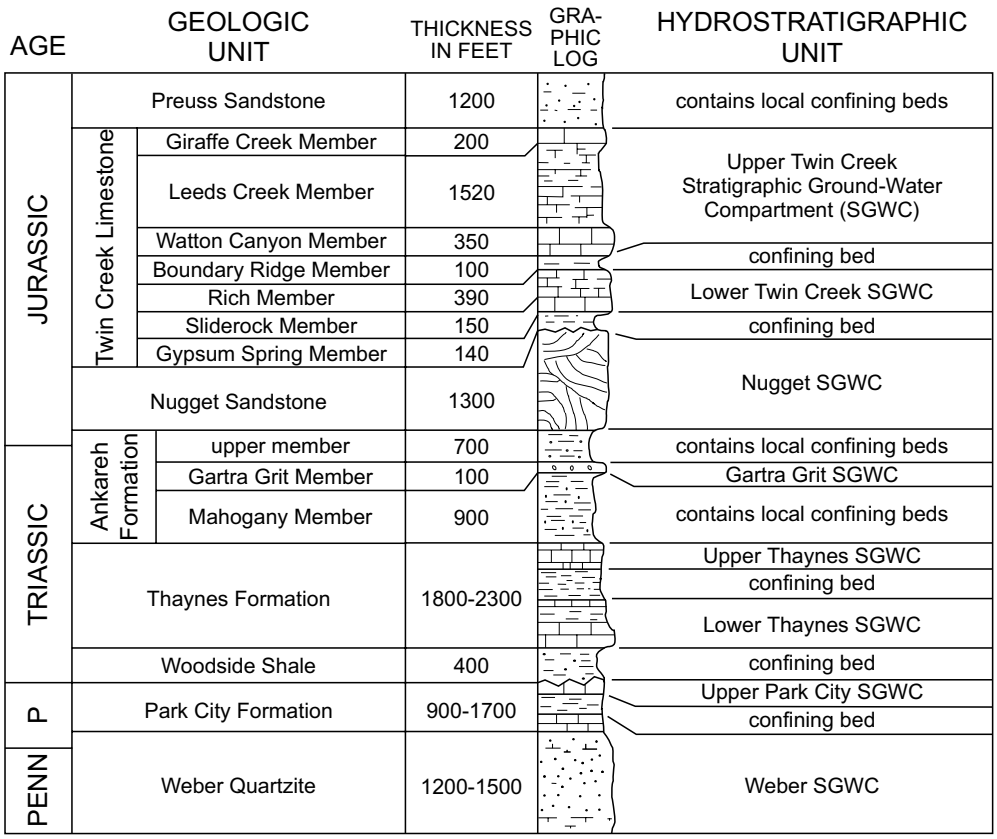

Figure 19. *Proposed hydrostratigraphy for the study area. Stratigraphic ground-water compartments consisting of fractured limestone and sandstone beds are separated by fracture-poor shale beds. Hydraulic conductivity of fracture-poor shale beds as measured perpendicular to bedding may approach that of intact shale.*

Bogan Shaft: Boutwell (1912) reported excessive water inflows during excavation of the Bogan Shaft (Silver King Consolidated; NW$^1/_4$ section 20, T. 2 S., R. 4 E.) through the Woodside Shale, whereas mine workings beneath the Woodside Shale in the Silver King mine were relatively dry (Boutwell, 1912; K. Gee, United Park City Mines Co., verbal communication, 1995). An examination of mining history in the central part of the Park City mining district reveals the importance of the basal part of the Woodside Shale as a regional confining bed.

Early in the history of the mining district, water inflows had hampered attempts to mine ore in the Weber Quartzite. At the Ontario Mine (figure 20) considerable efforts to dewater mine workings had been undertaken by the late 1880s. In 1888, the Ontario No. 2 drain tunnel was begun at the 1500-foot level (457 m) (depth) in the mine. Mining at the Silver King Mine, located to the northwest and upgradient of the Ontario mine workings, began in 1894 shortly after completion of dewatering efforts in the Ontario Mine. The Silver King Mine eventually penetrated the entire Park City Formation and the upper part of the Weber Quartzite. Dry conditions were encountered in the mine, and water actually had to be imported for use during mining. We interpret the dry conditions in the Silver King Mine to be the result of dewatering of the Weber SGWC by the Ontario No. 2 drain tunnel.

In 1903, excavation of the Bogan Shaft began slightly west-northwest of the crest of the ridgeline above the Silver King Mine. The shaft was collared in the basal Thaynes Formation, but penetrated only 38 feet of this unit before encountering the top of the Woodside Shale. Given that the Woodside Shale was known to be barren of ore (Boutwell, 1912), the location of this shaft is enigmatic, but excessive water inflows into the excavation indicate the effectiveness of the basal part of the Woodside Shale as a confining bed. The inability of the miners to cope with the water inflows as they attempted to deepen the shaft eventually caused them to abandon the mine without ever fully penetrating the Woodside Shale. Based on this and similar accounts, Boutwell (1912) described the formation's ability to "retain" water. We interpret the excessive water inflows in the Bogan Shaft as indicating that the gypsifersous and fracture-poor basal part of the Woodside Shale inhibited the downward flow of water into the underlying formations, which had been effectively dewatered as much as nine years earlier.

Spiro Tunnel: The Spiro Tunnel (plate 1) was completed in 1916 to drain mine workings in the western part of the Park City mining district. Table 7 shows that several of the major inflows reported while advancing the tunnel were at geologic contacts. Significant inflows occurred near the Thaynes/Woodside contact; in the uppermost lower third of the Woodside above the basal, gypsiferous bed; in the lower Park City Formation; and near the upper contact of the Weber. Water accumulation at the first two contacts was likely caused by the inability of ground water to flow downward through low-permeability shale beds.

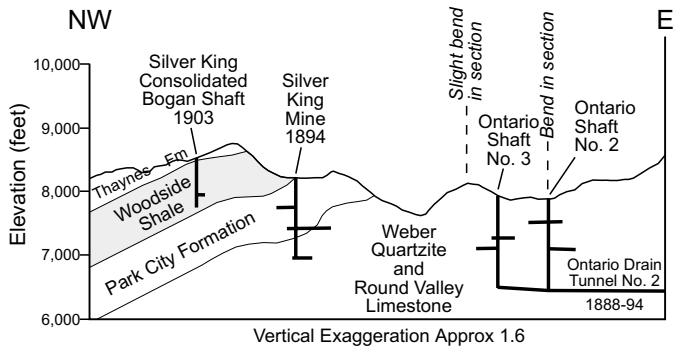

Historical Accounts of Dewatering Efforts and Ground-Water Inflows

1888-94: Construction of the Ontario Drain Tunnel No. 2 culminated attempts to dewater the Weber SGWC in the vicinity of the Ontario Mine. The Weber SGWC includes the lower part of Park City Formation.

1894: Silver King Mine began excavation. A shaft was eventually excavated to 1,300 feet (396 m), penetrating the Weber SGWC. Boutwell (1912) describes the mine as "dry," and water was imported for use in the mine. Dry condition indicates the Ontario Drain Tunnel No. 2, in combination with dewatering efforts at other nearby mine workings and tunnels, had effectively dewatered the Weber SGWC.

1903: Construction began on Bogan Shaft nine years after completion of Ontario Drain Tunnel No. 2. The shaft penetrated the lowermost Thaynes Formation and 800 feet (244 m) of the Woodside Shale. Water inflows plagued excavation attempts and the mine was eventually abandoned. Below the bottom of the shaft is the relatively unfractured, basal gypsiferous layer of the Woodside Shale which likely has very low permeability and inhibits the downward flow of ground water into underlying compartments. Water inflows continue today above the gypsiferous basal layer in the Spiro Tunnel located to the west of the Bogan Shaft.

Figure 20. *Schematic geologic cross section across the central Park City mining district showing sequential dewatering and ground-water inflow history.*

Table 7.
Summary of major ground-water inflows during excavation of the Spiro Tunnel, 1916.

Distance from portal (feet)	Formation/Contact	Seasonal Discharge (gallons/minute)
2,765	Thaynes/Woodside contact	58-198
6,600	Lower Woodside Shale	718-1,105
12,500	Lower Park City Formation	853-2,065
12,700	near Park City/Weber contact	3,188-4,040
14,246	Weber Quartzite	4,490-6,375

Middle School and Park Meadows Wells Aquifer-Test Results

Aquifer-test results (J.M. Montgomery, 1991) for the Middle School ($SW^1/_4SW^1/_4$ section 3, T. 2 S., R. 4 E.) and Park Meadows ($NE^1/_4NE^1/_4$ section 8, T. 2 S., R. 4 E.) wells indicate the lack of interaction between separate SGWCs isolated by confining beds. During the test both wells were pumped at high flow rates (1,100 gal/min [0.07 m^3/sec]). The Middle School well was pumped continuously for six days and both wells pumped simultaneously for an additional 24 hours. Four wells (Middle School, Park Meadows, Osguthorpe, and Mountain Top), all completed in fractured rock, were monitored during the test. The Middle School and Park Meadows wells are completed in the lower and upper parts of the Thaynes Formation, respectively, and are separated by a shale unit (possibly the mid-red shale) (figure 21). The Mountain Top well ($NE^1/_4SE^1/_4$ section 5, T. 2 S., R. 4 E.) is likely completed in the middle third of the Mahogany Member of the Ankareh Formation which directly overlies the upper part of the Thaynes Formation. The Mountain Top well is separated from the upper Thaynes SGWC by shale beds in the lower Mahogany Member and may be completed, at least in part, in the confining unit. The Osguthorpe well is likely completed in either the lowermost Thaynes Formation or uppermost Woodside Shale, and is thus in the lower Thaynes SGWC. Dority Spring, which is likely discharging from the upper Thaynes SGWC, was also monitored. Pumping from the Middle School well did not affect water levels in any of the wells except the Osguthorpe well, which is likely in the same SGWC. In addition, pumping from the Park Meadows well did not affect water levels in any of the other wells, but did significantly affect the flow rate at Dority Spring, which is in the same SGWC, to the point where no flow emanated from the spring.

The lack of hydraulic communication among wells/springs separated by confining beds indicates that ground water does not readily flow across shale beds. This appears to be true even where a set of joints normal to bedding is observed. Our fracture mapping in the area of the aquifer test indicates that the three prominent fracture sets include a northeast-striking set of high-angle faults and joints, east-northeast-striking north-dipping bedding fractures, and a north-northwest-striking (normal to bedding) set of high-angle joints. Whereas the latter set is a potential conduit for ground-water flow normal to bedding, these joints likely terminate at shale partings or ductile, fracture-poor shale beds and are likely tight or clay-infilled.

The aquifer-test results demonstrate the effectiveness of the confining beds to prevent short-term hydraulic communication between wells in separate SGWCs during continuous, high-flow-rate pumping. At present, the Middle School and

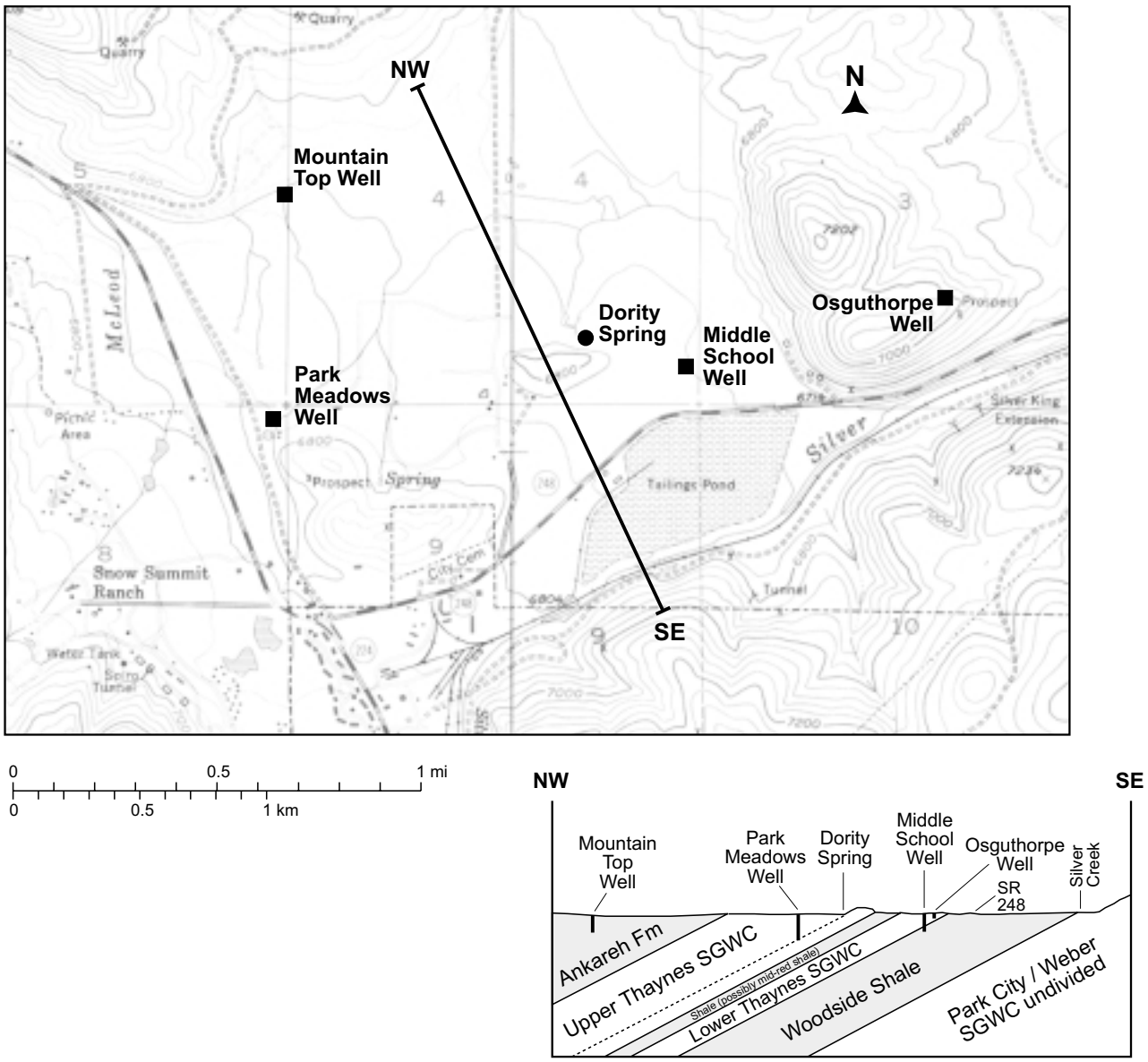

Figure 21. *Schematic geologic cross section showing stratigraphic ground-water compartments (SWGWCs) in the Thaynes Formation. Location of Dority Spring and welss monitored during aquifer test of Middle School well also shown. Testing showed hydraulic communication occurred only between wells and springs in the same SGWC. Location map shows that Dority Spring is closest to Middle School well; however, intervening shale bed prevents hydraulic communication between the well and spring. Location map modified from J.M. Montgomery (1991).*

Park Meadows wells are two of the most productive water-supply wells in the study area and capable of sustaining high flow rates with reasonable drawdown (safe yield). Most wells currently pump at much lower flow rates. Thus, where two low-flow-rate wells are separated by similar confining beds, little or no hydraulic communication is likely between the wells during continuous pumping.

The hydraulic communication between the Park Meadows well and Dority Spring and between the Middle School and Osguthorpe wells, respectively, suggests the existence of fracture networks consisting of interconnected bedding fractures and high-angle fractures in the upper and lower Thaynes SGWCs. Thus, we predict that future wells completed nearby in either SGWC may interfere with existing wells/springs in the same compartment, and the extent of the interference will be a function of well pumping rates and distance.

Summit Park Wells Numbers 7 and 8 Aquifer-Test Results

Recent aquifer-test results (Weston Engineering, Inc., 1996a) from newly completed Summit Park wells numbers 7 and 8 (figure 22) confirm that, at least locally, the Gypsum Spring Member of the Twin Creek Limestone acts as a confining bed. Well number 7 penetrated the lower part of the Twin Creek Limestone and upper part of the Nugget Sandstone (figure 23). Limestone beds in the lower Twin Creek Limestone are separated from sandstone in the Nugget Sandstone by mudstone and possibly gypsiferous mudstone beds in the Gypsum Spring Member. As drilling proceeded, ground water was initially encountered in the Twin Creek Limestone approximately 130 feet (40 m) below the ground surface. After completion of the well, following penetration of the Gypsum Spring Member and upper Nugget Sandstone,

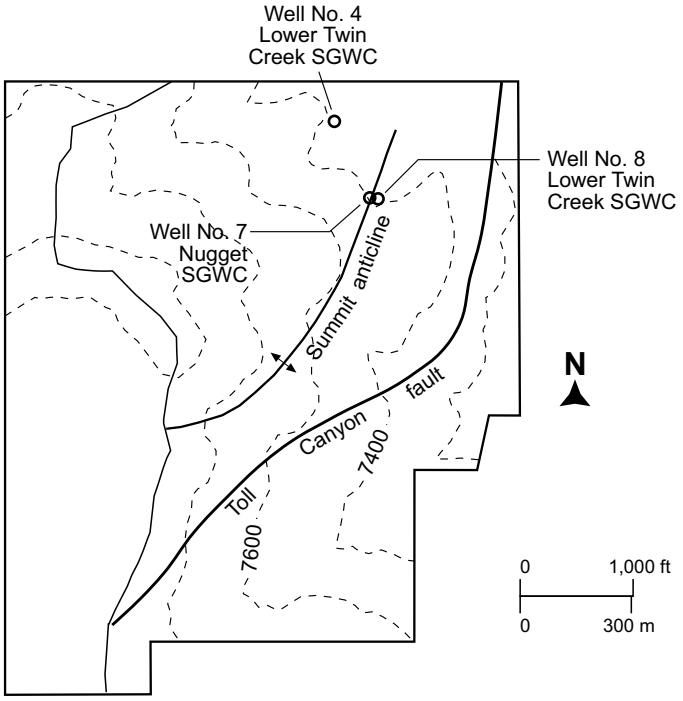

Figure 22. *Structural setting of Summit Park wells numbers 7 and 8. Wells are located on crest of Summit anticline (Weston Engineering, Inc., 1996a) partly because of the likelihood of enhanced fracturing at the structural location. The Toll Canyon fault (Crittenden and others, 1966) is located to east of wells and severs the SGWCs. Map modified from Weston Engineering, Inc. (1996a). Surface water divide (solid line) coincides with county line.*

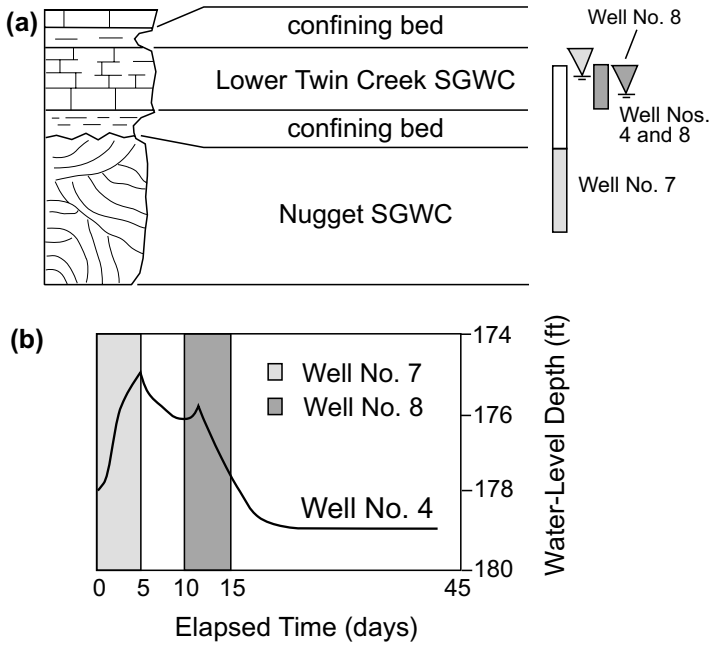

Figure 23. *Geology and aquifer-test results of Summit Park wells numbers 7 and 8. (a) Wells numbers 4 and 8 are completed in the lower Twin Creek SGWC and are isolated from well number 7 by the basal Gypsum Spring Member of the Twin Creek Limestone which acts as a confining bed. Water levels in well number 7 are higher than in adjacent well number 8 indicating confined ground water exists in the Nugget SWGC. (b) Ground-water level in monitoring well number 4 during pumping of wells 7 and 8 (time period of pumping shaded). Aquifer testing revealed no hydraulic communication between wells in separate SGWCs, however results suggest hydraulic communication between wells numbers 4 and 8 which are in the same SGWC.*

the static water level in the well rose to approximately 27 feet (8 m) below the ground surface. These observations indicate that ground water in the Nugget Sandstone is confined beneath the mudstones of the Gypsum Spring Member and that there is a head difference of approximately 100 feet (30 m) between the Lower Twin Creek SCWC and the Nugget SGWC. Data from a nearby observation well (number 4) completed in the Lower Twin Creek SGWC suggest that during a five-day constant-rate pumping aquifer test there was no hydraulic communication between wells completed in the Lower Twin Creek and Nugget SGWCs.

Following testing of well number 7, well number 8 was completed in the Lower Twin Creek SGWC above the Gypsum Spring Member. Data collected during a five-day constant-rate pumping aquifer test from well number 7 confirmed a lack of hydraulic communication between the Lower Twin Creek and Nugget SGWCs. Water-level data from well number 4 show an increasing rate of decline during the latter part of the aquifer test and suggest possible hydraulic communication between the two wells (numbers 4 and 8) completed in the Lower Twin Creek SGWC.

The local structural setting of wells numbers 7 and 8 (figure 22) confirms observations by Stone (1967) and Bruce (1988) that shale beds act as confining beds even where folded and overlying units are fractured. The well location was selected along the crest of a plunging anticline (Summit anticline) (Jarvis and Yonkee, 1993) because of the likelihood of through-going high-angle extensional fractures in such a structural setting (Huntoon, 1993). Water-yielding zones above and below mudstone beds in the Gypsum Spring Member appear to confirm the presence of such fractures. Nevertheless, the integrity of the Gypsum Spring Member as a confining bed appears to be preserved in this structural setting. Bruce (1988) indicated that the integrity of the Gypsum Spring Member as a regional confining bed may be locally broken as a result of the unit acting as a detachment during thrusting. This may imply that in some areas, such as west of Kimball Junction where lower Twin Creek Limestone underlies the Mount Raymond-Medicine Butte thrust, the member may not act as an effective confining bed.

Role of Macroscopic Faults in Regional Ground-Water Flow

Macroscopic faults, such as the Mount Raymond-Medicine Butte thrust, Toll Canyon fault, and Crescent fault, likely act in a complex manner as ground-water conduit-barrier systems (see Caine and others, 1993) (figure 24). Such fault zones likely have high permeability parallel to the fault, especially where brittle rock types comprise the wall rock, and low permeability perpendicular to the fault. These faults also sever (figure 25) the SGWCs described above, further segmenting the fractured-rock units (see Stacy, 1994).

Macroscopic Fault Zones as Ground-Water Conduit-Barrier Systems

Macroscopic faults are generally composite zones of deformation that may consist of one or more of the following:

1. irregular, branching, and anastomosing planes of discrete shear (Wallace and Morris, 1986);

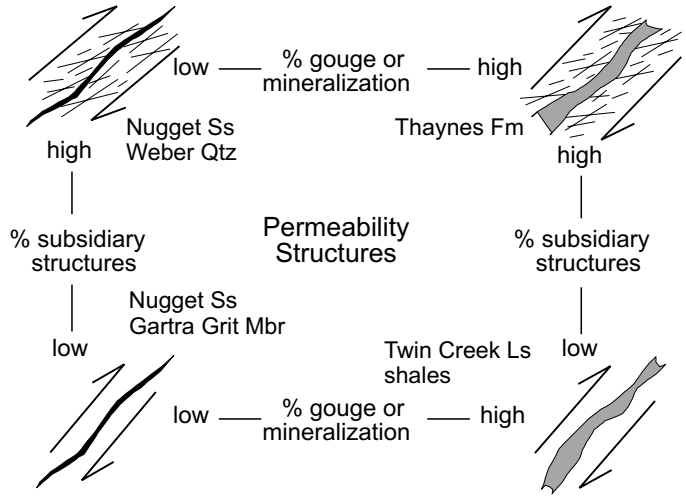

Figure 24. *Permeability structures associated with macroscopic fault zones. Caine and others (1993) recognized that macroscopic faults act as complex barrier-conduit systems and identified four end-member permeability structures. Faults consisting of only discrete shear planes (lower left) likely only nominally enhance rock permeability. Fault zones with interconnected subsidiary fracture zones or damage zones (upper left) likely enhance permeability and act as fault-parallel ground-water conduits. Fault zones with a high percentage of fine-grained gouge or mineralization (lower right) likely act as low-permeability boundaries and inhibit the flow of ground water perpendicular to the zone. The upper right illustration shows a composite case where faulting generates low-permeability fault gouge or subsequent mineralization forms a low-permeability zone, but a subsidiary fracture zone also exists adjacent to the fault, enhancing wall-rock permeability. Formations in which these permeability structures are common are listed. Diagram is modified from Caine and others (1993).*

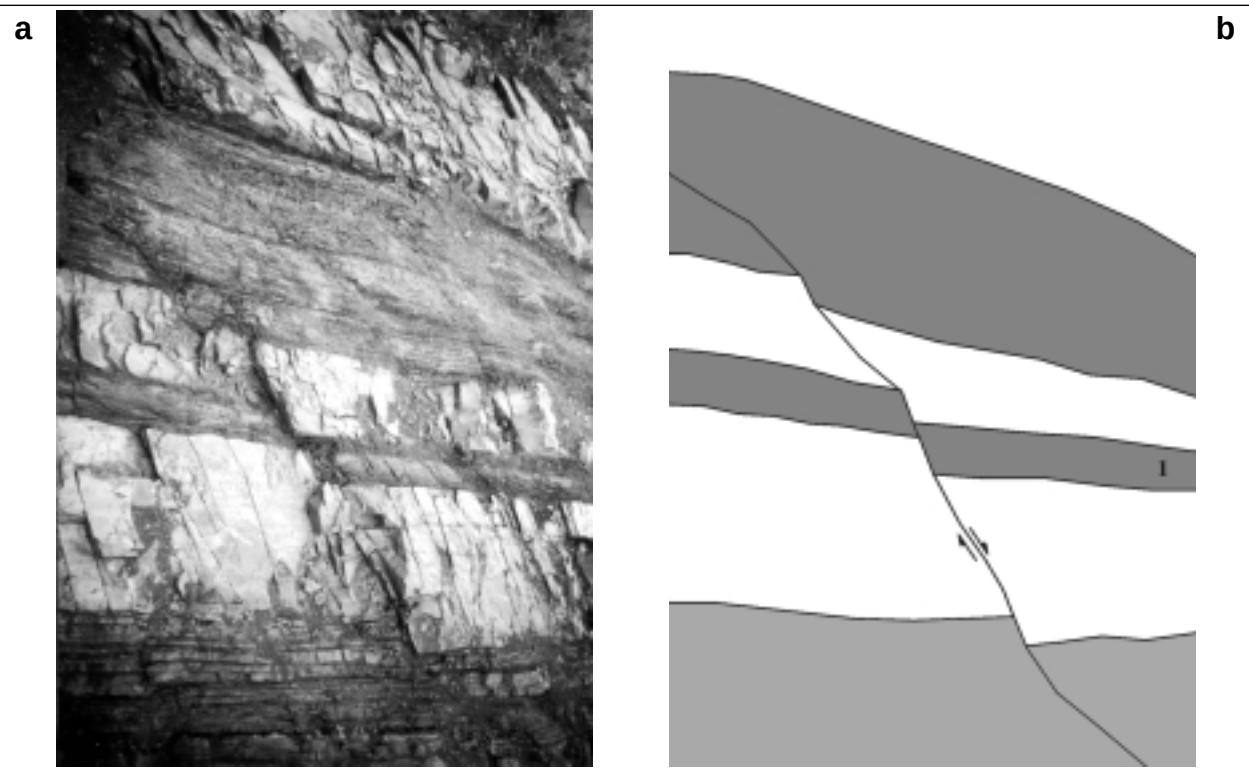

Figure 25. *Severing of a stratigraphic layer by a fault. (a) Photograph of shale (dark) and limestone layers cut by a fault. (b) Sketch of photograph shown in (a). Layer 1 is nearly completely severed by the fault. Severing of the layer inhibits the continuous flow of ground water along bedding fractures in the lower part of the layer.*

2. zone(s) of subsidiary fracturing in adjacent wall rock;
3. breccia or gouge zone(s) of variable composition and grain size, the width of which may be proportional to the total displacement (Engelder, 1974; Robertson, 1982; Wallace and Morris, 1986);
4. zones of ductile deformation (folding); and
5. mineralization.

The type of deformation in the surrounding wall rock is largely a function of rock type, thus hydraulic properties of the macroscopic fault zone will vary along strike and downdip. Where two different rock types are juxtaposed by faulting, hydraulic properties will vary across the fault zone. Subsidiary fracture zones are common in the Nugget, Thaynes, and Weber Formations and are likely wherever brittle rock types (sandstone and limestone) form the wall rock. As discussed previously, these fractures likely form ground-water conduits parallel to the fault. Breccia or gouge zones are likely in most macroscopic fault zones regardless of rock type, but may be locally absent. Clay gouge zones are common wherever limestone or shale forms the wall rock and such zones likely act as barriers to ground-water flow. Three macroscopic fault zones (Toll Canyon, Ecker Hill, and Snyderville) are exposed in roadcuts that enable these composite zones to be described in detail. In all three examples, a low-permeability core separates permeability-enhanced wall rock

from wall rock where permeability is negligibly enhanced or reduced.

Toll Canyon fault zone: In the SW$^1/_4$ section 11, T. 1 S., R. 3 E., the Toll Canyon fault zone is partly exposed in a roadcut. Intensely sheared and fractured Nugget Sandstone (figure 26) on the southeast is juxtaposed against the Mahogany Member of the Ankareh Formation on the northwest. The numerous, tight, interconnected fractures in the sheared Nugget wall rock form a subsidiary fracture zone that may act as a fault-parallel ground-water conduit on the southeast side of the fault (left side in figure 26). Although not exposed, the fault zone likely has a zone of relatively impermeable sheared shale (shale smear) or clay gouge derived from the Mahogany Member. Wall-rock deformation in the Mahogany Member possibly resulted in ductile deformation (see folds described adjacent to the Ecker Hill strand in the following section) and some fracturing. Fractures are likely tight, terminate against thin, ductile shale layers, are clay infilled, or have shale smears (faults), and thus have low permeabilities. Fault-zone characteristics likely reverse sides farther southwest where the fault juxtaposes the Nugget Sandstone on the northwest against the Twin Creek Limestone on the southeast.

Ecker Hill fault-strand zone: In the NE$^1/_4$ section 14, T. 1 S., R. 3 E., a probable strand of the Toll Canyon fault that we refer to as the Ecker Hill strand juxtaposes the Thaynes Formation on the northeast against the Mahogany Member on the southwest. Deformation in the Mahogany Member includes mesoscopic folding (figure 27) and fracturing. Mesoscopic faults typically have thin, highly polished shale smears. Tight, high-angle-to-bedding joints have very low persistence because they terminate against thin ductile shale layers in the Mahogany Member. Both fracture types in the Mahogany Member likely have low permeabilities. In contrast, fracture persistence is much higher in the Thaynes Formation. Persistent bedding fractures are prevalent near the fault, but generally become less frequent with increasing distance from the fault zone. Fractures in the Thaynes likely act as ground-water conduits parallel to the fault. The two formations are separated by a clay gouge zone (figure 28a) derived from the Thaynes Formation and a shale smear derived from the Mahogany Member (figure 28b) that likely have very low permeability.

Snyderville backthrust: In the NW$^1/_4$SE$^1/_4$ section 36, T. 1 S., R. 3 E., a roadcut exposes a southeast-dipping fault that was interpreted as the Mount Raymond-Medicine Butte thrust by Crittenden and others (1966), but has been reinterpreted as a backthrust (B. McBride, verbal communication, 1996). We refer to this fault as the Snyderville backthrust. The fault juxtaposes Nugget Sandstone on the southeast against the lower part of the Twin Creek Limestone on the northwest. Intensely sheared, fractured, and altered Nugget wall rock (figure 29) likely enhances permeability and acts as a ground-water conduit parallel to the fault. Although the Twin Creek Limestone is fractured adjacent to the fault, fracture intensity is an order of magnitude less than in the Nugget Sandstone. Low-permeability calcite-infilled veins are common. A zone of sheared shale separates the Nugget Sandstone from the limestone in the Twin Creek and likely acts as a boundary to ground-water flow normal to the fault.

Severing of Stratigraphic Ground-Water Compartments

Macroscopic faults sever the SGWCs described in previous sections of the report, subdividing these into discrete ground-water compartments (GWCs) (see Stacy, 1994). Severing of stratigraphy is recognized in compartmentalization of hydrocarbon accumulations (Bergosh and others, 1982; Al-Raisi and others, 1996) and ground-water aquifers (Huntoon, 1993; Stacy, 1994). Recent research (Gee, 1994; Weston Engineering, Inc., 1996a) suggests that many GWCs in the study area are bounded by macroscopic faults.

Figure 26. *Subsidiary fault zone in the Nugget Sandstone adjacent to the Toll Canyon fault. Interconnected subsidiary faults likely act as a ground-water conduit parallel to the fault (located to right of photograph). View is to the southwest. Hammer is shown for scale. Outcrop is located in SW$^1/_4$ section 11, T. 1 S., R. 3 E.*

Figure 27. *Ductile folding in the Mahogany Member of the Ankareh Formation adjacent to the Ecker Hill fault strand. Isoclinal fold in footwall of thrust and lack of persistent fractures indicate that ductile deformation dominated in this member during thrusting. View is to the east. Hammer is shown for scale. Outcrop is located in NE¼ section 14, T. 1 S., R. 3 E.*

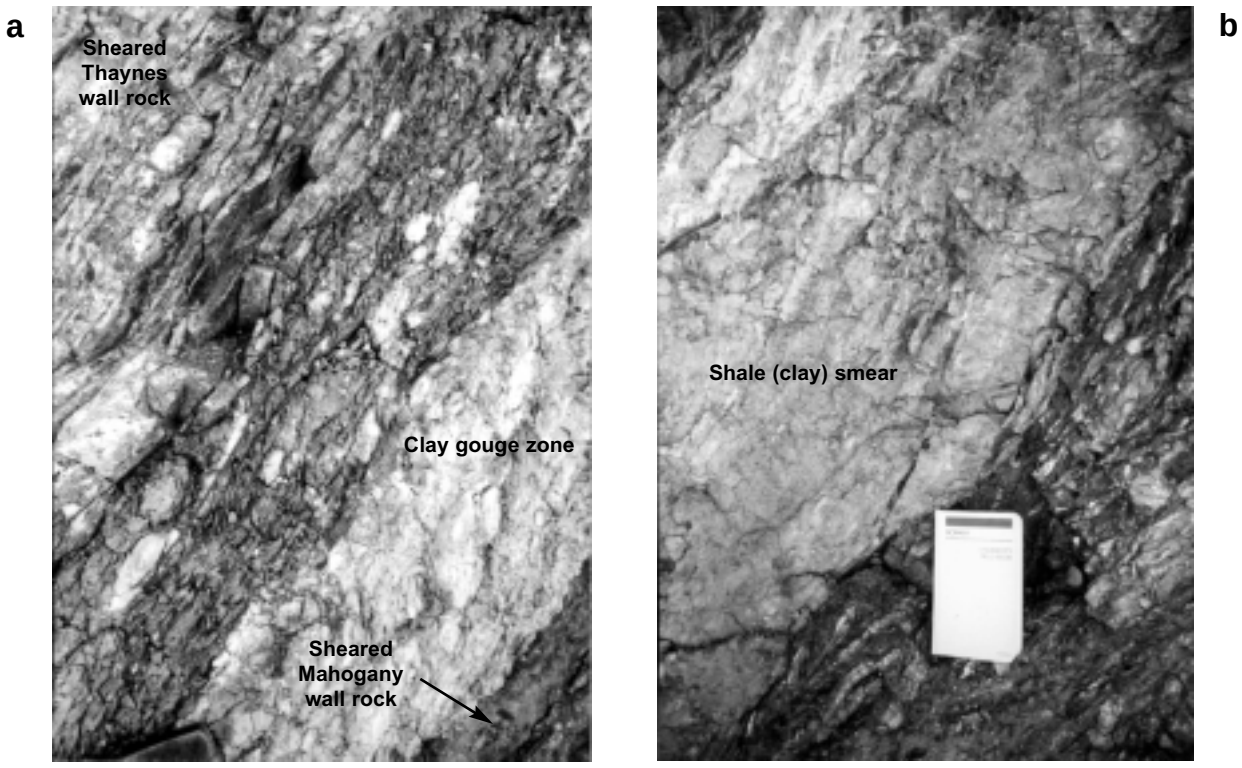

Figure 28. *Low-permeability clay-gouge zone and shale smear. (a) Clay-gouge zone is derived from Thaynes wall rock in hanging wall (left side) of fault zone. Part of hammer shown for scale. (b) Shale (clay) smear derived from Mahogany Member of Ankareh Formation in footwall (right side) of fault zone. Field book shown for scale. Clay gouge zone and shale smear form low-permeability core of fault zone. Views are to the east. Outcrop is located in NE¼ section 14, T. 1 S., R. 3 E.*

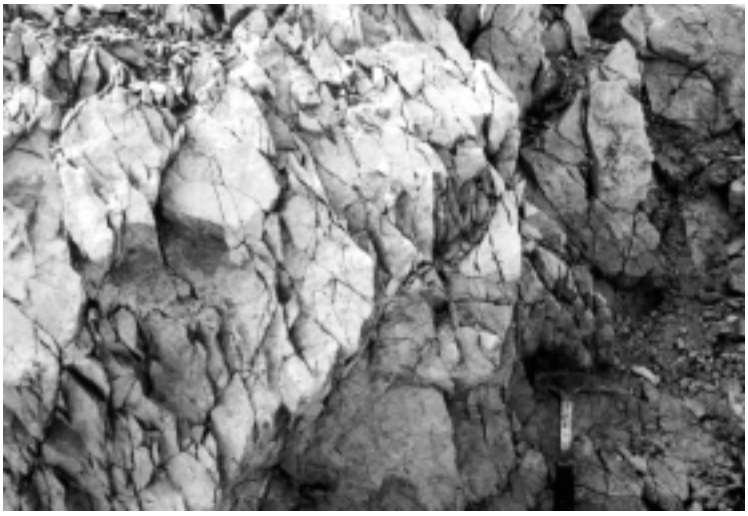

Figure 29. *Intensely sheared and fractured Nugget Sandstone adjacent to the Snyderville backthrust. These subsidiary fractures likely enhance permeability and form a ground-water conduit parallel to the backthrust. Outcrop is located in SE¼ section 36, T. 1 S., R. 3 E. Hammer shown for scale. View is to the southeast.*

Ground-Water Inflow and Dewatering Problems Associated with Excavation of the Anchor Shaft as Evidence for Ground-Water Compartments

The existence of ground-water compartments in the study area can be inferred from historical accounts of the excavation of the Anchor Shaft (Boutwell, 1912) in combination with subsurface geologic information (Gee, 1994). The Anchor Shaft is in the upper part of Empire Canyon (SW¼ section 29, T. 2 S., R. 4 E.). The shaft is northwest and in the hanging wall of the northwest-dipping Ontario-Daly West fault zone (figure 30). The Ontario-Daly West fault is a normal fault and rocks in the hanging wall (northwest side) are dropped down relative to rocks in the footwall side (southeast). The fault completely severs the Woodside Shale and members of the Thaynes and Park City Formations. As a result, the fault juxtaposes the upper Thaynes member (on the northwest) against the lower Thaynes member and Woodside Shale (on the southeast) near the ground surface. Thus, the Upper Thaynes SGWC is juxtaposed against the Lower Thaynes SGWC.

Historical accounts also suggest that the Ontario-Daly West fault zone acts as a composite barrier-conduit system. Similar macroscopic faults that sever limestone formations, such as the Thaynes and Park City Formations, form low-permeability clay gouge cores with enhanced permeability subsidiary fracture zones in adjacent wall rock. The presence of the Woodside Shale in the footwall of the uppermost part of the fault zone increases the likelihood that a low-permeability core exists caused by shale (clay) smears.

Boutwell (1912) indicated that as excavation of the shaft proceeded toward the fault through the Upper Thaynes SGWC, ground-water inflows increasingly plagued operations. Several factors likely contributed to the inflows, including the probable steep hydraulic gradients in the upper part of Empire Canyon above the shaft site and enhanced permeability associated with the subsidiary fracturing near the fault. The shaft was excavated only to a depth of about 600 feet (180 m) before ground-water inflows caused the miners to abandon operations. At one point the shaft filled nearly to the ground surface with water.

In an effort to dewater the shaft an ambitious drain tunnel was excavated. The tunnel, known as the Judge Tunnel, was started in 1888, approximately 6,600 feet (2012 m) downslope of the shaft. The tunnel was driven through the Weber, Park City, and Woodside Formations and the lower part of the Thaynes Formation. In addition, the tunnel crossed the Ontario-Daly West fault zone about 500 feet (152 m) downslope (northeast) of the shaft. The tunnel was driven to a location about 600 feet (183 m) directly beneath the bottom of the Anchor Shaft (1 on figure 30), but failed to drain the shaft.

The failure of the Judge Tunnel to drain the shaft demonstrates both stratigraphic and structural ground-water compartmentalization in the Empire Canyon area. Stratigraphic compartmentalization is demonstrated by the failure of the shaft in the upper Thaynes SGWC to drain despite the tunnel penetrating the lower Thaynes SGWC. The two SGWCs are separated by the mid-red shale member of the Thaynes Formation which inhibits the flow of ground water between the two compartments. In addition, the tunnel failed to drain the shaft despite its crossing the Ontario-Daly West fault zone. An explanation for this failure is that the inferred subsidiary fracture zone adjacent to the fault in the upper Thaynes SGWC is not present in the intervening mid-red shale member, and thus does not allow ground water to flow downdip along the fault. Although a similar subsidiary fracture zone is also likely in the lower Thaynes SGWC, these zones are separated by the mid-red shale member and the low-permeability fault-zone structures likely present in the shale-dominated member.

Subsequent attempts to dewater the shaft further demonstrate compartmentalization of ground water. A borehole was drilled from the bottom of the shaft toward the tunnel (2 on figure 30). The borehole was aborted at a depth of 300 feet (91 m) below the bottom of the shaft when a fire burned down the drill rig. The borehole likely penetrated the Park City Formation, but probably terminated in the phosphatic shale member that acts as a confining bed. A second borehole was drilled upward from the tunnel to within 50 feet (15 m) of the bottom of the shaft (3 on figure 30), but also failed to drain the shaft. The shaft failed to drain most likely because this borehole failed to penetrate the low-permeability core of the fault zone. Frustrated, but not defeated, the miners raised an explosive charge (torpedo) to the top of the second borehole and detonated it in an attempt to enhance

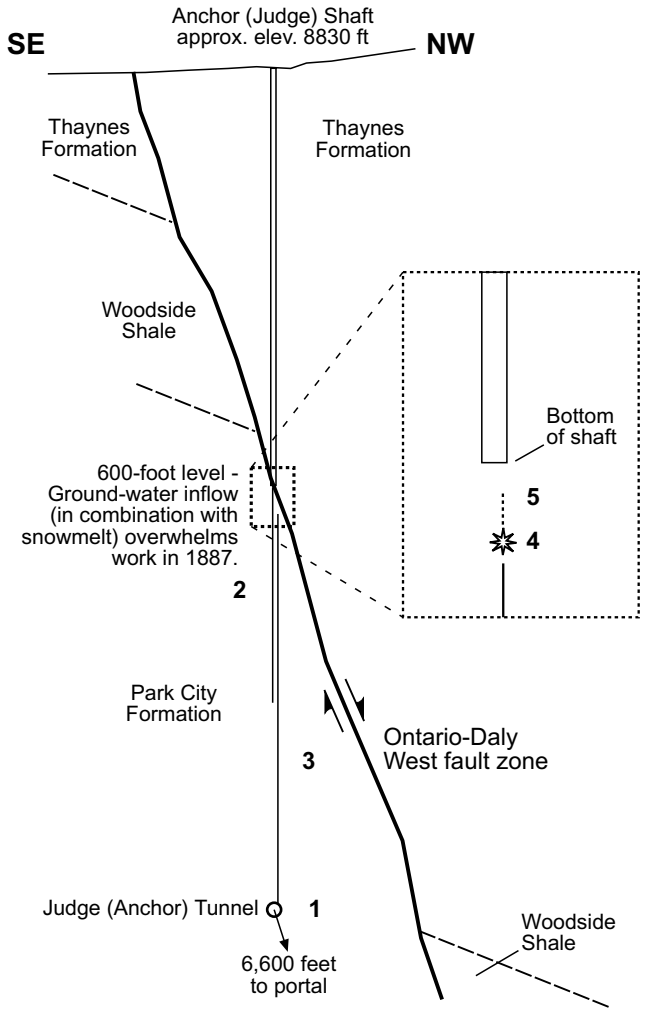

Figure 30. *Schematic geologic cross section of the Anchor Shaft. Historical accounts and subsurface geology based on Boutwell (1912). Geology at the 1,200-foot level (366 m) (Judge Tunnel) modified from Gee (1994). Near-surface geology modified from Baker and others (1966). See text for explanation.*

fracturing and permeability in the intervening 50 feet (15 m) between the top of the second borehole and the bottom of the shaft (4 on figure 30). This effort also failed to drain the shaft, possibly because zones of clay remained between the blast-fractured rock and the bottom of the shaft. Finally, the shaft was drained when the borehole was drilled upward, despite some inherent danger to miners in the tunnel below, to within 20 feet (6 m) of the bottom of the shaft (5 on figure 30). The extended borehole likely penetrated the low-permeability fault zone core and intercepted transmissive fracture zones that crossed the shaft.

Discrete Ground-Water Compartments

Twin Creek Limestone

We recognize a minimum of four separate Twin Creek GWCs (plates 3, 4, and 5). Three of these could be further subdivided on the basis that the Boundary Ridge Member divides the Twin Creek Limestone into upper and lower SGWCs. We are unable to show this subdivision, however, because the detailed mapping of the Twin Creek Limestone members was beyond the scope of our work:

1. Summit Park-Jeremy Ranch GWC: this GWC (plate 3, cross sections E-E' and F-F') includes all members overlying the Gypsum Spring Member (figure 2) that crop out, or are present in the subsurface, between the western boundary of the study area and the eastern edge of Jeremy Ranch. The GWC may be subdividable into three additional separate compartments bounded by the Toll Canyon fault.
2. Kimball Junction GWC: this GWC (plate 3, cross section D-D') includes all members overlying the Gypsum Spring Member that crop out, or are present in the subsurface, between Hi Ute Ranch and Silver Creek Junction. The Mount Raymond-Medicine Butte thrust bounds the aquifer to the south, whereas an unnamed fault (Crittenden, 1974; Bryant, 1990) bounds it on the north.
3. Bear Hollow GWC: this GWC (plate 3, cross section C-C') includes the thin belt of Twin Creek Limestone that overlies the Nugget Sandstone and is bounded on the southeast by the Snyderville backthrust (the Mount Raymond thrust of Crittenden and others, 1966). The GWC consists mostly of the lower part of the formation (Lower Twin Creek SGWC) particularly in the Kimball Junction area.
4. Parleys Park GWC: this GWC (plate 4) includes the belt of Twin Creek Limestone that flanks the eastern and southern Parleys Park area, and the area south and southeast of the Silver Summit subdivision. We speculate that the entire thickness of the formation crops out southeast of Silver Summit. Mapping by others (Crittenden and others, 1966; Crittenden, 1974; Bryant, 1990) suggests that the upper part may be faulted out by the Mount Raymond-Medicine Butte thrust or an imbricate strand west of the eastern edge of Parleys Park. However, we favor the alternate interpretation of the thrust location (Lamerson, 1982; McBride, 1996, verbal communication) in which the upper part of the Twin Creek Limestone is not faulted out. The GWC likely continues east from the Silver Summit area beyond the study-area boundary, but may be covered by a substantial thickness of Keetley Volcanics or interrupted by intrusive igneous rocks.

Nugget Sandstone

We recognize a minimum of five discrete Nugget GWCs (plates 3, 6, and 7).

1. Summit Anticline GWC: this GWC includes the Nugget exposed in the core of the Summit anticline (Jarvis and Yonkee, 1993, figure 9; Weston Engineering, Inc., 1996a) and that underlies the Twin Creek Limestone. The upper branch of the Toll Canyon fault bounds the aquifer on the east and south. The GWC is overlain by the Gypsum

Spring Member of the Twin Creek Limestone in the majority of the Summit Park area.

2. Summit Syncline GWC: this GWC (plates 3, cross section F-F′) underlies the Twin Creek Limestone in the southern part of Summit Park, but its recharge area crops out farther to the south along the southeastern flank of the Summit syncline (Jarvis and Yonkee, 1993, figure 9). The lower (main) branch of the Toll Canyon fault bounds the GWC on the north.
3. Gorgosa GWC: this GWC (plate 3, cross sections D-D′ and E-E′) includes the arcuate belt of Nugget Sandstone that crops out near Gorgosa (Pinebrook). The GWC is located in the hanging wall of the Toll Canyon fault. It is overlain by the Gypsum Spring Member north of Kimball Junction and northwest of Pinebrook and bounded by an unnamed fault (Crittenden, 1974; Bryant 1990) on the north. The GWC is separated from the Summit Anticline GWC to the west by the upper branch of the Toll Canyon fault (Jarvis and Yonkee, 1993; Weston Engineering, Inc., 1996a) and from the Summit Syncline GWC by the lower branch of the Toll Canyon fault. At Kimball Junction, it is bounded on the south by the Mount Raymond-Medicine Butte thrust.
4. Willow Draw Anticline GWC: this GWC (plate 3, cross section C-C′) includes the Nugget Sandstone exposed in the core of the Willow Draw anticline and that underlies the Gypsum Spring Member northwest of the Snyderville backthrust. The GWC is severed from the Nugget exposed at Iron and Quarry Mountains by the backthrust, except possibly in the uppermost upland recharge area to the southwest.
5. Iron Mountain - Round Valley GWC: this GWC (plate 3, cross section C-C′) includes the folded belt of Nugget exposed between White Pine Canyon and the Silver Summit area. The GWC may continue east-northeast to the study-area boundary, but may be covered by a substantial thickness of Keetley Volcanics or interrupted by intrusive igneous rocks.

Thaynes Formation

We recognize a minimum of five discrete Thaynes GWCs (plates 3, 8, and 9). These GWCs can be further subdivided on the basis that the mid-red shale member separates each into upper and lower compartments. We are unable to show this subdivision, however, because the detailed mapping of the Thaynes Formation members was beyond the scope of our work:

1. Twomile Canyon GWC: this GWC (plate 3, cross section E-E') includes the folded belt of Thaynes Formation that crops out south and east of Twomile Canyon. The Ecker Hill strand of the Toll Canyon fault (see description above) bounds the aquifer on the north. The aquifer is overlain by the Mahogany Member of the Ankareh Formation in the nose region of the Twomile Canyon fold. The overturned west limb of the fold places the Thaynes over the Ankareh, at least at shallow depths.
2. Ecker Hill GWC: this GWC (plate 3, cross section E-E′) includes the Thaynes Formation where it crops out at Ecker Hill. The Toll Canyon fault and the Ecker Hill strand bound the aquifer on the north and south, respectively. The GWC is underlain by the Woodside Shale on the southeast.
3. Hi Ute GWC: this GWC (plate 3, cross sections D-D′ and E-E′) includes the belt of Thaynes Formation underlying the unconsolidated deposits east of Pinebrook. Faults bound the GWC on the south and east. The GWC is overlain by the Mahogany Member of the Ankareh Formation.
4. Park Meadows GWC: this GWC (plate 3, cross sections A-A′, B-B′, and C-C′) consists of the folded belt of Thaynes Formation that extends from the eastern part of the study area to the West Monitor Flats area. Evidence for subdivision of this GWC into upper and lower SGWCs was described previously.
5. Frog Valley GWC: this GWC (plate 3, cross section A-A′) consists of the lower part of the Thaynes Formation that crops out to the east of the Frog Valley thrust. This GWC is underlain by the Woodside Shale and overlain, in some areas, by the Keetley Volcanics and Quaternary unconsolidated deposits.

Weber Quartzite

We recognize a minimum of two discrete Weber GWCs (plates 3, 10, and 11). Although the Weber SGWC includes the lower part of the Park City Formation below the phosphatic shale bed, we show the top of the Weber GWCs as the upper contact of the Weber Quartzite because detailed mapping of the Park City Formation members was beyond the scope of our work.

1. Park City Anticline GWC: this GWC (plate 3, cross sections A-A′, B-B′, and C-C′) includes the Weber Quartzite where it crops out in the core of the Park City anticline north of the Ontario No. 2 drainage tunnel. The Weber Quartzite is overlain by the Park City Formation north and west of Park City. The Frog Valley thrust bounds the GWC on the east, and faulting has increasingly severed the Weber SGWC to the north. This has resulted in structural separation of the Park City Anticline GWC from the Queen Esther GWC.
2. Queen Esther GWC: this GWC (plate 3, cross sections A-A′ and B-B′) includes the Weber Quartzite in the footwall of the Frog Valley thrust. The GWC is at relatively shallow depths along the southeastern edge of the study area, but becomes increasingly deeper to the northeast of Deer Valley.

Safe Yields

The discrete GWCs vary considerably in extent, thickness, physiography, and hydrology. These factors will influ-

ence the maximum safe yield. Whereas some of the larger GWCs have large recharge areas, other have small recharge areas. Still others may be recharged mostly by flow of ground water along bounding faults (Queen Esther GWC) or by infiltration from overlying saturated unconsolidated deposits (Hi Ute GWC). Whereas some of these GWCs may supply large safe yields over the long term, those of smaller extent may supply only small safe yields over the long term. Such a wide variability in gross characteristics implies that each of the discrete GWCs may require separate long-term management plans to prevent exceeding safe yield.

Structure and Thickness

To assist engineers, hydrogeologists, well drillers, public officials, and others interested in siting future wells in the discrete GWCs, we have constructed cross sections (plate 3) and structure-contour and isochore (vertical thickness) maps (plates 4 through 11) of the Twin Creek, Nugget, Thaynes, and Weber Formations (refer to discussion regarding actual GWC boundaries in previous sections). Some uncertainty is implicit in the maps due to the lack of data that constrain the geometry of the formations in many areas. We did not extend the maps into most upland recharge areas because the present focus of water-resource development is mostly in lowland discharge areas. We also did not attempt to extend the maps into the Park City mining district due to our lack of detailed knowledge in this complexly faulted area (Barnes and Simos, 1968). Proprietary, detailed geologic data available from the numerous mine workings could, in the future, be used to prepare maps that would supersede our reconnaissance evaluation.

The structure-contour maps (plates 4, 6, 8 and 10) show the elevation of the upper contact of each formation. Because structure contours are strike lines, the maps also show bedding attitude in the uppermost part of the formations and allow interpretation of the overall structure. Note that because of faulting and erosion, the upper contact is not always present and an incomplete section of the formation may exist (Ecker Hill GWC and Bear Hollow GWC). The isochore maps (plates 5, 7, 9, and 11) show the vertical thickness of each formation. The elevations and thicknesses shown on these maps are approximate. The maps are suitable for estimating purposes, but are not intended to be a substitute for site-specific detailed geologic studies prior to selecting a water well location. Further description of how to use the maps in selecting well locations is presented in appendix F.

Fracture Domains

Fracture domains are areas with distinct fracture patterns (Mabee and others, 1994) that differ significantly from surrounding areas. Fracture domain boundaries are commonly geologic structures or contacts, but in some cases (such as boundaries in the Keetley Volcanics) they do not correspond to a known geologic feature. In most cases, boundaries are somewhat transitional even where a well-defined geologic feature delineates the boundary. Members of one particular fracture set within a domain are commonly found across the boundary in the margins of adjacent domains, but their frequency typically decreases rapidly with increasing distance from the boundary.

Recent studies (Ritzi and Andolsek, 1992; Cheema and Islam, 1994) demonstrated that in fractured-rock aquifers the direction of maximum hydraulic conductivity is parallel to the direction of the predominant fracture trend or fracture-connection pathways. Regional ground-water flow in fractured rock is controlled by the spatial distribution of hydraulic conductivity and degree of anisotropy (Greene and Rahn, 1995). The approximate anisotropy can be estimated based on the shape of the hydraulic conductivity ellipse from rose diagram plots (as shown on plates 12 through 15) of fracture trends. Such an understanding allows the prediction of the shape of the cone of depression surrounding a high-yield well (Ritzi and Andolsek, 1992) and the potential for hydraulic communication with nearby wells.

Two examples show how fracture patterns can be used to characterize the hydraulic conductivity of a fracture domain (figure 31). The rose diagram in figure 31a shows the fracture pattern of a mesoscopic fault domain. The rose diagram shows that the predominant set and the secondary set trend nearly ninety degrees apart. Note that the predominant set is bimodal and trends northwest. A "best fit" ellipse can be superimposed over the plot by placing the long axis of an ellipse over the median line between the two modes of the predominant set. The shape of the resulting ellipse in this case suggests slight anisotropy (anisotropic hydraulic conductivity). A circle would indicate isotropy. The degree of anisotropy can be expressed in the form of a ratio of the lengths of the axes of the ellipse, or evaluated visually. Actual ground-water flow paths are likely complex, but flow along the four directions of the two bimodal sets is favored. Figure 31b is an example of a rose diagram from a domain where the maximum hydraulic conductivity is oriented east-northeast. Note that the mode of the predominant set is parallel to the long axis of the ellipse in this case, which is more common in the study area than the bimodal case presented in figure 31a.

The fracture domain maps (plates 12 through 15) show the prominent trends of fractures, but exclude bedding joints. Although bedding joints are excluded from the mesoscopic joint domain maps, bedding faults are not excluded from the

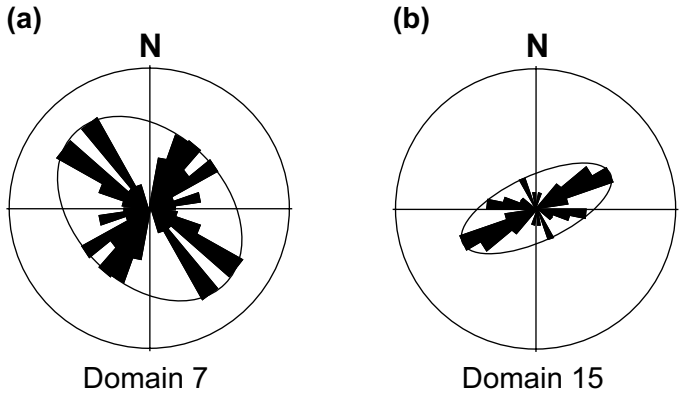

Figure 31. *Estimation of the shape of the hydraulic conductivity ellipse using rose diagrams. Maximum hydraulic conductivity is inferred to be parallel to long axis of ellipse. (a) Rose diagram showing example of a slightly anisotropic hydraulic conductivity. Long axis of ellipse is inferred to occupy the median position between the two predominant modes. (b) Rose diagram showing example of an anisotropic hydraulic conductivity. Long axis of ellipse is parallel to the predominant fracture trend.*

mesoscopic fault domain map. We excluded bedding joints because of the difficulty of accounting for their enhanced frequency near the ground surface. In general, the fracture patterns constrain the flow paths of ground water in the discrete GWCs and possibly predict the long axis of the hydraulic conductivity ellipse (Cheema and Islam, 1994; bulk permeability ellipse of Davis, 1969) for the domain, except in areas where ground-water flow is significant along bedding joints. In such areas, flow along bedding must also be considered and superimposed onto the other fracture data in order to predict ground-water flow.

Correlation of Linear-Trace Trends with Outcrop-Fracture Trends

Linear traces (O'Leary and others, 1976) are linear features visible on aerial photographs that are less than 1 mile (1.6 km) in length. Linear traces may include topographic, vegetation, and tonal alignments and do not necessarily represent a geologic feature such as a fracture. We evaluated the coincidence of linear-trace trends with fracture trends determined from outcrop data in three of the largest fracture domains. We considered trends to be coincident if the modes were within a 15 degree half-width of each other. Coincident linear traces that trend parallel to prominent fracture sets are referred to as fracture-correlatable (Mabee and others, 1994) traces. Figures 32 and 33 show that linear-trace trends are more frequently coincident with secondary fracture trends in two of the three domains than with predominant fracture trends. A high percentage of linear-trace trends coincide with the predominant fracture trend only in domain 2 (figure 33).

The paucity of outcrops made it impossible to define mesoscopic fracture domains across the entire study area. Therefore we attempted to extend fracture-domain boundaries beyond the limits we imposed (1 kilometer [0.63 mile] to the closest outcrop) in our mesoscopic fracture domain-mapping using linear-trace data. We chose domain 2 because it demonstrated a high frequency of fracture-correlatable linear traces and the highest percentage of traces coincident with the predominant mesoscopic fracture trend. Figure 34 shows that the majority of linear traces outside of mesoscopic fracture domain 2 are not coincident (are not fracture-correlatable) with prominent mesoscopic fracture trends in the domain. We interpret the lack of coincidence to indicate that the traces consist predominantly of linear features that do not correspond to macroscopic fractures in rock.

Subsurface Fracture Trends

So far we have discussed mostly trends of fractures mapped at or near the ground surface, or of linear traces obtained from aerial photos. However, because water wells drilled into rock are typically completed at depths exceeding several hundred to a thousand feet, we evaluated the available subsurface fracture-trend data and compared them with the surface fracture-trend data. Subsurface data are limited to the Park City mining district, and no data exist for the northern two-thirds of the Snyderville basin. The sources of our information included published accounts of fractures encountered in underground workings, and unpublished geologic maps and information provided by Kerry Gee of United Park City Mines Company. Geologic maps of underground mine workings and tunnels typically describe only faults that show discernable offset and mineralized fractures. Data on joint trends are generally absent.

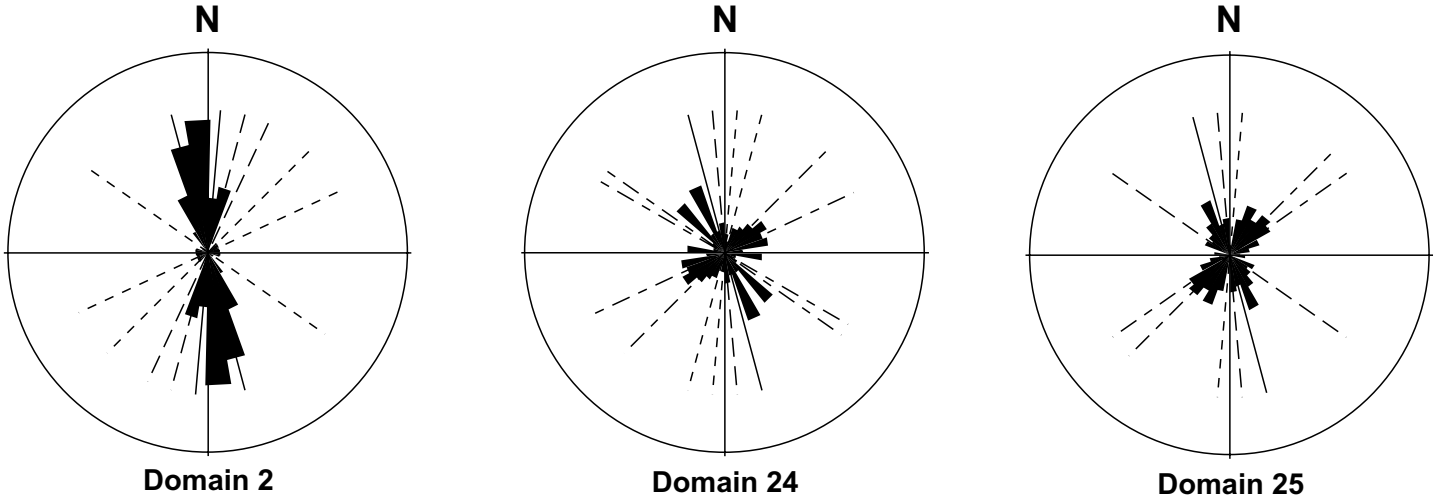

Figure 32. *Coincidence of linear-trace modes and prominent fracture trends in three selected domains.*

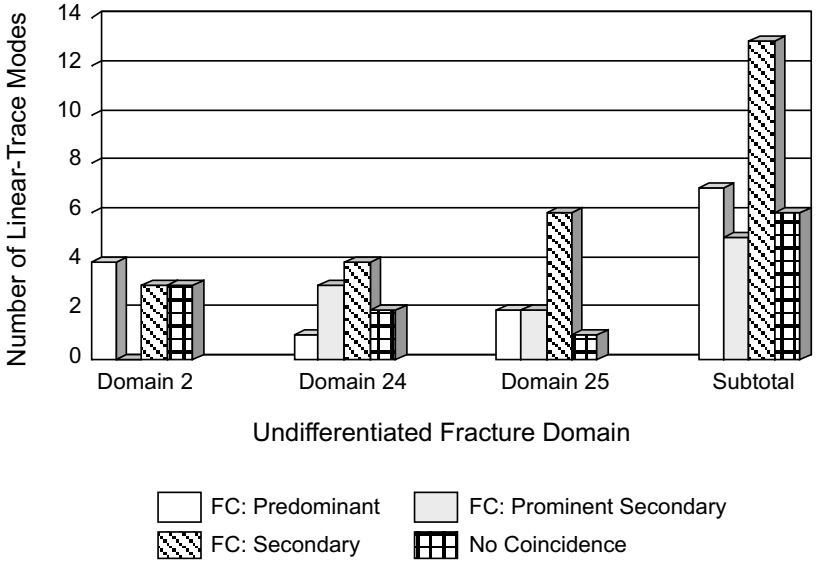

Figure 33. *Coincidence of linear-trace modes and prominent fracture trends. Most traces in these domains can be classified as being "fracture correlatable" (FC) (Mabee and others, 1994), but linear traces correlate more frequently with secondary fracture trends rather than predominant trends in two of the three domains.*

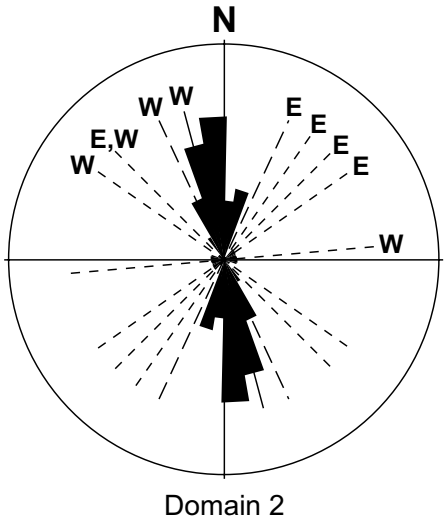

Explanation

Linear-trace mode parallel to (±15 degrees) predominant undifferentiated fracture trend: fracture-correlated linear trace.

Linear-trace mode parallel to secondary undifferentiated fracture trace trend: fracture-correlated linear trace.

Linear-trace mode that does not coincide with mapped undifferentiated fracture trends.

E **W** Direction of sample area from mapped domain.

Rose diagram shows prominent fracture trends as determined from outcrop mapping.

Figure 34. *Comparison of linear-trace trends in areas adjacent to domain 2 to prominent fracture trends. Linear traces outside arbitrary boundary of domain 2 show poor correlation with prominent fracture trends of domain 2. Seventy percent of linear-trace modes show no correlation with prominent fracture trends.*

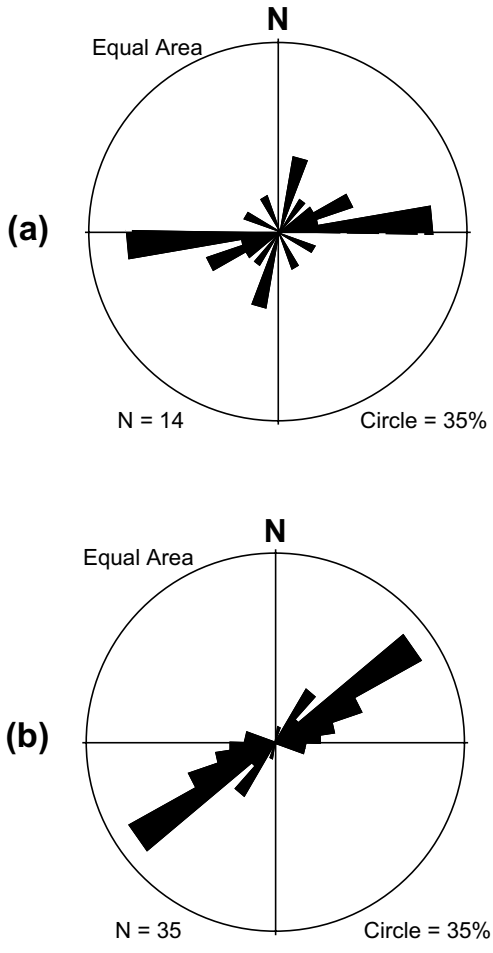

Figure 35. *Subsurface fault trends as reported by Boutwell (1912). Trends of major mineralized fault zones (a) and other major faults (b).*

Subsurface fracture-trend data are relatively consistent with surface fracture-trend data in the Park City mining district. Figure 35 shows that the trends of the major ore-bearing fault zones and other major faults encountered in the mine workings are predominantly east-west and northeast, respectively (Boutwell, 1912). The subsurface data for the major ore-bearing (macroscopic) fault zones (figure 35a) are consistent with the surface data for macroscopic fault domain II that contains most of the fault zones (see plate 14). This confirms that the trend of faults within the domain does not change significantly with depth. The northeast subsurface trend of the other major faults (figure 35b) reported by Boutwell (1912) is rotated slightly clockwise with respect to surface data from domain I, and is rotated slightly counterclockwise with respect to domain II. Because the plot includes measurements from both domains I and II, it likely presents a mean trend value of the combined domains.

Mesoscopic fracture-trend data obtained from geologic maps of underground workings and tunnels are also consistent with surface data (figure 36; table 8). Predominant trends at three separate subsurface sites are reasonably constrained by surface data, and also appear to confirm the location of domain boundaries that are defined solely by surface data. Data from the Keystone Lower Tunnel ($SE^1/_4NW^1/_4$ section 30, T. 2 S., R. 4 E.) illustrate the consistency between surface and subsurface fracture trends. The portal of the tunnel is near the boundary between macroscopic fault domains Ic and IIa, from which the tunnel extends southeastward into domain IIa. The predominant subsurface fracture trend at the Keystone Lower Tunnel is north-northeast (azimuth 025°), and deviates only slightly from the predominant north-northeast (azimuth 015°) trend in domain Ic. The secondary trend in the tunnel is east-west (azimuth 080°), and again deviates only slightly from the predominant east-northeast (azimuth 075°) trend of the adjacent domain IIa. The consistency of the secondary trend data in the tunnel improves (azimuth 075°) if only fault trends are evaluated (not shown in figure 36).

Potential Ground-Water Resources in the Weber Ground-Water Compartments

Although no wells are presently completed in the Weber GWC (includes lower Park City Formation) in the study area, data from mine workings indicate that highly permeable fracture zones may be capable of yielding large quantities of ground water. During Spiro Tunnel construction in 1916, peak inflows from the Weber interval exceeded 4,500 gal/min (284 L/s), contributing seventy percent of the peak discharge at the portal (K. Gee, United Park City Mines Company, unpublished data, 1995). Today, very little inflow is observed within the first 13,500 feet (4,100 m) of the Spiro Tunnel. The Thaynes, Park City, and Weber Formations in the majority of this interval are drained and dry to nominally

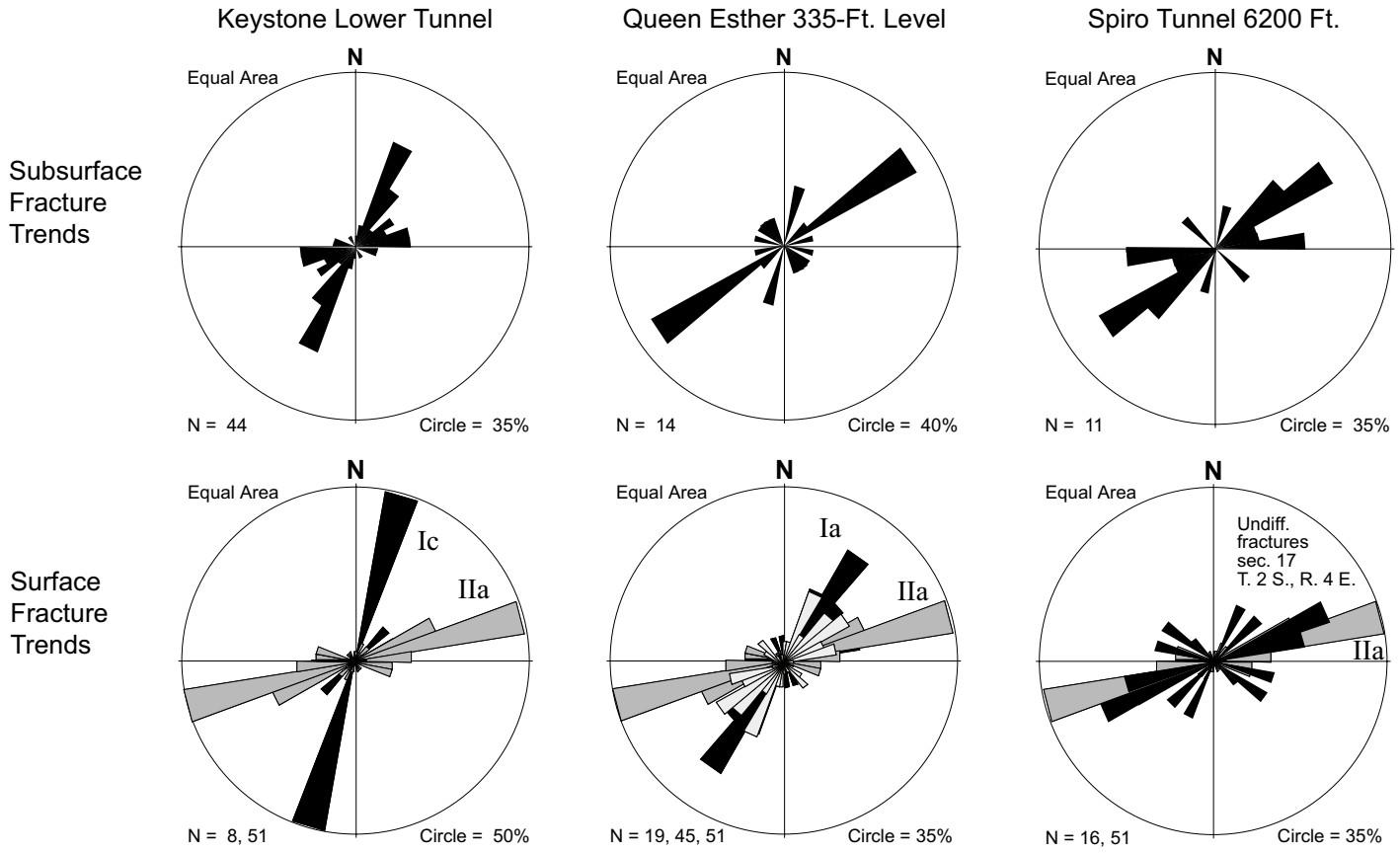

Figure 36. *Comparison of subsurface and surface fracture trends in the Park City mining district. Subsurface trends determined from maps of tunnels and underground mine workings provided by K. Gee of United Park City Mines Company. Subsurface fractures consist primarily of faults. Rose diagrams for surface fracture domains directly above sites of subsurface mapping are shown for comparison. See table 8 for comparison of predominant modes. Roman numerals indicate macroscopic faults. Others are mesoscopic fractures.*

Table 8.
Comparison of subsurface and surface fracture trends.

Location	Subsurface Fracture Trends		Surface Fracture Trends			
	Predominant Azimuth (degrees)	Secondary Azimuth (degrees)	Macroscopic Azimuth[1] (degrees)		Mesoscopic Azimuth[1] (degrees)	
Keystone Lower Tunnel	025	080	015	075		
Queen Esther - 335' Level	055		035	075	025	055
Spiro Tunnel - 6,200'	055	085	075		065	

[1] *Two trends reported where bimodal.*

wet. Most of the present inflow of ground water into the Spiro Tunnel is from its southwesternmost extension. Beneath Thaynes Canyon, the tunnel bends southwestward and extends to the West Monitor Flat area. There the tunnel terminates in the lower part of the Park City Formation (K. Gee, United Park City Mines Company, verbal communication, 1995). Some exploratory drifts extend outward, from near the tunnel's face, into both the Park City and Weber Formations. Other than these exploratory drifts, the area is not penetrated by extensive mine workings. The West Monitor Flat area is, in terms of ground-water conditions, analogous to what the remainder of the mining district must have been like in the second half of the nineteenth century prior to extensive mining. The influence of existing mine workings on ground-water flow should be considered in the selection of a well site in either of the Weber GWCs.

Changes in Fracture Aperture

Fracture aperture near a well may decrease over time with continued pumping. Decreasing production reported in some wells (T. Jarvis, Weston Engineering, Inc., unpublished data, 1996) may reflect closing of fractures as fracture pore pressure is reduced by continuous pumping. Progressively decreasing production, if attributable to fracture closing, may not recover without well-enhancement measures. The reported decrease in well production may be attributable to other factors such as silting in of wells or microbial growth, but well-production-history data (see reference above) suggest otherwise. The fact that well production varies seasonally suggests that well design or condition has little to do with restricting flow into the well (T. Jarvis, Weston Engineering, Inc., written communication, 1996).

Solution widening may increase fracture aperture in limestone beds. Although no direct field evidence was observed to confirm ongoing solution widening, Huntoon (1995) indicates that it is reasonable to assume some dissolution even where evidence is lacking. Borehole video tapes of wells in Park City and anecdotal evidence concerning wells in the Pinebrook area, all completed in the Thaynes Formation, suggest at least some solution enhancement (T. Jarvis, Weston Engineering, Inc., written communication, 1996). Huntoon (1993) indicated that solution widening may occur along crests of anticlines, enhancing the permeability of extensional fractures.

Transient Storage

Production-history data (T. Jarvis, Weston Engineering, Inc., written communication, 1996) indicate that some wells completed in fractured-rock GWCs experience seasonal production fluctuations. Larger well yields in the spring result from rapid recharge during spring runoff. Lower well yields occur in the fall and winter months. Similar seasonal ground-water inflow fluctuations are reported from tunnels (K. Gee, United Park City Mines, verbal communication, 1995). These seasonal fluctuations suggest relatively low storativity of the fractured-rock GWCs precluding long-term storage of recharge (T. Jarvis, Weston Engineering, Inc., written communication, 1996).

The Importance of Fracture Dip on Well Yield

Figure 37 shows that most fractures in the study area are high angle (dips exceed 45 degrees). Because in many areas bedding fractures are low angle, they will be the most common fracture type encountered in shallow vertical wells. Better well yields might be achieved by drilling inclined holes so that they encounter the high-angle fracture zones (Banks, 1992), or drilling deeper and increasing the total number of high- and low-angle fractures encountered as well as increasing the potential for intersecting a high-angle fracture zone. Inclined drilling may be most useful where bedding fractures are less common, such as in the Keetley, Nugget, and Weber Formations.

SUMMARY

Ground water in the Snyderville basin is present in shallow unconsolidated deposits and discrete fractured-rock GWCs. The limited extent and thickness of the unconsolidated deposits makes them secondary to the fractured-rock aquifers in terms of their potential for future development.

The unconsolidated deposits consist primarily of alluvium and glacial till and outwash in the lowlands of the study area. Unconsolidated deposits consist of only a thin veneer of glacial or colluvial deposits in most upland areas. In lowland areas, the thickness of the deposits generally exceeds 40 feet (12 m), and may be as much as 275 feet (84 m) in the southern part of Parleys Park. The exceptional thickness of unconsolidated deposits and shallow water table in the south-

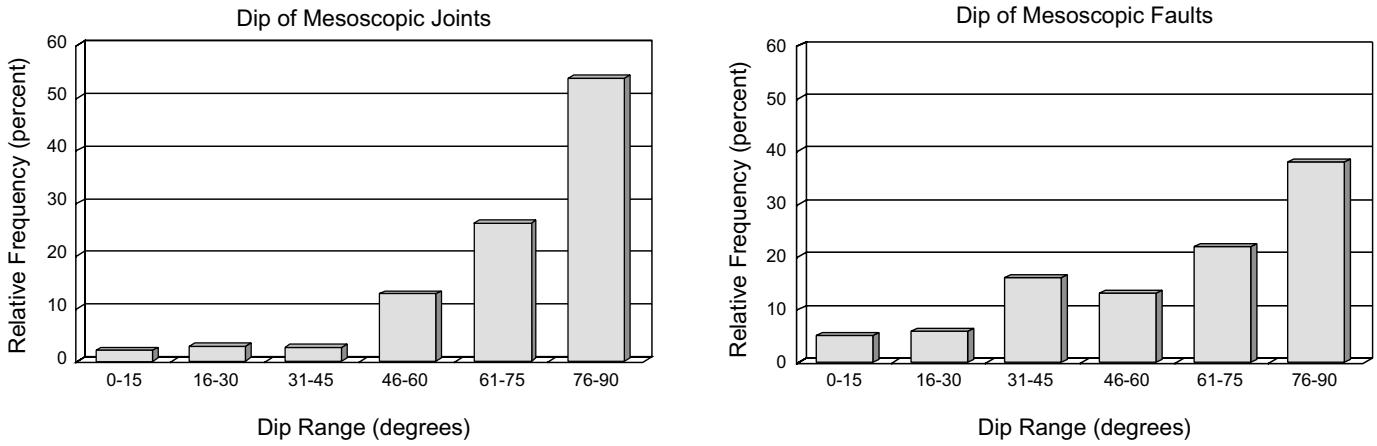

Figure 37. *Dip of mesoscopic joints and faults. Histograms show that the majority of joints and faults dip greater than 45 degrees. Over 50 percent of joints and 35 percent of faults are nearly vertical.*

ern part of Parleys Park suggest that the unconsolidated aquifer is more substantial here than elsewhere in the study area. However, descriptions of the deposits, although commonly of poor quality, suggest that the deposits are typically fine grained and unlikely to produce high-yielding wells.

Fractured sedimentary rocks are becoming an increasingly important source of ground water in the study area. Permeability in these rocks is primarily a result of fracturing which may be locally enhanced by solution-widening in limestone and other calcareous units. Some primary permeability in Cretaceous sedimentary rocks and locally in the Keetley Volcanics may also yield small quantities of water to wells. Primary permeability in Jurassic or older limestones and sandstones is probably negligible, but has not been studied in detail.

Fracture characteristics are generally controlled by the rock properties of each formation and therefore do not vary significantly in a given formation. Joints, bedding joints, and cleavage fractures tend to enhance rock permeability or have a negligible effect. Faults may act as conduits, increasing permeability parallel to the fault, but generally inhibit ground-water flow perpendicular to the fault. High-angle-to-bedding fractures in limestone and sandstone are generally persistent, allowing ground-water flow perpendicular to beds. High-angle-to-bedding fractures in shale generally have very low persistence, terminate against shale partings or ductile beds, and are tight or clay-infilled. Whereas persistent bedding fractures in shale may act as ground-water conduits parallel to bedding, non-persistent high-angle-to-bedding fracture characteristics likely inhibit ground-water flow perpendicular to bedding. Hydraulic conductivities of fracture-poor shale beds, such as the gypsiferous shale bed in the lower part of the Woodside Shale, likely approach that of intact shale.

Fractured limestone and sandstone beds are separated by shale confining beds that have very low hydraulic conductivities perpendicular to bedding. Aquifer-test results indicate a lack of hydraulic communication between wells completed in separate fractured limestone and sandstone SGWCs. Historical accounts from mine workings also indicate stratigraphic control of ground water flow. Water accumulations above fracture-poor shale beds likely reflect the inability of ground water to flow perpendicular to these beds.

Macroscopic faults act in a complex manner as ground-water conduit-barrier systems and also sever the continuity of SGWCs. Fault-zone cores commonly consist of gouge zones that likely act as barriers to ground-water flow. Gouge-zone width is a function of wall rock type and the amount of displacement on the fault. Zones of interconnected subsidiary fractures in brittle wall rock may act as conduits parallel to the fault, but may terminate along strike at contacts.

At least sixteen discrete GWCs are recognized. Several of these, in the Twin Creek Limestone and Thaynes Formation, may be subdividable on the basis that they contain an intraformational confining bed. GWCs vary considerably in extent, thickness, physiography, and hydrology. Recharge areas for some may be small and for these safe yields may be low.

Fracture trends vary across the study area, but fracture domains with distinct fracture trends are recognizable. In many cases, fracture-domain boundaries occur at major structures or geologic contacts; however, others do not and are transitional. Fracture patterns as presented on rose diagrams are useful in predicting hydraulic communication between wells in a single GWC and help predict the shape of drawdown cones. Fracture-trend data determined from outcrops correlate well with subsurface fracture data, but correlate poorly with linear-trace data.

Other factors may affect the production history or yields of wells completed in fractured rock. Continuous pumping may result in closing of fractures as pore pressures are reduced. Fracture aperture may not recover, resulting in diminishing well yields over time. Solution widening in limestone and calcareous rocks may increase fracture permeability and can favor specific structural settings such as the crests of anticlines. As a result of the steep dip of most fractures, vertical wells are less likely to intercept transmissive fracture zones. Inclined drilling may result in higher well yields, particularly in formations such as the Nugget Sandstone and Weber Quartzite where moderate- to low-angle bedding fractures are rare. Water well production-history data suggest that fracture storage characteristics may preclude long-term storage of recharge.

RECOMMENDED FUTURE STUDIES

Conclusions and observations in this report are preliminary due to the regional scope of the study. In this section, we present our recommendations for future investigations that would supplement this study and add further to the understanding of the ground-water resources in the study area.

1. Long-duration, constant-pump-rate aquifer tests are required to demonstrate the anisotropy and compartmentalization of the fractured rock throughout the study area. Although the limited data available to us during this study appear to support these concepts, our speculation regarding the anisotropy of fractured rock is based solely on fracture-pattern data. To determine the anisotropy of discrete fractured-rock GWCs, aquifer tests must be conducted using monitoring wells that are completed in the compartment, and that are located so that the shape of the cone of depression can be defined. Additional monitoring wells must be situated in adjacent compartments or confining beds to test the integrity of the latter.
2. More detailed fracture data are required to predict hydraulic communication among wells in a local area or within single subdivisions. Although we collected much fracture data, our focus was on understanding as much of the basin as possible. In the process of collecting data, we recognized certain areas that were structurally complex and where fracture patterns varied widely among outcrops. In such areas, our data are only preliminary and more detailed studies are required.
3. Additional investigations are needed to determine ground-water storage characteristics of fractured rock. We are aware of no studies to determine the primary permeabilities of rock types in the study area. We observed evidence suggesting high primary permeability locally in the Frontier Formation, Gartra Grit Member of the Ankareh Formation, and the Keetley Volcanics that may yield low to moderate amounts of ground water to wells. Primary permeability data may give insights into specific retention (water that is not yielded to wells) in fractured rock, and may be useful in understanding the long-term production history of existing wells. In addition, fracture connectivity should be evaluated in detail to determine its variability across a single fractured-rock ground-water compartment. The degree of connectivity is proportional to the permeability of a fracture set or network (combination of fracture sets) (Ohlmacher, 1994). Poorly connected fractures may contain ground water that may be difficult to recover from wells.
4. Recharge areas of the discrete GWCs should be identified using the hydrostratigraphic concepts and an understanding of the role of macroscopic faults as complex barrier-conduit systems presented herein. This is an important step in estimating the safe yields of each GWC and identifying potential sources of ground-water contamination.

ACKNOWLEDGMENTS

This study was largely funded by the Utah Division of Water Rights (WR). We thank Boyd Clayton, John Mann, and Jerry Olds, WR, for their help in obtaining well logs and digital map data, and for notifying us of projected well starts. We thank Lynette Brooks and Geoffrey Freethey, USGS WRD; Todd Jarvis and Bill Loughlin, Weston Engineering, Inc.; and Kerry Gee, United Park City Mines Company for their valuable input during discussions of geologic and hydrologic conditions in the Snyderville basin. We especially thank Kerry Gee for providing access to the Spiro Tunnel as this greatly improved our understanding of subsurface geologic and ground-water conditions in the basin. Technical reviews of this report were provided by Michael Hylland of the UGS; James P. Evans of Utah State University; Todd Jarvis of Weston Engineering, Inc.; and Lynette Brooks, Geoffrey Freethey, and Jim Mason of the USGS WRD.

REFERENCES

Al-Raisi, M.H., Slatt, R.M., and Decker, M.K., 1996, Structural and stratigraphic compartmentalization of the Terry Sandstone and effects on reservoir fluid distributions - Latham Bar Trend, Denver Basin, Colorado: The Mountain Geologist, v. 33, no. 1, p. 11-30.

Baker, A.A., Calkins, F.C., Crittenden, M.D., Jr., and Bromfield, C.S., 1966, Geologic map of the Brighton quadrangle, Utah: U.S. Geological Survey Geologic Quadrangle Map GQ 534, scale 1:24,000.

Baker, C.H., Jr., 1970, Water resources of the Heber-Kamas-Park City area, north-central Utah: Utah Department of Natural Resources Technical Publication No. 27, 79 p.

Banks, David, 1992, Optimal orientation of water-supply boreholes in fractured aquifers: Ground Water, v. 30, no. 6, p. 895-900.

Barnes, M.P., and Simos, J.G., 1968, Ore deposits of the Park City district with a contribution on the Mayflower lode, *in* Ridge, J.D., editor, Ore deposits of the United States, 1933-1967: New York, American Institute of Mining, Metallurgical and Petroleum Engineers, p. 1102-1126.

Bergosh, J.L., Good, J.R., Hillman, J.T., and Kolodzie, S., 1982, Geological characterization of the Nugget Sandstone, Anschutz Ranch East: Utah Geological Association Publication 10, p. 253-265.

Boutwell, J.M., 1912, Geology and ore deposits of the Park City district, Utah: U.S. Geological Survey Professional Paper 77, 231 p.

Bradley, M.D., and Bruhn, R.L., 1988, Structural interactions between the Uintah arch and the overthrust belt, north-central Utah - implications of strain trajectories and displacement modeling: Geological Society of America Memoir 171, p. 431-445.

Bromfield, C.S., 1968, General geology of the Park City region, Utah: Utah Geological Society Guidebook to the Geology of Utah No. 22, p. 10-29.

—1989, Gold deposits in the Park City mining district, Utah: U.S. Geological Survey Bulletin 1857-C, p. C14-C26.

Bromfield, C.S., Baker, A.A., and Crittenden, M.D., Jr., 1970, Geologic map of the Heber quadrangle, Wasatch and Summit Counties, Utah: U.S. Geological Survey Geologic Quadrangle Map GQ-864, scale 1:24,000.

Bromfield, C.S., and Crittenden, M.D., Jr., 1971, Geologic map of the Park City East quadrangle, Summit and Wasatch Counties, Utah: U.S. Geological Survey Geologic Quadrangle Map GQ-852, scale 1:24,000.

Bruce, C.L., 1988, Jurassic Twin Creek Formation - a fractured limestone reservoir in the overthrust belt, Wyoming and Utah: Carbonate Symposium, Rocky Mountain Association of Geologists, p. 105-120.

Bryant, Bruce, 1990, Geologic map of the Salt Lake City 30′ x 60′ quadrangle, north-central Utah, and Uintah County, Wyoming: U.S. Geological Survey Miscellaneous Investigations Series Map I-1944, scale 1:100,000.

—1992, Geologic and structure maps of the Salt Lake City 1° x 2° quadrangle, Utah and Wyoming: U.S. Geological Survey Miscellaneous Investigations Series Map I-1997, scale 1:125,000.

Caine, J.S., Forster, C.B., and Evans, J.P., 1993, A classification scheme for permeability structures in fault zones: EOS, Transactions of the American Geophysical Union, v. 74, p. 677.

Cheema, T.J., and Islam, M.R., 1994, Experimental determination of hydraulic anisotropy in fractured formations: Bulletin of the Association of Engineering Geologists, v. XXXI, no. 3, p. 329-341.

Crittenden, M.D., Jr., 1974, Regional extent and age of thrusts near Rockport Reservoir and relation to possible exploration targets in northern Utah: American Association of Petroleum Geologists Bulletin, v. 58, no. 12, p. 2428-2435.

Crittenden, M.D., Jr., Calkins, F.C., and Sharp, B.J., 1966, Geologic map of the Park City West quadrangle, Utah: U.S. Geological Survey Geologic Quadrangle Map GQ-535, scale 1:24,000.

Davis, S.M., 1969, Porosity and permeability of natural materials, in De Wiest, R.J.M., editor, Flow through porous media: New York, Academic Press, p. 54-89.

Downhour, P.A., and Brooks, L.E., 1996, Selected hydrologic data for Snyderville basin, Park City, and adjacent areas, Summit County, Utah, 1967-95: U.S. Geological Survey Open-File Report 96-494, 52 p.

Eardley, A.J., 1968, Regional geologic relations of the Park City District: Utah Geological Society Guidebook to the Geology of Utah No. 22, p. 3-9.

Eberly, P.O., 1985, Brittle fracture petrofabric along a west-east traverse from the Connecticut Valley to the Narragansett Basin: Amherst, University of Massachusetts, Department of Geology and Geography, Contribution No. 57, 137 p.

Economics Research Associates, 1981, The outlook for growth, Park City/Snyderville Basin, a market perspective: San Francisco, 57 p.

Engelder, J.T., 1974, Cataclasis and the generation of fault gouge: Geological Society of America Bulletin, v. 85, p. 1515-1522.

Faill, R.T., 1969, Kink band structure in the Valley and Ridge Province, central Pennsylvania: Geological Society of America Bulletin, v. 80, p. 2539-2550.

—1973, Kink band folding, Valley and Ridge Province, Pennsylvania: Geological Society of America Bulletin, v. 84, p. 1289-1314.

Freeze, R.A., and Cherry, J.A., 1979, Groundwater: Englewood Cliffs, New Jersey, Prentice Hall, 604 p.

Gee, Kerry, 1994, Flagstaff Mountain at Deer Valley - an expansion of the Deer Valley Resort and the hydrogeology of the Judge Tunnel, Park City, Utah: Park City, Utah unpublished consultant's report, 6 p.

Gill, H.E., and Lund, W.R., 1984, Engineering geology of Park City, Summit County, Utah: Utah Geological and Mineral Survey Special Studies 66, 42 p.

Granger, A.E., 1953, Stratigraphy of the Wasatch Range near Salt Lake City, Utah: U.S. Geological Survey Circular, 14 p.

Greene, E.A., and Rahn, P.H., 1995, Localized anisotropic transmissivity in a karst aquifer: Ground Water, v. 33, p. 806-816.

Hintze, L.F., 1988, Geologic history of Utah: Brigham Young University Geology Studies, Special Publication 7, 202 p.

Holmes, W.F., Thompson, K.R., and Enright, M., 1986, Water resources of the Park City area with emphasis on ground water: Utah Department of Natural Resources Technical Publication No. 85, 81 p.

Huntoon, P.W., 1993, The influence of Laramide foreland structures on modern ground-water circulation in Wyoming artesian basins, *in* Snoke, A.W., Steidtmann, J.R., and Roberts, S.M., editors, Geology of Wyoming: Geological

Survey of Wyoming Memoir No. 5, p. 756-789.

—1995, Is it appropriate to apply porous media groundwater circulation models to karstic aquifers?, *in* El-Kadi, A.I., editor, Groundwater models for resources analysis and management: Boca Raton, Florida, Lewis Publishers, p. 339-358.

Imlay, R.W., 1967, Twin Creek Limestone (Jurassic) in the western interior of the United States: U.S. Geological Survey Professional Paper 540, 105 p.

International Society for Rock Mechanics, 1980, Commission on classification of rocks and rock masses - basic geotechnical description of rock masses: International Journal of Rock Mechanics, v. 18, p. 85-110.

Jarvis, Todd, and Loughlin, Bill, 1996, Addendum to final report on Summit Park Well No. 7: Laramie, Wyoming, Weston Engineering, Inc., unpublished technical memorandum, 3 p.

Jarvis, Todd and Yonkee, W.A., 1993, Summit Park and Timberline Water Special Service Districts test well siting program: Laramie, Wyoming, Weston Engineering, Inc., unpublished technical memorandum, 10 p.

J.M. Montgomery, 1991, Park City municipal corporation 1991 well pump test - observations and results of the Middle School well and Park Meadows well pump test: Provo, Utah, unpublished consultant's report, unpaginated.

Kildale, M.B., 1956, Geology and mineralogy of the Park City district, Utah: Mineralogical Society of Utah Bulletin, v. 8, no. 2, p. 5-10.

Lachmar, T.E., 1993, The influence of fracture properties on ground-water flow at the Bunker Hill Mine, Kellog, Idaho: Bulletin of the Association of Engineering Geologists, v. XXX, p. 395-407.

Lamerson, P.R., 1982, The Fossil Basin area and its relationship to the Medicine Butte thrust fault system, in Powers, R.B., editor, Geologic studies of the Cordilleran Thrust Belt, 1982: Denver, Colorado, Rocky Mountain Association of Geologists, p. 279-340.

LaPointe, P.R., and Hudson, J.A., 1985, Characterization and interpretation of rock mass joint patterns: Geological Society of America Special Paper 199, 37 p.

Lattman, L.H., 1958, Technique of geologic fracture traces and lineament mapping on aerial photographs: Photogrammetric Engineering, v. 24, p. 568-576.

Mabee, S.A., Hardcastle, K.C., and Wise, D.U., 1994, A method for collecting and analyzing lineaments for regional-scale fractured-bedrock aquifer studies: Ground Water, v. 32,

no. 6, p. 884-894.

Mendenhall, William, and Sincich, Terry, 1992, Statistics for engineers and the sciences: New York, MacMillan Publishing Company, 963 p.

Morrow, C.A., Shi, L.Q., and Byerlee, J.D., 1984, Permeability of fault gouge under confining pressure and shear stress: Journal of Geophysical Research, v. 89, p. 3193-3200.

Mount, D.L., 1952, Geology of the Wanship-Park City region, Utah: Salt Lake City, University of Utah, unpublished M.S. thesis, 35 p.

Ohlmacher, G.C., 1994, Fracture networks, fracture connectivity, and environmental implications [abs]: American Association of Petroleum Geologists Bulletin, v. 78, no. 3, p. 497.

O'Leary, D.W., Friedman, J.D., and Pohn, H.A., 1976, Lineament, linear, lineation--some proposed new standards for old terms: Geological Society of America Bulletin, v. 87, p. 1463-1469.

Ritzi, R.W., Jr., and Andolsek, R.H., 1992, Relation between anisotropic transmissivity and azimuthal resistivity surveys in shallow, fractured, carbonate flow systems: Ground Water, v. 20, p. 774-780.

Robertson, E.C., 1982, Continuous formation of gouge and breccia during fault displacement: 23rd Symposium of Rock Mechanics Association of America, p. 387-404.

Stacy, M.E., 1994, Karstic groundwater circulation in the fault-severed Madison aquifer in the Casper Mountain area of Natrona County, Wyoming: Laramie, University of Wyoming, M.S. thesis.

Stokes, W.L., 1977, Subdivisions of the major physiographic provinces in Utah: Utah Geology, v. 4, no. 1, p. 1-17.

Stone, D.S., 1967, Accumulation theory, Big Horn Basin: American Association of Petroleum Geologists Bulletin, v. 51, no. 10, p. 2056-2114.

Sullivan, J.T., Nelson, A.R., LaForge, R.C., Wood, C.K., and Hansen, R.A., 1986, Regional seismotectonic study for the back valleys of the Wasatch Mountains in northeastern Utah: Denver, unpublished U.S. Bureau of Reclamation report, 317 p.

Suppe, John, 1985, Principles of structural geology: Englewood Cliffs, Prentice-Hall, 537 p.

Tearpock, D.J., and Bischke, R.E., 1991, Applied subsurface geological mapping: Englewood Cliffs, New Jersey, Prentice-Hall, 648 p.

Terzaghi, R.D., 1965, Sources of errors in joint surveys: Geotechnique, v. 15, p. 287-304.

Twiss, R.J., and Moores, E.M., 1992, Structural geology: New York, W.H. Freeman and Company, 532 p.

U.S. Department of Agriculture Soil Conservation Service, 1977, Soil survey and interpretations, Parleys Park portion of soil survey of Summit Valley, Summit County, Utah: Utah Agricultural Experiment Station, in cooperation with Summit County Commission and Park City Planning Commission, Bulletin 495, 317 p., scale 1:24,000.

Wallace, R.E., and Morris, H.T., 1986, Characteristics of faults and shear zones in deep mines: Pure and Applied Geophysics, v. 124, p. 107-124.

Weston Engineering, Inc., 1996a, Final well report - Summit Park Water Special Service District Well No. 7 located in $NW^1/_4NE^1/_4$, section 16, T. 1 S., R. 3 E., Summit County, Utah: Park City, Utah, unpublished consultant's report, 13 p.

—1996b, Source delineation report - Gorgoza Mutual Water Company (System No. 22030), T. 1 S., R. 3 E., Summit County, Utah: Park City, Utah, unpublished consultant's report, unpaginated.

Willis, G.C., 1999, The Utah thrust system – an overview, *in* Spangler, L.E., editor, Geology of northern Utah and vicinity: Utah Geological Association Publication 27, p. 1-9.

Wilson, C.L., 1959, Park City Mining District, in Williams, N.C., editor, Guidebook to the geology of the Wasatch and Uintah Mountains transition area: Intermountain Association of Petroleum Geologists Tenth Annual Field Conference, p. 182-188.

Wise, D.U., 1964, Microjointing in basement, middle Rocky Mountains of Montana and Wyoming: Geological Society of America Bulletin, v. 75, p. 287-306.

Yonkee, W.A., Evans, J.P., and DeCelles, P.G., 1992, Mesozoic tectonics of the northern Wasatch Range, Utah: Utah Geological Survey Miscellaneous Publication 92-3, p. 429-460.

GLOSSARY

Anticline - a fold, the core of which contains stratigraphically older rocks, and is convex or closes upward

Aperture - thickness of fracture opening (may be infilled)

Descriptive term	Aperture (mm)
tight	no visible opening
slightly open	<1
moderately open	1-3
open	3-10
moderately wide	10-30
wide	>30

Asperities - irregularities on a fracture surface

Axial surface (plane) inclination

Descriptive term	Dip (degrees)
gently	0-30
moderately	31-60
steeply	61-80
upright	81-90

Bedding spacing

Descriptive term	Spacing (cm)
massive	>200
layered	<200
thinly laminated	<0.3
thickly laminated	0.3-1
very thinly bedded	1-3
thinly bedded	3-10
medium bedded	10-30
thickly bedded	30-100
very thickly bedded	>100

Bifurcates - branches

Cleavage - a planar fabric in a rock normal to the direction of shortening that forms at relatively low metamorphic grades

Common joints - joints that are less than 5 meters in length

Compass directions

Descriptive term	Azimuth range (degrees)
north-south	346-014
north-northeast	015-030
northeast	031-059
east-northeast	060-075
east-west	076-089; 270-284 (270=090)
west-northwest	285-300
northwest	301-329
north-northwest	330-345

Note that strike lines are horizontal lines. Their attitude can therefore be described as being either north or south, northeast or southwest, etc. Directions other than north, south, east, or west were abbreviated using compass directions in the northern two quadrants, for example northeast versus northeast-southwest.

Country rock - the rock intruded by and surrounding an igneous intrusion

Dip slip - slip direction, or component thereof, is roughly parallel to dip direction of the fault; rake is between 70 and 90 degrees

Disharmonic - a description of folds that die out within a couple of half-wavelengths or less; in layered rocks

Disjunctive - a type of cleavage that is not pervasive, but rather characterized by spaced cleavage domains

Fold tightness

Descriptive term	Interlimb angle (degrees)
isoclinal	0-10
tight	10-30
close	30-70
open	70-120
gentle	120-180

Footwall - the lower block of a non-vertical fault

Fracture persistence

Descriptive term	Trace length (m)
very low	<1
low	1-3
medium	3-10
high	10-20
very high	>20

Fracture spacing

Descriptive term	Spacing (cm)
extremely close	<2
very close	2-6
close	6-20
moderate	20-60
wide	60-200
very wide	200-600
extremely wide	>600

Hanging wall - the upper block of a non-vertical fault

Hydraulic conductivity - a coefficient of proportionality describing the rate at which water can flow through a permeable medium that is a function of both the porous or fractured medium and the density and viscosity of water

Macrojoints - joints that exceed 5 meters in length

Macroscopic - regional scale

Mesoscopic - visible at the scale of outcrops and hand samples

Microjoints - tiny joints that are spaced less than 3 millimeters apart

Microscopic - visible under the microscope

Mode - the value that occurs with the greatest frequency

Normal fault - a fault where the hanging wall appears to have moved downward relative to the footwall

Permeability - a coefficient describing the rate of which water can flow through a medium that is only a function of the porous or fractured medium

Plumose - a joint surface pattern that resembles a feather; indicative of an extensional mode of origin

Plunge - the angle that a linear structure such as a fold axis makes with respect to a horizontal plane measured in a vertical plane

Descriptive Term	Plunge (degrees)
horizontal	0-10
gently	11-30
moderately	31-60
steeply	60-90

Predominant - most common

Prominent - projecting outward (as on a histogram or rose diagram); immediately noticeable

Reverse fault - a high-angle fault where the hanging wall appears to have moved upward relative to the footwall

Slickenside - a highly polished surface that is the result of frictional sliding

Storativity - the volume of water that an aquifer releases from or takes into storage per unit surface area of the aquifer per unit change in head

Strike slip - slip direction, or component thereof, is parallel to the strike of the fault; rake is between 0 and 20 degrees

Stylolitic - widely spaced disjunctive cleavage; commonly the result of pressure (strain) solutioning

Syncline - a fold, the core of which contains stratigraphically younger rocks, and is convex or closes downward

Thrust fault - a low-angle fault where the hanging wall appears to have moved upward relative to the footwall

Wall rock - the rock mass comprising the wall of the fault

APPENDIX A

Methods

Unconsolidated Deposits

Water-Well Log Interpretation and Correlation

Our knowledge of the subsurface geology of unconsolidated deposits in the study area is chiefly from water-well drillers' logs. These logs give descriptions of the types of materials encountered during drilling. These logs vary in quality and their use requires caution in their interpretation due to inadequate geological information. Exact depths and specific deposit types cannot always be defined in the unconsolidated valley fill from the logs. However, correlation and interpretation of the logs do provide enough information to prepare generalized cross sections.

Seismic-Refraction Soundings

Seismic-refraction soundings are useful for delineating the thickness of the unconsolidated materials and depth to bedrock. Seismic-refraction techniques artificially induce vibrations into the ground and measure the average velocity of the vibrations in subsurface materials. Unconsolidated deposits transmit the induced vibrations slower than consolidated bedrock. By measuring the velocities in different units one can calculate depth to bedrock.

We conducted seismic-refraction surveys using an in-line profiling method. We used 12 hertz (Hz) geophones and an energy source placed first at one end and then at the other end of the line of geophones to generate reverse profiles. Intervals between uniformly spaced geophones varied from 25 to 40 feet (7-12 m), depending on the area available to accommodate total line length and the expected depth to bedrock. The reversed profiling method allowed the construction of symmetrical time-distance graphs. The recording instrument was an EG&G Geometrics ES-1225 portable field seismograph. This instrument is a microprocessor-based multichannel shallow-exploration seismograph, consisting of a 12-channel recorder and amplifying unit. The instrument permits signal enhancement, and multiple seismic impulses at each site were used to enhance the signal and help cancel background noise. The energy source was a Bison elastic wave generator (EWG). Bison's EWG creates a high-energy, high-frequency seismic impulse using a 300-pound (136-kg) hammer driven into a steel anvil on the ground surface.

Ten sites were selected for seismic-refraction soundings (one 10 channel and nine 12 channel soundings) to supplement the drillers' logs used in the construction of four cross sections (figures 8-11). The soundings indicated that unconsolidated deposits are homogeneous with respect to seismic velocity. Unconsolidated surficial deposits had seismic velocities ranging from 2,000 to 6,000 feet per second (610 to 1830 m/s). The velocity in bedrock ranged from 10,000 to 12,000 feet per second (3,050 to 3,660 m/s) for sedimentary bedrock and from 5,500 to 6,200 feet per second (1,680 to 1,890 m/s) for volcanic bedrock.

Preparation of Isopach Map

To prepare the isopach map (figure 12), we used the best available information on the depth to bedrock, mostly water-well drillers' records and seismic-refraction data. Where data are not available, we interpolated to estimate the thickness of unconsolidated deposits. For the most part, figure 12 is a crude approximation.

Fractured Rock

Field Methods

Because of the significant contribution of fractures to the total permeability of rock aquifers, we evaluated fracture characteristics across the study area. Outcrop mapping of surface exposures was supplemented with linear-trace analysis, using aerial photographs, in areas of limited or no outcrop.

Outcrop mapping: Outcrop mapping of mesoscopic fractures (visible at the scale of outcrops and hand specimens) was performed at 111 sites in the study area. We used a modified scan-line survey technique at sites with nearly vertical cut walls. The technique involves recording characteristics of fractures that cross a line (measuring tape) that is stretched across an outcrop or rock cut. We recorded scan-line trends so that directional biases could be recognized. The fracture characteristics recorded include attitude, fracture type, mineralization or alteration effects, infilling type, aperture, persistence, and surface planarity and roughness (see glossary). Some outcrops were not well suited for the scan-line survey technique and selective mapping was used to obtain uniform sampling of the fractures at these sites.

To determine true fracture spacings, we measured spacings of selected fracture types and trends at sixteen sites. Our purpose was to develop a preliminary understanding of fracture spacing values, as well as to determine whether trends could be established between fracture spacing and depth. Fracture spacing was measured in centimeters normal to the fracture planes with an estimated precision of ±0.5 millimeters (±0.02 in). We measured spacings for fracture sets demonstrating only small variations in attitude. All measurements were taken at depths less than 5 meters (16 ft) below the top-of-rock. We measured joint spacing in most of the formations underlying the Preuss Sandstone. In addition, we measured the spacing of bedding fractures in the Preuss, Twin Creek, and Nugget Formations, and of faults within a northeast-trending fault zone in the Nugget Sandstone.

Linear-trace analysis: We used aerial photographs to identify linear traces (O'Leary and others, 1976) throughout the Snyderville basin. Natural linear traces visible on aerial photographs and continuous for less than one mile are sometimes referred to as fracture traces (Lattman, 1958). They may include topographic, vegetation, or soil tonal alignments. Although a linear trace can be the direct manifestation of a macroscopic (regional) joint or a fault, it may also be the surface expression of another geologic feature such as a contact between two different rock types. Alternatively, a linear trace may not represent a geologic feature at all. Linear traces, however, have been correlated successfully with both joints and other geologic structures (Cheema and Islam, 1994).

Linear traces were mapped by a single observer, and therefore have not been filtered through use of a reproducibility test (Mabee and others, 1994). The traces were transferred to topographic maps and the trend and length determined for each. Trace intensity in the Keetley Volcanics was locally extremely high and prohibited including all data into the analysis. A selective sample of at least twenty-five traces was collected by placing a small square grid over an area of high linear-trace density. The data were compared with the total population of linear traces near the sample area to evaluate whether the sample was representative of the entire population of observed traces.

Limitations: Directional sampling methods, such as the scan-line survey technique used, can bias the fracture-trend (attitude) data. We chose a scan-line survey technique, however, because it reduces some of the subjectivity in sampling that can result otherwise. An orientation effect (Terzaghi, 1965; Lapointe and Hudson, 1985) is inherent in directional sampling because of the dependency of fracture frequency to the angle between the scan line and the predominant fracture orientations. The orientation effect is reduced or eliminated by taking two or more scan-line surveys at large acute angles to each other in any given area where fracture trends will be defined. In areas with multiple stations (where the number of stations [m] is greater than 1 in the tables on plates 12, 13, 14, and 15) and oriented as described, the orientation effect will be reduced. Modifications to the sample collecting technique were also made to include scan-line-parallel fractures. The modification potentially reintroduces some subjectivity into the data collection. The potential for a bias resulting from the orientation effect is greatest where trends are shown based on single scan-line stations. No correction was made to the trend data presented in this study, but instead the scan-line direction was recorded so that the potential for directional bias could be identified. Where the prominent trends are at small acute angles to the scan-line direction, the relative frequency relationships shown in the rose diagrams are likely representative. Alternatively, where prominent trends are nearly perpendicular to the scan-line direction, there is a potential that their relative frequency is overestimated (Lapointe and Hudson, 1985).

Other limitations that influence quantitative determination of fracture aperture and persistence became apparent during the outcrop mapping. Natural surficial processes and other disturbances have increased fracture aperture at the outcrop. Surficial processes include ice and root wedging, natural decrease in lateral stresses due to erosion, and toppling. Disturbance due to root wedging was the most easily recognized and noted. Other disturbances include blast-induced widening of fractures, mechanical disturbance of the rock mass, and excavation-induced stress release effects. The aperture values reported in this study likely reflect widening from natural surficial processes and other disturbances, although widening was noted in field logs wherever recognized. Fracture-persistence measurements were restricted by the size of the outcrops. Only a few of the available outcrops exceeded 5 meters (16 ft) in length in all directions, and mapping of true fracture length was limited to fractures with lengths less than the outcrop dimensions. In general, only a minimum length could be determined for fractures.

The linear-trace data are also subject to some limitations. A modified version of domain overlap analysis (Mabee and others, 1994) was employed in areas where outcrop mapping was performed to evaluate the nature of the traces (figures 32, 33, and 34). In areas where outcrops were absent or access was restricted, the nature of the traces could be evaluated only by projection from the closest available outcrop data. We chose not to present the raw linear traces because they were not filtered to eliminate traces that do not meet a reproducibility criteria and do not correlate with outcrop fracture data.

Preparation of Structure Cross Sections

We constructed cross sections using available geologic data (Crittenden and others, 1966; Bromfield and Crittenden, 1971; Crittenden, 1974; Bryant, 1990; Jarvis and Yonkee, 1993) supplemented with limited geologic mapping and structural analysis. In constructing the cross sections, we reinterpreted previous mapping (Crittenden and others, 1966; Bromfield and Crittenden, 1971). In many cases, the contacts on published maps, although shown as approximate, required relocation on the cross sections. However, in many of these areas, the contacts are covered by colluvium and are difficult to locate in the field. In other cases, mapping errors were noted and revised on the cross sections. In a few cases, we inferred additional faults that do not appear on the previously published maps.

We developed cross sections using the kink method (Faill, 1969, 1973; Suppe, 1985) which assumes that limbs of folds have a constant dip. The assumption of constant dip is generally valid over short distances in most of the study area, and allows for easier prediction of the approximate depth to a specific contact. We did not attempt to balance the cross sections; however, the kink method ensures proper line length and area balancing where sufficient data are available (Tearpock and Bischke, 1991). Our use of the kink method does not imply that we believe all macroscopic folds have angular hinge zones. Rather, the method allowed us to impose some realistic constraints in developing the cross sections. The method also allows the engineer or other user to estimate the depth to a layer or contact because a well site will generally be located within a single constant dip domain.

We used formation thicknesses from published measured sections and thicknesses (Boutwell, 1912; Granger, 1953; Bromfield, 1968; Hintze, 1988). In addition, we estimated thicknesses using descriptive geometry techniques and published maps. Table C.1 in appendix C shows the wide range of formation thicknesses from these sources and the ranges used in the cross sections. In most cross sections, we assumed constant formation thickness along the section line. However, formation thicknesses are, in many cases, significantly different in the hanging wall than in the footwall of the Mount Raymond-Medicine Butte thrust (table 1).

Preparation of Structure-Contour and Isochore Maps

We developed structure-contour and isochore maps using the cross sections and published map data. Elevations and thicknesses were determined from the cross sections and plotted along the section lines. Elsewhere, we plotted structure-contour lines using geometric techniques or directly from geologic-map data. We constrained structure-contour-line trends using bedding attitude data at the ground surface. We estimated trends of isochore lines on the basis of inferred fold geometry and bedding attitude. In areas of outcrop between the traces of the upper and lower contacts, we ignored second-order thickness variations due to topography to simplify the isochore lines, but acknowledge that estimates of isochore thickness will vary from actual vertical thickness observed in wells due to such topographic effects.

Determination of Fracture Domains

We analyzed mesoscopic and macroscopic fracture and linear-trace data to delimit fracture domains in the study area. We plotted fracture trends (strike directions) on rose diagrams using a 10-degree class interval. A minimum of four measurements was required before a rose diagram would be plotted for a single fracture type at a station. Prominent fracture trends were determined from the rose diagrams. We plotted the prominent trends onto interim maps to evaluate the spatial distribution of specific fracture trends. Clusters of stations with similar prominent trends defined preliminary domains. In many cases, we established boundaries between domains using a trial and error method. This method involved adding fracture data from adjacent stations to a preliminary domain fracture set to evaluate whether the addition altered the fracture pattern in the domain. Wherever possible, we attempted to select reasonable geologic features as boundaries. On our final domain maps, we terminated the domains wherever the distance to the nearest outcrop station exceeded one kilometer. In a few areas, we were able to extend the boundaries on the basis of linear-trace data, where such trends correlated (±15 degrees) with the outcrop data. Unfortunately, in most areas where outcrop data were lacking, trace trends showed poor correlation with prominent fracture trends of adjacent fracture domains (figure 34). Macroscopic fault trends were measured from published geologic maps.

APPENDIX B

Use of the Structure-Contour and Isochore Maps and Cross Sections

Use of the Structure-Contour Maps

The structure-contour maps allow the user to estimate the depth to the upper contact of an underlying ground-water compartment or formation. The maps show the subsurface elevation of the top of the unit (figure B.1a). Contour lines are typically shown until the approximate depth of the upper contact exceeds 2,500 feet (762 m). The depth to the top of the unit, or the thickness of the overlying deposits, can be estimated by subtracting the elevation of the upper contact from the ground-surface elevation at the well site.

The traces of where the upper and lower contacts intersect the ground surface are also shown on the maps. Due to topography, the traces are irregular. The ground-water compartment or formation crops out at the surface, except where covered by overlying Tertiary or Quaternary deposits, between the traces of the upper and lower contacts. The contour lines of the upper contact would be above the ground surface in this interval and therefore are not shown.

Use of the Isochore Maps

The isochore maps allow the user to estimate the total vertical thickness of an underlying compartment or formation (figure B.1b). The trace of the lower contact's intersection with the ground surface represents the zero-thickness line. Wells must be located on the "downdip" side of this trace where the unit crops out to encounter the unit. Isochore thickness increases progressively in this "downdip" direction from the lower contact to the upper contact. Wells between the traces of the upper and lower contacts will penetrate only a portion of the unit, in addition to some thickness of overlying Tertiary or younger deposits. For wells between the upper and lower contacts and in areas underlain by unconsolidated deposits, the depth to the bottom of the unit can be estimated by adding the isochore thickness to the estimated thickness of unconsolidated deposits (figure 12). For wells located on the "downdip" side of the upper contact, isochore thickness varies directly with the dip of the formation. The depth to the bottom of the unit can be estimated by adding the isochore thickness to the depth to the upper contact, determined from the structure-contour map as described above.

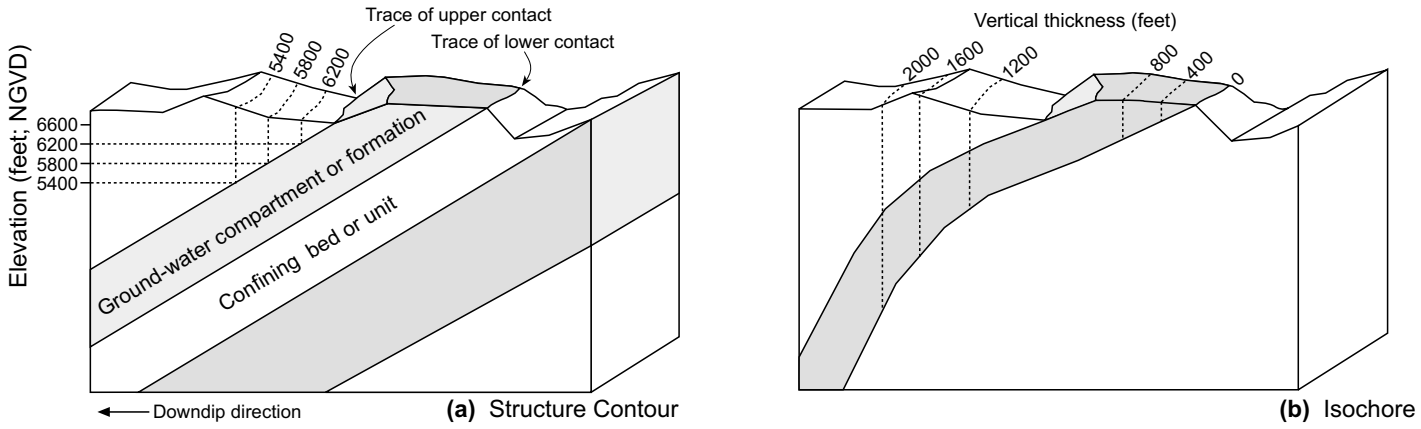

Figure B.1. *Explanation of information shown on structure-contour and isochore maps.*

Example Demonstrating the Use of the Maps and Cross Sections

To demonstrate how to use the maps and cross sections to site future water wells, we have selected a hypothetical proposed well located in Park City as an example. We locate this hypothetical well 2,000 feet south and 400 feet west of the northwest corner of section 10, T. 2 S., R. 4 E. at an old prospect site shown by an "x" (plate 10). The ground-surface elevation at this site is approximately 6,780 feet. In this demonstration we will show how the maps and cross sections assist in the following:

1. identifying potential ground-water compartments at depth,
2. determining the depth to the top of the ground-water compartment/formation,
3. determining the vertical thickness of the ground-water compartment/formation,
4. indicating whether an overlying confining bed will provide protection with respect to water quality, and
5. evaluating whether continuous pumping will affect nearby GWC.

Identifying Ground-Water Compartments at Depth

The structure-contour map (plate 10) shows that the Park City Anticline ground-water compartment underlies the well site. Historical accounts of water inflows from the Park City mining district indicate the presence of highly permeable fracture zones in the Weber Quartzite. Although not shown on the plate, the lower part of the Park City Formation may also yield water to the well.

Depth to the Top of the Weber Quartzite

The depth to the top of the Weber Quartzite can be determined by subtracting the elevation of the upper contact, shown on plate 10 to be approximately 6,150 feet, from the ground-surface elevation at the site.

6,780' - 6,150' = 630 feet

Vertical Thickness of the Weber Quartzite

The isochore map (plate 11) indicates the vertical thickness of the aquifer exceeds 1,600 feet at the well site. If the well is designed to be 1,500 feet deep and the top of the Weber Quartzite is at a depth of 630 feet, then the well will be completed only in the upper part of the Park City Anticline GWC. The estimated thickness of Weber Quartzite intercepted by the well is:

1500' - 630' = 870 feet

Presence of an Overlying Confining Bed

Because the well is located where the upper contact is in the subsurface, overlying formations are intercepted by the well. At this site, evaluating the nearest cross section (B-B' on plate 3) indicates that the subsurface geology consists of a thin veneer of colluvium/alluvium overlying the Park City Formation and the Weber Quartzite.

The phosphatic shale member of the Park City Formation (figure 19) is a confining bed that may protect the underlying GWC from contamination due to surface infiltration near the well site and to the north. The phosphatic shale member separates the Weber Quartzite SGWC (Park City Anticline GWC) from the overlying Upper Park City SGWC that is in turn separated from the Lower Thaynes SGWC (lower part of the Park Meadows GWC shown in cross section B-B' in plate 3) by the lower part of the Woodside Shale.

Evaluating Effect of Continuous Pumping on Adjacent GWCs

The cross sections (A-A' and B-B' on plate 3) and structure-contour maps (plates 8 and 10) show two important GWCs nearby, the Queen Esther and Park Meadows. As described above, several confining beds separate the Park City Anticline GWC from the Park Meadows GWC and therefore pumping from one will not likely affect the other. Cross sections A-A' and B-B' (plate 3) show that the Frog Valley thrust severs the Weber SGWC. In addition, the thrust likely acts as a ground-water barrier-conduit. Several other unnamed faults between the well site and the Queen Esther GWC (cross section B-B') likely act as boundaries to ground-water flow. It is therefore unlikely that continuous pumping at the well site will affect water levels in any wells in the Queen Esther GWC.

Table C.1.
Summary of formation thicknesses.

	Thickness (ft)										
Formation **Source**	**Weber Quartzite**	**Park City Fm.**	**Woodside Shale**	**Thaynes Fm.**	**Ankareh Fm.**	**Nugget Ss.**	**Twin Creek Ls.**	**Preuss Ss.**	**Kelvin Fm.**	**Frontier Fm.**	**Keetley Volcanics**
Boutwell (1912) Big Cottonwood Canyon Treasure Hill sequence Silver King Consolidated Shaft	>1,350	 590 700	1,180 1,090 700	1,190 1,290	 1,150	>500	—	—	—	—	—
Mount (1952) Silver Creek Area north of Round Valley Pace section	—	—	725	1,376	—	 1,000	 1,350	—	—	—	—
Granger (1953) Salt Lake City area	—	974	384	1,971	1,299	830	2,821	1,020	1,669	8,724	—
Barnes and Simos (1968)	1,235 1,215-1,350	670	680-700	1,150	—	—	—	—	—	—	—
Bromfield (1968)	—	—	700-800	—	1,400-1,450	—	—	—	—	—	—
Hintze (1988) Park City-Kamas-Coalville near Salt Lake City	 1,300 1,200-1,500	 650 900-1,700	 600-700 400	 1,150 1,800-2,300	 1,230 1,700	 1,000-1,400 1,300	 1,380 2,850	 1,000 1,000	 3,250 1,700	 6,800- 8,760 7,000 -8,000	 up to 2,000
Bromfield (1989)	1,300-1,500	550-650	650-820	1,100-1,300	1,640	820					up to 1,640
Jarvis and Yonkee (1993) Summit Park	—	—	—	—	—	1,350	2,520-2,760	—	—	—	—
Range reported in literature	1,215-1,500 1,200(SLC)- 1,500	550-700 550- 1,700(SLC)	600-1,180 384(SLC)- 1,180	1,100-1,376 1,100 -2,300 (SLC)	1,150-1,640 1,150 -1,700 (SLC)	820-1,400	1,350-2,760 1,350 -2,850 (SLC)	1,000-1,020	3,250 1,700 (SLC)	6800-8,760	up to 1,640- 2,000
As determined from 7.5' geologic quadrangle maps: Ecker Hill area Big Cottonwood Canyon area Daly West shaft area	 1,380	 785-1,230	 910	 2,050-2,350 1,335 1,225	 1,290 1,550	— 	— 	— 	— 	— 	—
Used in cross sections	1400	600-950(?)	725-1,000	1,375-2,200	1,150-1,700	1,150-1,350	1,500-2,600	1000	ns	ns	ns

1. Thickness reported adjacent to name of source(s) where specific location of measured section is not specified. In most cases, the reported thickness is for the Park City mining district.
2. SLC = Salt Lake City area.
3. ns = total thickness not shown on cross sections.

Table D.1.
Summary of mesoscopic fold geometry.

Formation	Site Number	**Bedding Attitude** Strike, Dip	**Fold Axis Attitude** Plunge, Bearing	**Axial Plane Axial Trace** Strike, Dip or Dip	Fold Type	Fold Shape	Fold Description
Twin Creek Limestone:	1	044, 27 SE 038, 65 SE	04, 216	034, 43 NW moderately inclined	WNW-verging, E-closing asymmetric fold	rounded hinge planar limbs i = 142, gentle	WNW-verging, moderately inclined SSW-trending, gentle anticline
	2		subhorizontal?, 110		neutral		
	3		08, 327	approx 30 NE	synform? closes to NE	i = approx 110	
	4		subhorizontal, 110	approx 45 S	antiform part of N-verging S-fold	rounded? hinge i = approx 90	
	5	272, 40 N 286, 30 N 314, 46 SW	18, 295 to 10, 304	185, 19 W to 170, 13 W gently inclined to recumbent	teepee structure closes to N	angular hinge planar limbs i = 72-78 open	gently inclined to nearly recumbent, gently plunging, open fold
	6	293, 87 N 291, 83 N 295, 48 S 288, 71 S	02, 293 to 04, 291 or 12, 112 to 06, 110	281, 18 N 344, 15 NE	S-closing fold below teepee fold	subrounded hinge planar to sl. curved limbs i = 130-150; gentle	gently inclined, gentle, S-closing fold
	7	307, 74 SW 294, 65 SW 320, 47 SW 307, 46 SW	00, 307	307, 31 NE	drag folding in footwall of NE-directed thrust	i = 153 gentle	moderately inclined, gentle, S-closing fold
	8			approx 30 SE	W-closing fold	subrounded hinge planar limbs i = approx 105 part of S-fold	
	9	027, 60 SE 204, 70 SE 010, 86 E 012, 90	14, 199 27, 012	026, 65 E 011, 88 E curved AP	isoclinal antiform? closes to W-SW	rounded hinge sl. curved limbs? i = 4 to i = 10; isoclinal	steeply inclined to upright, gently plunging, isoclinal antiform?
	10	060, 50 NW 027, 78 NW	39, 017	336, 52 E	asymmetric anticline closes to SW younging on SW limb is toward NW	subrounded hinge planar limbs i = 140 gentle	asymmetric, moderately inclined, moderately plunging, gentle anticline
Thaynes Formation:	1	353, 89 W 030, 79 W	73, 350	284, 74 N	closes to NW?	i = 143 gentle	steeply inclined, steeply plunging, gentle antiform?
	2	010, 73 W 021, 72 W 044, 60 NW	71, 303 to 52, 356 57, 341	307, 70 NE	closes to NW? i = 147; gentle	subrounded hinge gentle antiform	steeply inclined, steeply plunging,

(continued on next page)

Table D.1. (continued)

Formation	**Site Number**	**Bedding Attitude** Strike, Dip	**Fold Axis Attitude** Plunge, Bearing	**Axial Plane Axial Trace** Strike, Dip or Dip	**Fold Type**	**Fold Shape**	**Fold Description**
	3	014, 39 W 008, 37 W 020, 36 W 021, 36 W 019, 58 W 008, 72 W 027, 78 W 028, 85 W	02, 018	013, 30 E	hanging-wall anticline	i = 142 gentle	moderately inclined, gentle anticline
Mahogany Member of the Ankareh Formation:	1		60, 028	302, 64 NE	isoclinal closes to NW	rounded hinge planar limbs	
	2		similar to above	bedding parallel	isoclinal	rounded hinge planar limbs	
	3		similar to above	bedding parallel	isoclinal	angular hinge	
Park City Formation:	1	348, 50 W 012, 18 W	10, 339	333, 59 NE	synform	rounded hinge? sl. curved limbs? i = 147; gentle	moderately inclined; gently plunging, gentle synform

Note: i is the interlimb angle, commonly shown as alpha.

Table D.2.
Summary of macroscopic fold geometry.

Informal Fold Name	Formations	Fold Axis Attitude Plunge, Bearing	Axial Plane Attitude Strike, Dip	Tightness	Fold Description
Round Valley anticline	Twin Creek Ls., Nugget Ss. Ankareh Fm. median	28, 291 26,293 27, 292	294, 84 S 300, 77 SW 297, 80 S	i = 138; gentle i = 153; gentle i = 145; gentle	gently WNW-plunging, steeply inclined to upright, gentle, asymmetric anticline
Quarry Mountain syncline	Nugget Ss. Ankareh Fm.	20, 304 21, 320	319, 87 NE 307, 82 SW	i = 133; gentle i = 138; gentle	gently NW-plunging, gentle syncline
Iron Mountain anticline (Park City anticline-NW)	Nugget Ss.	16, 304 to 24, 327; 21, 317	308, 78 SW to 329, 86 SW; 320, 84 SW	i = 153 to 156; 153 gentle	gently NW-plunging, gentle anticline
	Ankareh Fm.	22, 307 to 22, 338	312, 73 SW to 339, 87 SW	i = 152 to 156; gentle	gently NW- to NNW-plunging steeply inclined to upright gentle anticline
	Park City Fm.	30, 307 to 25, 335	307, 90 to 331, 81 NE	i = 166 to 177; gentle	gently NW- to NNW-plunging gentle anticline
Dutch Draw syncline	Twin Creek Ls., Nugget Ss.	02, 039 to 10, 045; 10, 045	040, 74 NW to 044, 85 SE; 044, 85 SE	i = 99 to 54; close to open	horitzonal to gently NE-plunging, steeply inclined to upright, close to open syncline
Willow Draw anticline	Twin Creek Ls., Nugget Ss.	040	040, 80-84 NW	i = 60-90; possibly up to 133?; close to gentle?	horizontal?, NE-trending, close to gentle anticline
	Nugget Ss., Ankareh Fm.	04, 027 06, 031 01, 038	026, 74 SE 030, 85 SE 038, 86 NW	i = 102; open i = 132; gentle i = 100; open	horizontal, NNE- to NE-trending, steeply inclined to upright, open to gentle, anticline
Ski Jump anticline	Nugget Ss.	05, 034 to 23, 024	032, 70 SE to 024, 90	i = 94 to 61; open to tight	horizontal to gently NNE- to NE-plunging, steeply inclined to upright, open to tight anticline.
Threemile Canyon syncline	Thaynes Fm.	40, 337	335, 88 NE	i = 106; open	moderately NNW-plunging, open syncline
Threemile Canyon anticline	Thaynes Fm.	29, 321 to 30, 316	330, 74 SW to 328, 69 SW	i = 131 to 121; gentle	gently NW-plunging, steeply inclined, gentle anticline
Toll Canyon syncline					
Sec 27 T1S R3E	Ankareh Fm. (Gartra Grit Mbr.)	26, 334	330, 82 NE	i = 69; close	gently NNW-plunging, close syncline
Sec 22S T1S R3E	Ankareh Fm. (Gartra Grit Mbr.), Nugget Ss.	17, 348 to 15, 349	347, 86 E to 348, 88 E	i = 84 to 79; open	gently NNW-plunging, open syncline
Sec 22N T1S R3E	Twin Creek Ls., Nugget Ss.	05, 011 to 06, 011	009, 72 E to 010, 80 E	i = 61 to 20; close to tight	horizontal, N-trending, steeply inclined, close to tight syncline
Sec 15 T1S R3E	Twin Creek Ls.	72, 047 to 59, 030 to 56, 047; 72, 047	012, 79 E to 064, 80 NW to 054, 77 NW; 012, 79 E	i = 39 to 87 to 98; close to open; 39; close	steeply NE-plunging, steeply inclined, close syncline
Twomile Canyon anticline see also Threemile Canyon anticline	Ankareh Fm. (Gartra Grit Mbr.)	34, 063 to 32, 017; 34, 063	008, 41 E to 013, 83 E; 008, 41 E	i = 63 to 131; close to gentle; 63; close	moderately ENE-plunging, moderately inclined, close anticline

Note: i is the interlimb angle, commonly shown as alpha.

APPENDIX E

Fracture Spacing

We measured true fracture spacing at fourteen selected sites (table E.1) in seven different formations. At each site, we measured spacing perpendicular to the fracture surfaces of the prominent systematic (Twiss and Moores, 1992) or persistent fracture set.

These measurements and our field observations suggest that zones of intense fracturing are isolated or surrounded by areas that are less fractured. Subsidiary fault zones, consisting of tight faults spaced close to extremely close, are typically adjacent to major faults. Subsidiary fault spacing increases, or the frequency of faults decreases, with increasing distance away from major faults.

Insufficient average-fracture-spacing data (table E.2) exist to establish unequivocal trends, but some insights are possible from close examination of the data. Table E.2 presents average spacing values for various fracture-set trends. The values are grouped by fracture type, formation, and trend. Although the data provide some insight into fracture spacing in the study area, the data are inadequate for site-specific characterization with respect to fracture spacing.

Table E.1.

Fracture-spacing measurements.

Formation	**Twin Creek Ls.**	**Twin Creek Ls.**	**Nugget Ss.**	**Preuss Ss.**	**Thaynes Fm.**	**Twin Creek Ls.**	**Nugget Ss.**	**Ankareh Fm. upper mbr.**	**Nugget Ss.**	**Weber Qtz.**	**Park City Fm.**	**Nugget Ss.**	**Nugget Ss.**	**Nugget Ss.**	**Nugget Ss.**	**Thaynes Fm.**	**Thaynes Fm.**	**Ankareh Fm. Mahogany Mbr.**
Feature type	Bedding	Calcite veins	Faults	Bedding	Undiff.	Bedding	Joints	Joints	Bedding	Joints	Joints	Joints	Bedding	Joints	Undiff.	Joints	Joints	Joints
Distance to top-of-rock	1-1.5 m	1-1.5 m	1-1.5 m	0-2 m	approx 2-3 m	0.3-3 m	approx 1m	0-approx 1 m	3 m	5 m	approx 1 m	approx 2-3 m	0-4 m	approx 1-3 m	approx 0.5 m	approx 1 m	at TOR	approx 0.5 m
Attitude strike	038 NE	278-284 EW	047-077 NE-ENE	074-078 EW	NE-ENE?	330-340 NNW	304-332 NW	350-008 NS	047-082 NE-EW	004-008 NS	276-298 EW-WNW	359-017 NS-NNE	084-285 EW	062 ENE	062 ENE 040 NE	351-010 NS	078 EW	053-078 NE-ENE
Dip	67 SE	74-85 N	78-88 NW	38 N	—	60-70 NE	72 NE-78 SW	72 E-82 W	32-47 NW	62-63 W	64-80 S	72-90 E	55-62 N	38 SE	74 SE	66-68 E	72 SE	80-90 E
Fracture spacing (cm)	11 18 9 13 7 4 4 3 4 3 10 12 **Avg: 8**	31 22 32 **Avg: 29**	12 6 2.5 21 6 16 12 **Avg: 11**	13 6 7 14 20 7 42 37 6 3 **Avg: 16**	9 5 5 5 8 7 11 15 38 11 7 **Avg: 11**	9 7 6 4 4 8 6 10 12 13 12 13 20 7 4 19 4 14 22 24 12 22 14 6 7 13 20 19 15 12 **Avg: 12**	28 12 16 9 103 17 181 **Avg: 52**	30 8 10 8 **Avg: 14**	17 10 11 10 3 20 40 23 24 16 30 23 28 26 **Avg: 20**	64 73 10 2 60 **Avg: 42**	3 6 3 1 7 1 2 0.5 2 1 0.5 0.25 2 2 2.5 **Avg: 2**	4 8 250 21 108 6 485 18 222 14 144 **Avg: 116**	27 44 34 15 27 29 10 34 26 29 37 27 29 33 18 5 48 51 56 **Avg: 30**	3 3 4 4 6 **Avg: 4**	8 10 12 5 4 3 15 7 5 23 2 3 5 4 15 15 **Avg: 9**	8 15 11 10 13 10 16 27 **Avg: 14**	32 7 7 31 10 18 11 4 9 22 14 10 31 11 14 10 11 **Avg: 15**	17 40 43 67 12 6 67 6 29 4 5 13 **Avg: 26**

Table E.2.
Summary of average-fracture-spacing data.

Fracture Type	Average Spacing (cm)	Formation	Average Spacing (cm) High-Angle	Average Spacing (cm) Bedding Fractures	Trend	Average Spacing (cm)
High-Angle Fractures	2 - 116	Preuss Ss.	—	16	NS	14 - 116
Joints	2 - 116	Twin Creek Ls.	29	8 - 12	NNE	—
Calcite Veins	29	Nugget Ss.	4 - 116	20 - 30	NE	8 - 26
Faults	11	Ankareh Fm. upper mbr.	14	—	ENE	4 - 26
Undifferentiated	9 - 11	Ankareh Fm. Mahogany Mbr.	26	—	EW	2 - 30
Bedding Fractures	8 - 30	Thaynes Fm.	11 - 15	—	WNW	2
		Park City Fm.	2	—	NW	52
		Weber Qtz.	42	—	NNW	12

APPENDIX F

Fracture Persistence

Persistence distributions that are corrected for biases introduced by the actual number of measurements in each formation (table F.1) suggest that joints with lengths that exceed 5 m (16 feet) are most frequent in the Nugget Sandstone and Weber Quartzite. The apparent tendency for higher persistence joints in these formations is likely due, in part, to the availability of large outcrop areas in both. Similarly, corrected persistence distributions suggest that faults with lengths that exceed 5 m (16 feet) are most frequent in the Keetley Volcanics, and somewhat less frequent in the Thaynes, Ankareh (sandstone beds that crop out), Weber, and Nugget Formations. This appears to confirm the tendency for higher persistence fractures in limestone and sandstone as well as in the undifferentiated volcanic rocks of the Silver Creek breccia.

Persistence versus trend (direction) distributions (table F.2) appear to show that certain trends are characterized by higher persistence fractures. Joints that strike north-northeast and east-west, and faults that strike northeast to east-west and northwest, exhibit the highest frequency of persistence values exceeding 5 m (16 feet). The tendency for higher persistence in east-west-striking fractures appears to be the least biased by the frequency of fractures with that trend.

Linear-trace persistence distributions as determined from aerial-photo mapping allow some comparison with mesoscopic persistence; however, the data are admittedly overwhelmed by non-fracture-correlated traces. Figure F.1 shows that traces that trend west-northwest have the longest average lengths, followed by traces that trend east-west, northwest, and east-northeast, listed in descending order. The high average length of east-west-trending traces is consistent with high persistence observed for both mesoscopic joints and faults with this trend. Surprisingly, traces with a northeast trend have the lowest average length, despite that higher persistence mesoscopic faults with this trend are common.

Table F.1.

Corrected relative frequency distribution of high-persistence fractures. Relative frequency (percent) of fractures with persistence greater than 5 m (16 ft).

Formation	Joints	Faults
Keetley Volcanics	5	26
Tertiary intrusives	5	—
Tertiary conglomerates	7	—
Frontier Formation	16	25
Kelvin Formation.	3.5	—
Preuss Sandstone	1.5	7
Twin Creek Limestone	1.5	1
Nugget Sandstone	29	8
Ankareh Formation	2.5	9
Thaynes Formation	3	9
Woodside Shale	2	5
Park City Formation	1	2
Weber Quartzite	21	8

Distributions corrected to reduce bias resulting from differences in the number of measurements in each formation. The high percentage of high-persistence faults shown in Frontier Formation is likely a product of the correction where there is a small number of actual measurements.

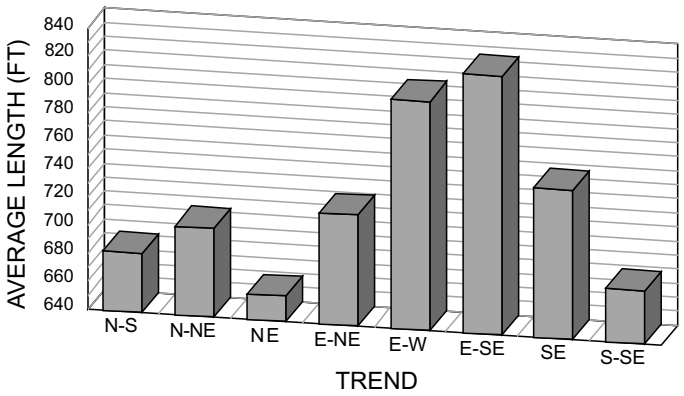

Figure F.1. *Linear-trace persistence versus trend. Histogram shows the average length of 2,298 linear traces separated by trend. Data set likely contains a high percentage of traces that are not the surface manifestation of fractures in rock. Linear traces were mapped from aerial photographs.*

Table F.2.

Relative frequency distribution of high-persistence fractures versus trend. Relative frequency (percent) of fractures with persistence greater than 5 m (16 ft).

Trend	NS	NNE	NE	ENE	EW	WNW	NW	NNW
Joints	15	20	18	7	18	10	5	7
Faults	5	12	24	17	19	7	14	2

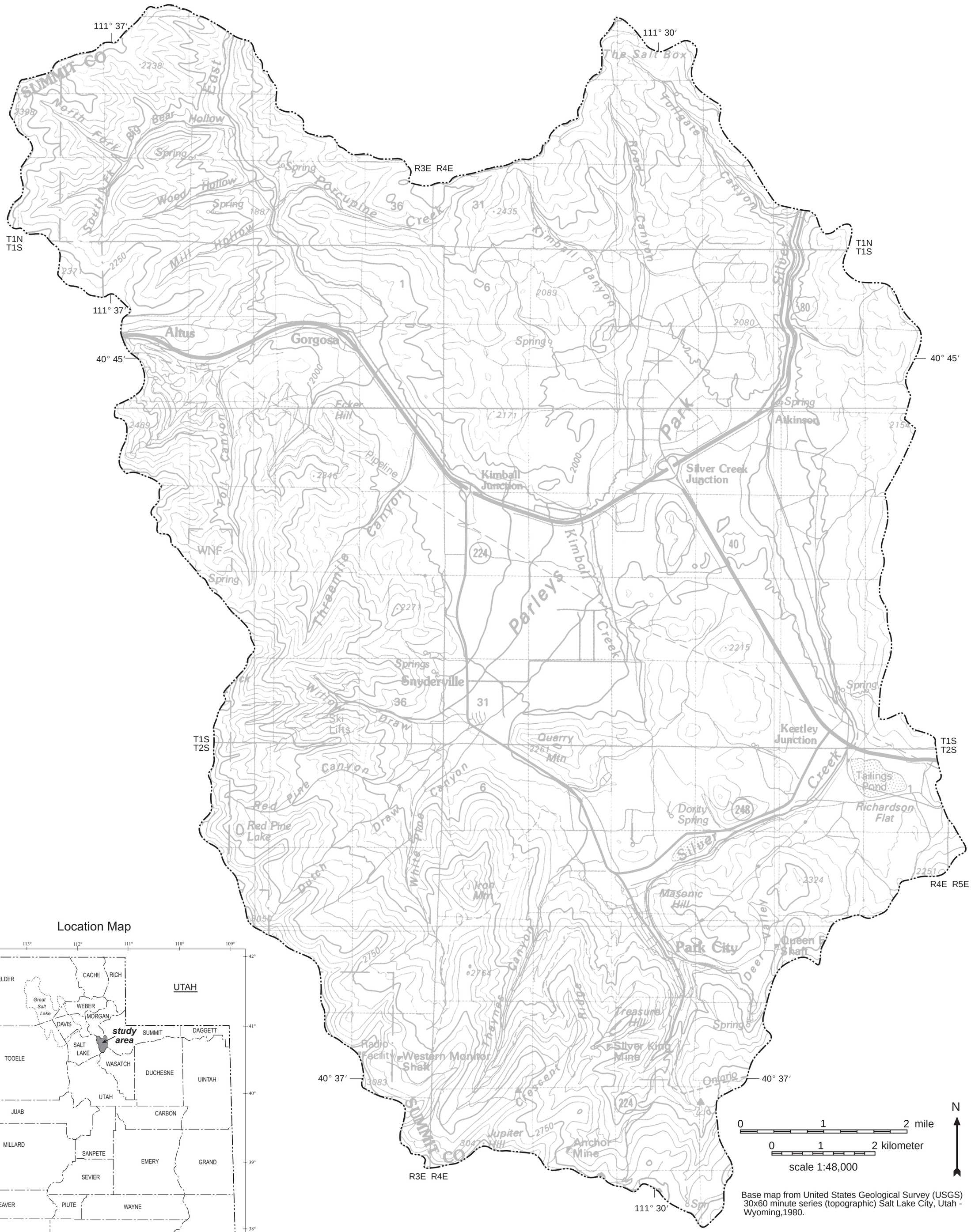

Location Map

0 1 2 mile

0 1 2 kilometer

scale 1:48,000

N

Base map from United States Geological Survey (USGS) 30x60 minute series (topographic) Salt Lake City, Utah - Wyoming,1980.

GEOGRAPHIC MAP OF THE SNYDERVILLE BASIN 2001

EXPLANATION

Qal	Alluvium, glacial outwash, and colluvium, undifferentiated
Qtp	Glacial till, Pinedale
Tk	Keetley Volcanics
Ti	Intrusive rock
Toc	Conglomerate
Twc	Conglomerate (Wasatch Formation)
Kf	Frontier Formation
Kfu	Upper member
Kfo	Oyster Ridge Sandstone Member
Kfl	Lower member
Kfcg	Conglomerate facies
Kk	Kelvin Formation
Kk	Upper member
Kkp	Parleys Member
Jp	Preuss Formation
Jtc	Twin Creek Limestone
Jn	Nugget Sandstone
Ra	Ankareh Formation
Rt	Thaynes Formation
Rw	Woodside Shale
Ppc	Park City Formation
IPw	Weber Quartzite
IPMu	Undifferentiated Carboniferous rock (cross section only)

A — A′ Section line

Contact

Fault, short dashed where concealed, teeth on upthrown side

Plunging anticline, arrows show direction of plunge

Plunging syncline, arrows show direction of plunge

Overturned syncline

0 1 2 mile

0 1 2 kilometer

scale 1:48,000

N

NOTES

1. Base map from United States Geological Survey (USGS) 30x60 minute series (topographic) Salt Lake City, Utah - Wyoming,1980.
2. Geologic-unit contacts modified from digitized contacts provided by USGS.
3. Geology modified from Crittenden and others, 1966; Bromfield, 1968; Bromfield and Crittenden, 1971; Bryant, 1990; and Jarvis and Yonkee, 1993.

GEOLOGIC MAP OF THE SNYDERVILLE BASIN
2001

UTAH GEOLOGICAL SURVEY
a division of
UTAH DEPARTMENT OF NATURAL RESOURCES

Plate 3
WATER RESOURCE BULLETIN 28

NORTHWEST SOUTHEAST

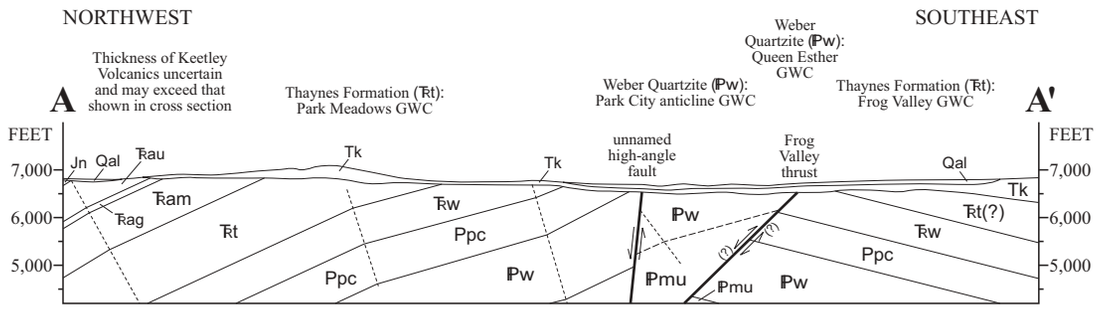

NORTHWEST SOUTHEAST

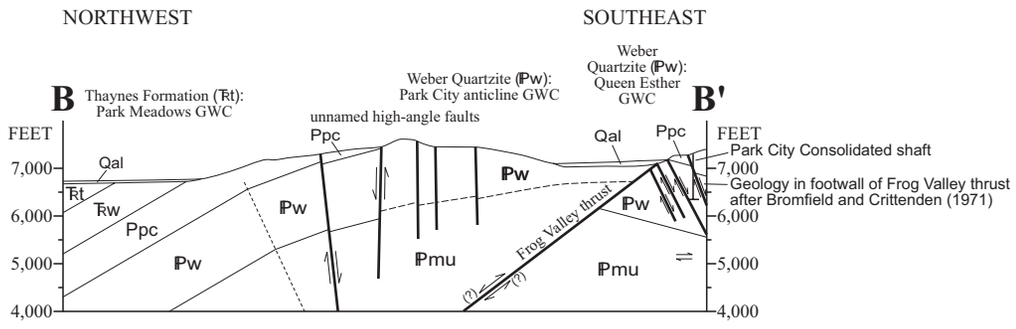

NORTHWEST SOUTHEAST

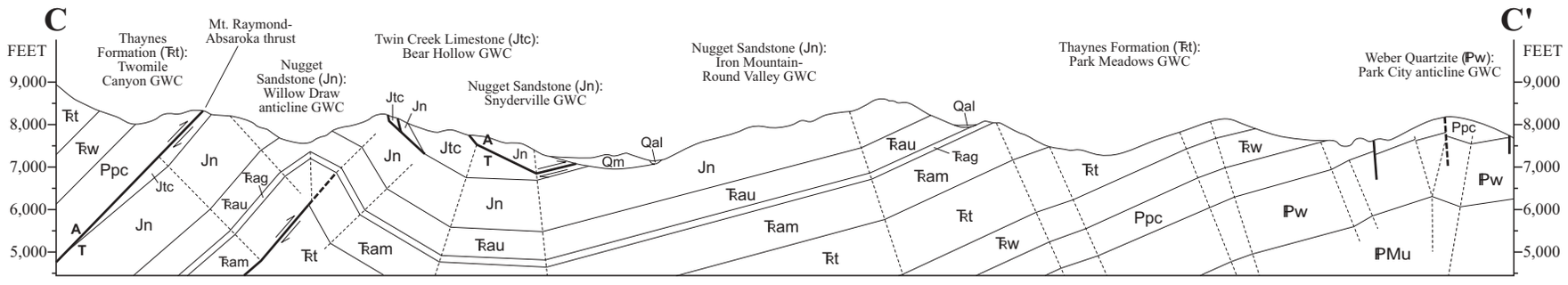

NORTHWEST SOUTHEAST

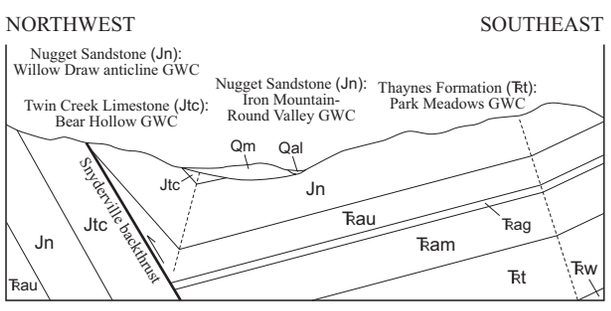

Alternate interpretation of part of C-C'

SOUTHWEST NORTHEAST

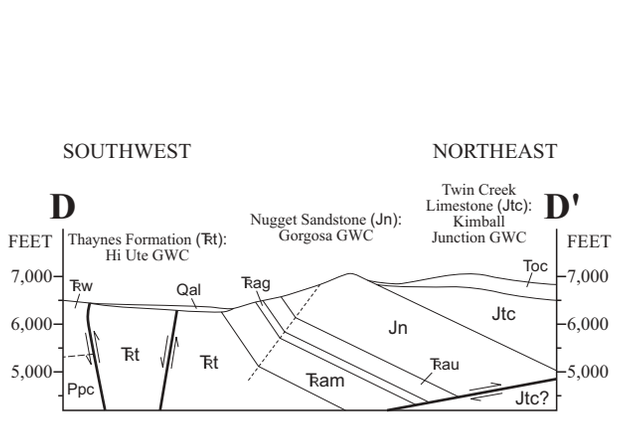

NORTHEAST SOUTHWEST

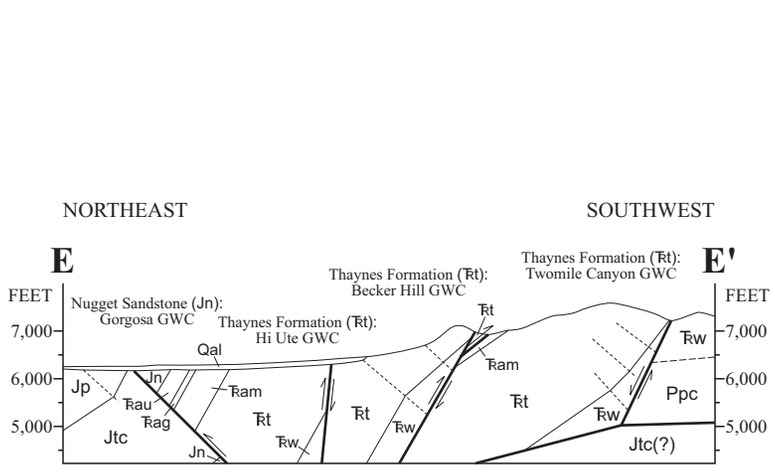

NORTH SOUTH

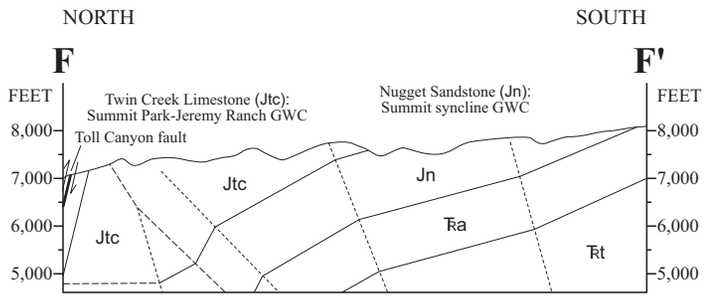

EXPLANATION

Fault

Axial trace

Contact, dashed where speculative

Mine workings

Fractured-Rock Ground-Water Compartments (GWCs)

Jtc	Twin Creek Limestone (upper and lower undivided)
Jn	Nugget Sandstone
Trt	Thaynes Formation (upper and lower undivided)
Pw	Weber Quartzite (includes lower Ppc)

See plate 2 for explanation of symbols and other geologic units shown in cross sections. See plates 2, 4, 6, 8, and 10 for locations of section lines.

0 1 2 miles

0 1 2 kilometers

scale 1:48,000

NOTES

1. Cross sections developed using the kink method (Faill, 1969, 1973; Suppe, 1985). The method depicts folds as having planar limbs and angular hinge zones. The depiction of planar fold limbs is generally valid over short distances in the study area, and allows the user to easily estimate the depth to an aquifer. Fold hinge shape varies from rounded to angular in the study area.

2. Cross sections are speculative where pre-Tertiary formations are covered by Tertiary and younger deposits.

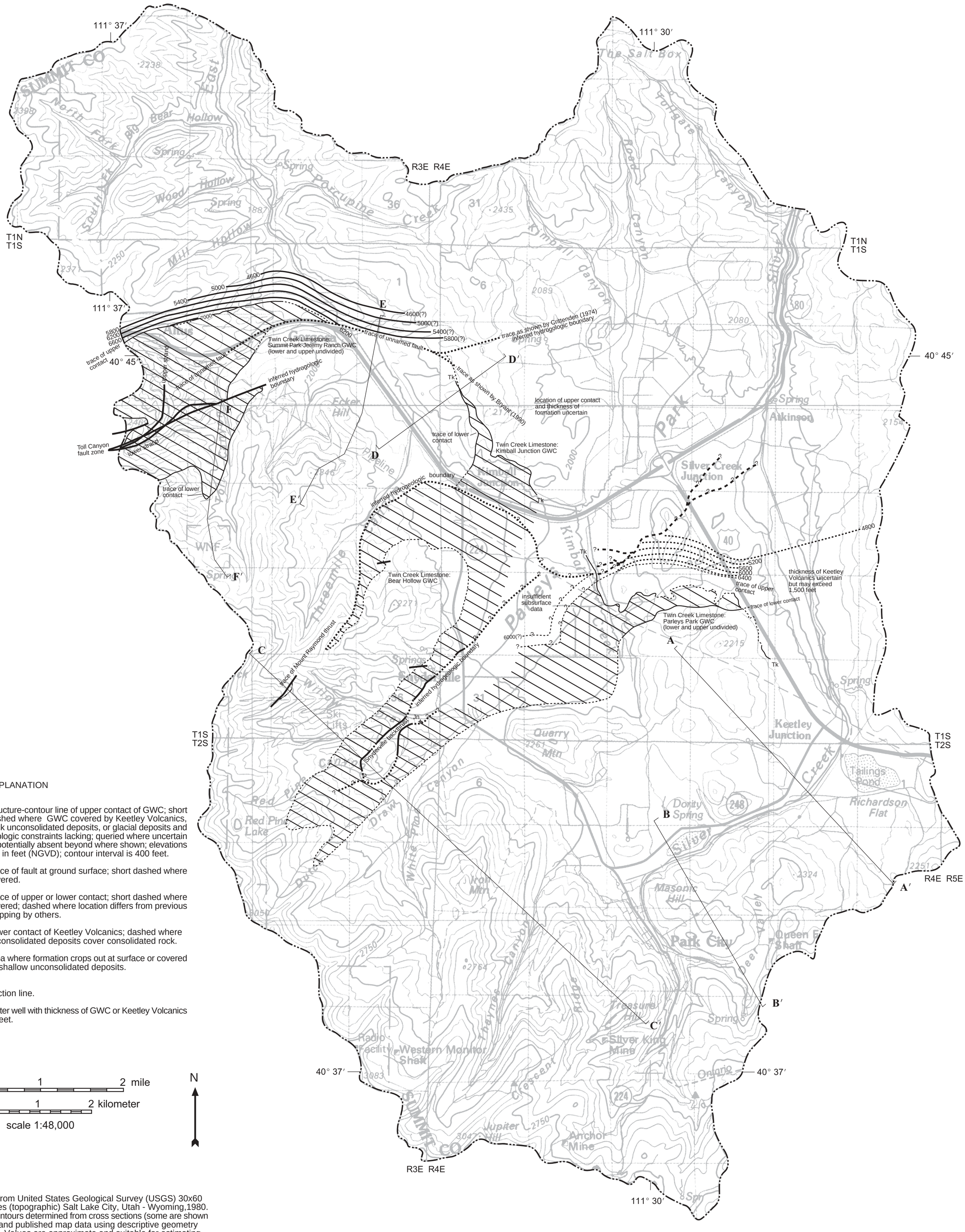

EXPLANATION

- Structure-contour line of upper contact of GWC; short dashed where GWC covered by Keetley Volcanics, thick unconsolidated deposits, or glacial deposits and geologic constraints lacking; queried where uncertain or potentially absent beyond where shown; elevations are in feet (NGVD); contour interval is 400 feet.
- Trace of fault at ground surface; short dashed where covered.
- Trace of upper or lower contact; short dashed where covered; dashed where location differs from previous mapping by others.
- Lower contact of Keetley Volcanics; dashed where unconsolidated deposits cover consolidated rock.
- Area where formation crops out at surface or covered by shallow unconsolidated deposits.
- A A′ Section line.
- Water well with thickness of GWC or Keetley Volcanics in feet.

0 1 2 mile
0 1 2 kilometer
scale 1:48,000

N

NOTES

1. Base map from United States Geological Survey (USGS) 30x60 minute series (topographic) Salt Lake City, Utah - Wyoming,1980.
2. Structure contours determined from cross sections (some are shown on plate 3) and published map data using descriptive geometry techniques. Values are approximate and suitable for estimating purposes only.
3. GWC = Ground Water Compartment, SGWC = Stratigraphic Ground Water Compartment, NGVD = National Geodetic Vertical Datum.

STRUCTURE-CONTOUR MAP OF THE TWIN CREEK LIMESTONE, SNYDERVILLE BASIN
2001

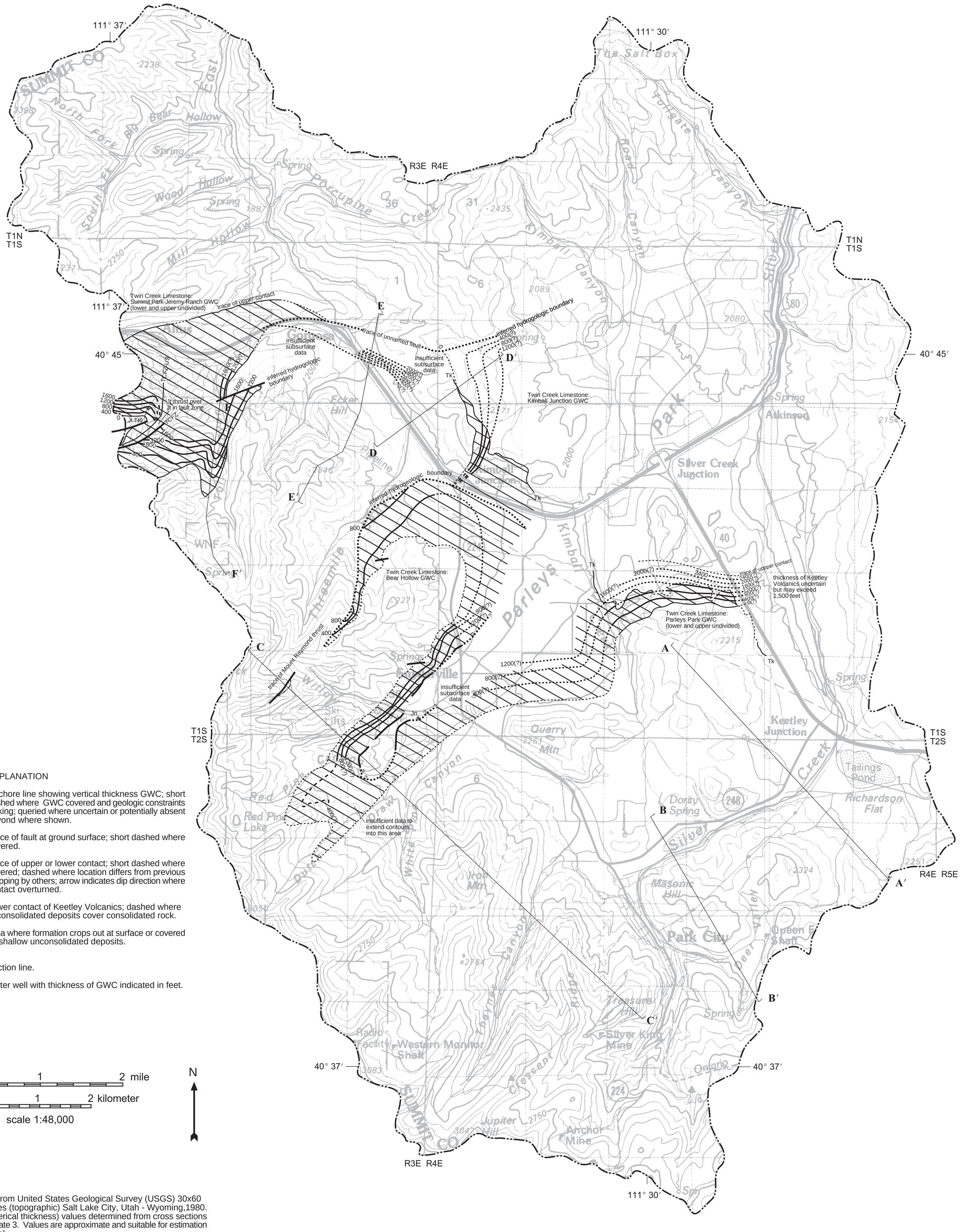

EXPLANATION

- Isochore line showing vertical thickness GWC; short dashed where GWC covered and geologic constraints lacking; queried where uncertain or potentially absent beyond where shown.
- Trace of fault at ground surface; short dashed where covered.
- Trace of upper or lower contact; short dashed where covered; dashed where location differs from previous mapping by others; arrow indicates dip direction where contact overturned.
- Lower contact of Keetley Volcanics; dashed where unconsolidated deposits cover consolidated rock.
- Area where formation crops out at surface or covered by shallow unconsolidated deposits.
- A — A′ Section line.
- Water well with thickness of GWC indicated in feet.

NOTES

1. Base map from United States Geological Survey (USGS) 30x60 minute series (topographic) Salt Lake City, Utah - Wyoming,1980.
2. Isochore (verical thickness) values determined from cross sections shown on plate 3. Values are approximate and suitable for estimation purposes only.
3. GWC = Ground Water Compartment, SGWC = Stratigraphic Ground Water Compartment, NGVD = National Geodetic Vertical Datum

ISOCHORE MAP OF THE TWIN CREEK LIMESTONE, SNYDERVILLE BASIN
2001

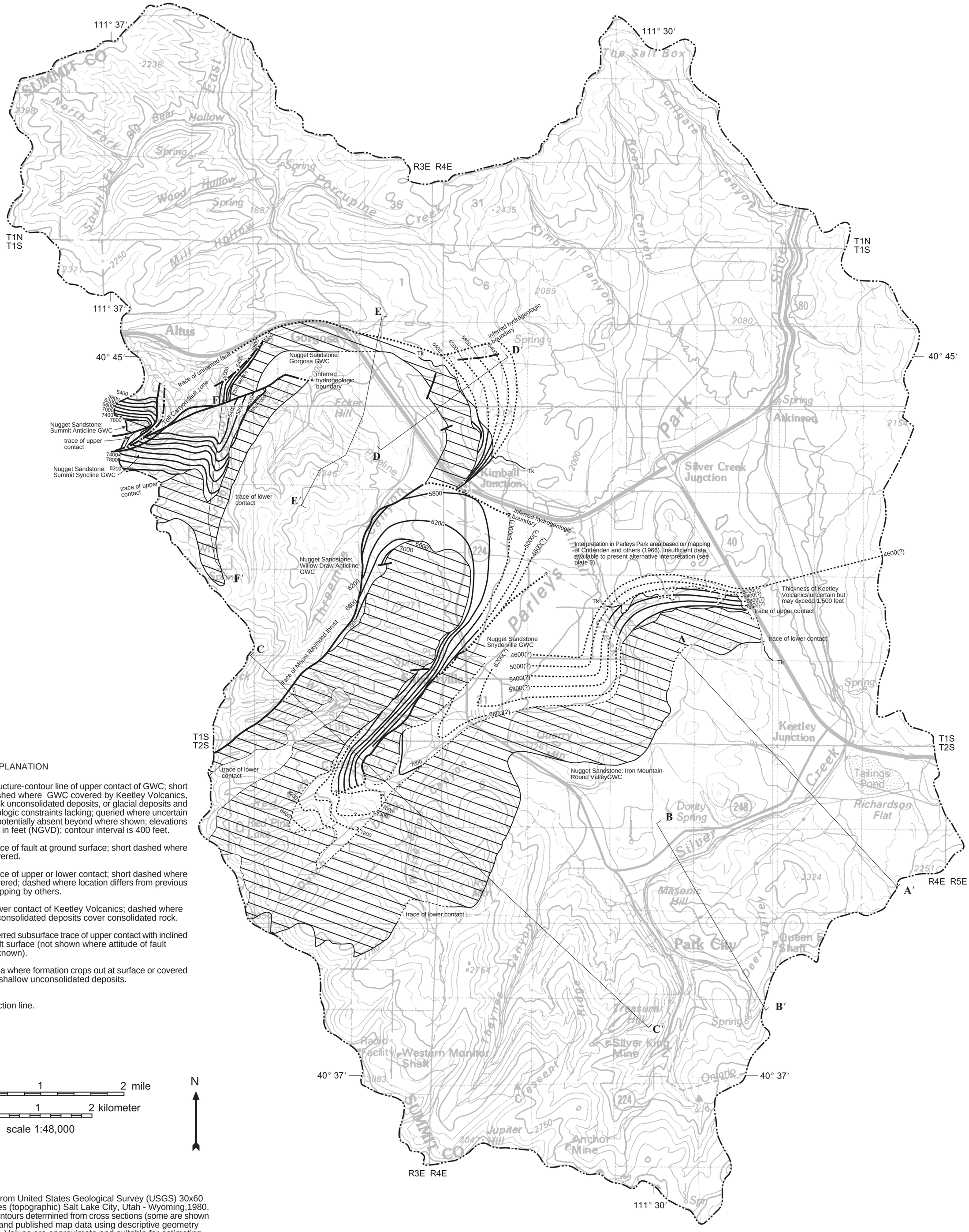

EXPLANATION

- Structure-contour line of upper contact of GWC; short dashed where GWC covered by Keetley Volcanics, thick unconsolidated deposits, or glacial deposits and geologic constraints lacking; queried where uncertain or potentially absent beyond where shown; elevations are in feet (NGVD); contour interval is 400 feet.
- Trace of fault at ground surface; short dashed where covered.
- Trace of upper or lower contact; short dashed where covered; dashed where location differs from previous mapping by others.
- Lower contact of Keetley Volcanics; dashed where unconsolidated deposits cover consolidated rock.
- Inferred subsurface trace of upper contact with inclined fault surface (not shown where attitude of fault unknown).
- Area where formation crops out at surface or covered by shallow unconsolidated deposits.
- A A′ Section line.

0 1 2 mile
0 1 2 kilometer
scale 1:48,000

N

NOTES

1. Base map from United States Geological Survey (USGS) 30x60 minute series (topographic) Salt Lake City, Utah - Wyoming,1980.
2. Structure contours determined from cross sections (some are shown on plate 3) and published map data using descriptive geometry techniques. Values are approximate and suitable for estimating purposes only.
3. Structure contours were not extended into upland areas.
4. GWC = Ground Water Compartment, SGWC = Stratigraphic Ground Water Compartment, NGVD = National Geodetic Vertical Datum.

STRUCTURE-CONTOUR MAP OF THE NUGGET SANDSTONE, SNYDERVILLE BASIN
2001

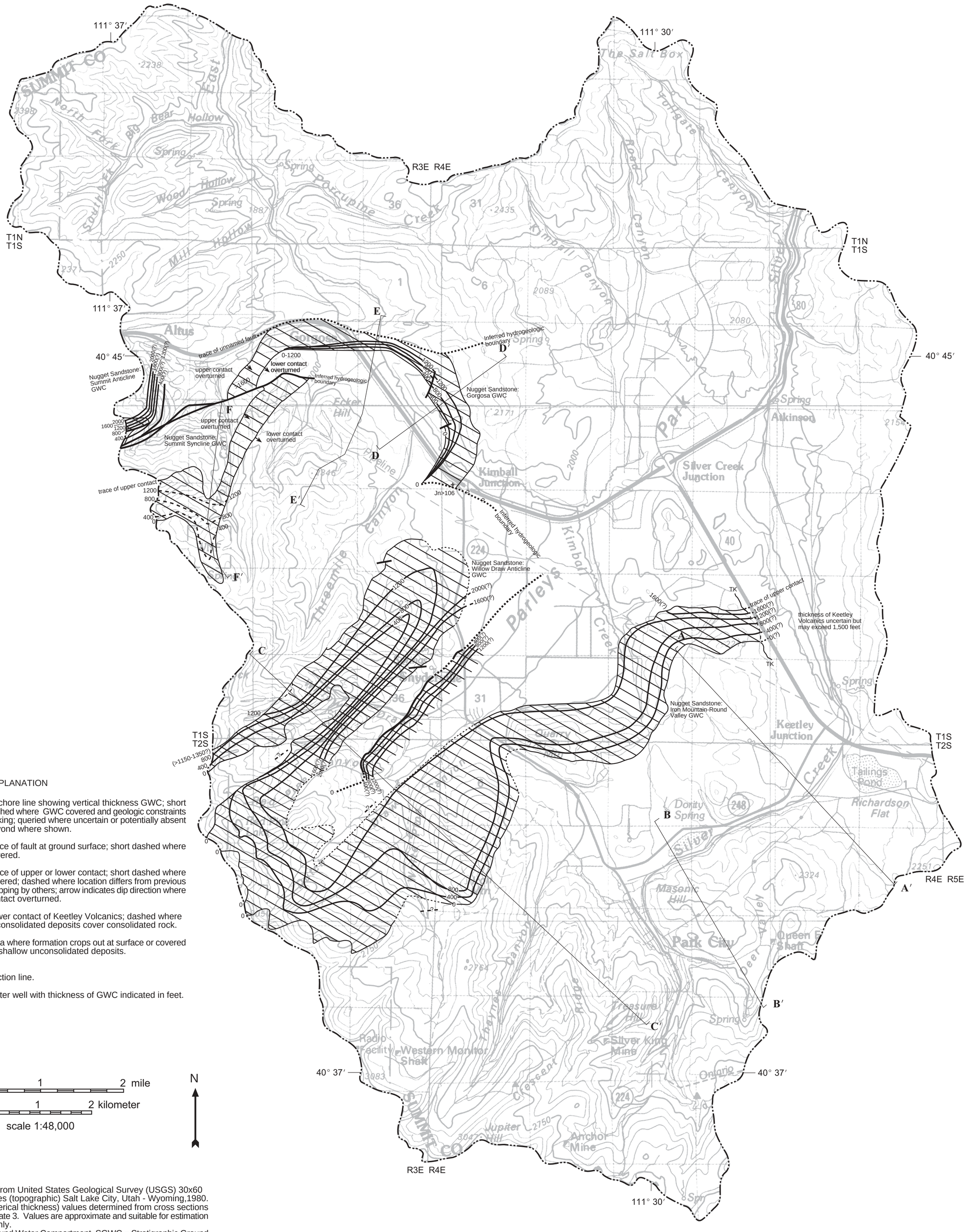

EXPLANATION

- Isochore line showing vertical thickness GWC; short dashed where GWC covered and geologic constraints lacking; queried where uncertain or potentially absent beyond where shown.
- Trace of fault at ground surface; short dashed where covered.
- Trace of upper or lower contact; short dashed where covered; dashed where location differs from previous mapping by others; arrow indicates dip direction where contact overturned.
- Lower contact of Keetley Volcanics; dashed where unconsolidated deposits cover consolidated rock.
- Area where formation crops out at surface or covered by shallow unconsolidated deposits.
- A — A′ Section line.
- Jn>106 Water well with thickness of GWC indicated in feet.

0 1 2 mile
0 1 2 kilometer
scale 1:48,000

N

NOTES

1. Base map from United States Geological Survey (USGS) 30x60 minute series (topographic) Salt Lake City, Utah - Wyoming,1980.
2. Isochore (verical thickness) values determined from cross sections shown on plate 3. Values are approximate and suitable for estimation purposes only.
3. GWC = Ground Water Compartment, SGWC = Stratigraphic Ground Water Compartment, NGVD = National Geodetic Vertical Datum

ISOCHORE MAP OF THE NUGGET SANDSTONE, SNYDERVILLE BASIN 2001

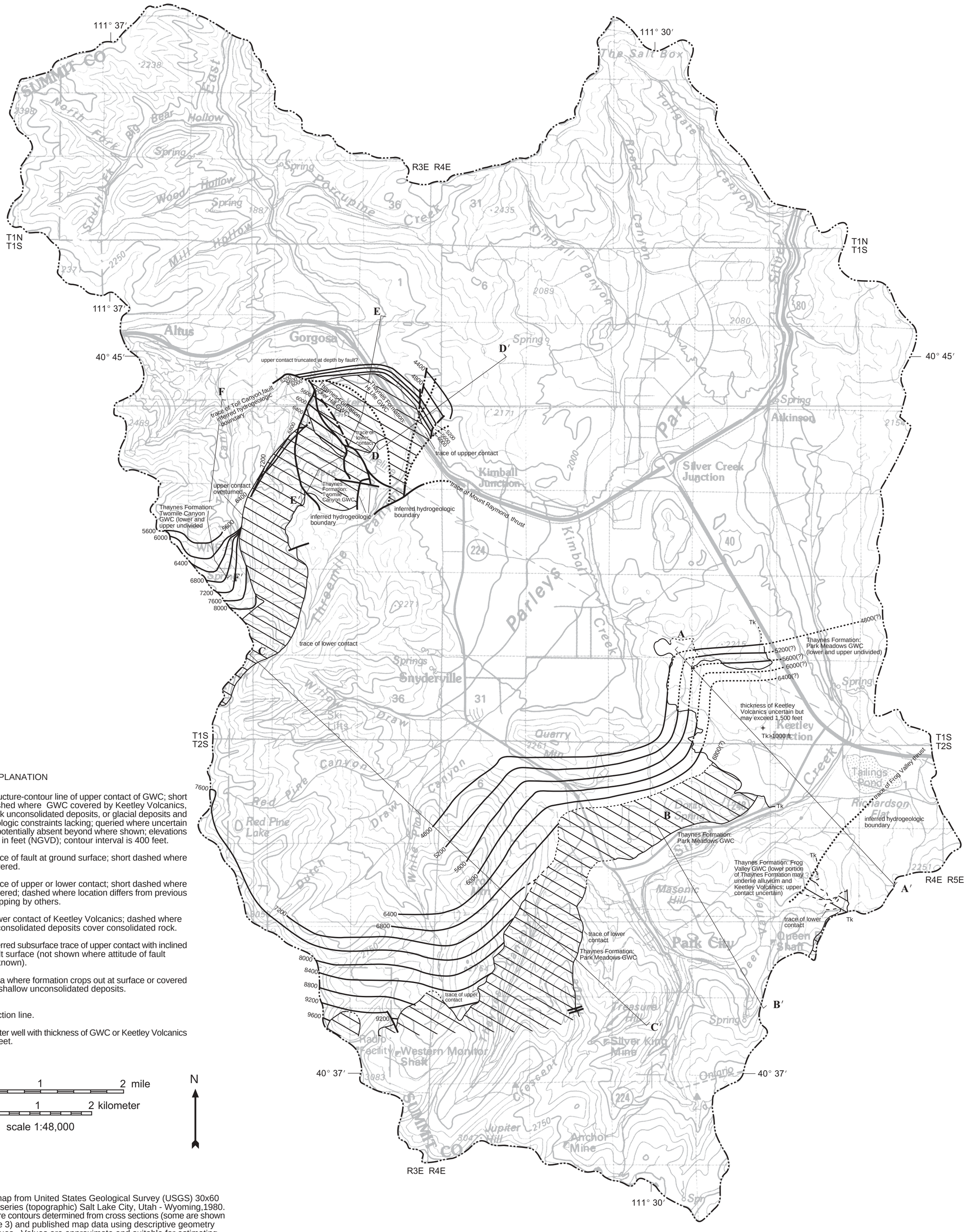

EXPLANATION

- Structure-contour line of upper contact of GWC; short dashed where GWC covered by Keetley Volcanics, thick unconsolidated deposits, or glacial deposits and geologic constraints lacking; queried where uncertain or potentially absent beyond where shown; elevations are in feet (NGVD); contour interval is 400 feet.
- Trace of fault at ground surface; short dashed where covered.
- Trace of upper or lower contact; short dashed where covered; dashed where location differs from previous mapping by others.
- Lower contact of Keetley Volcanics; dashed where unconsolidated deposits cover consolidated rock.
- Inferred subsurface trace of upper contact with inclined fault surface (not shown where attitude of fault unknown).
- Area where formation crops out at surface or covered by shallow unconsolidated deposits.
- A — A′ Section line.
- Water well with thickness of GWC or Keetley Volcanics in feet.

0 1 2 mile
0 1 2 kilometer
scale 1:48,000

N

NOTES

1. Base map from United States Geological Survey (USGS) 30x60 minute series (topographic) Salt Lake City, Utah - Wyoming,1980.
2. Structure contours determined from cross sections (some are shown on plate 3) and published map data using descriptive geometry techniques. Values are approximate and suitable for estimating purposes only.
3. GWC = Ground Water Compartment, SGWC = Stratigraphic Ground Water Compartment, NGVD = National Geodetic Vertical Datum.

STRUCTURE-CONTOUR MAP OF THE THAYNES FORMATION, SNYDERVILLE BASIN
2001

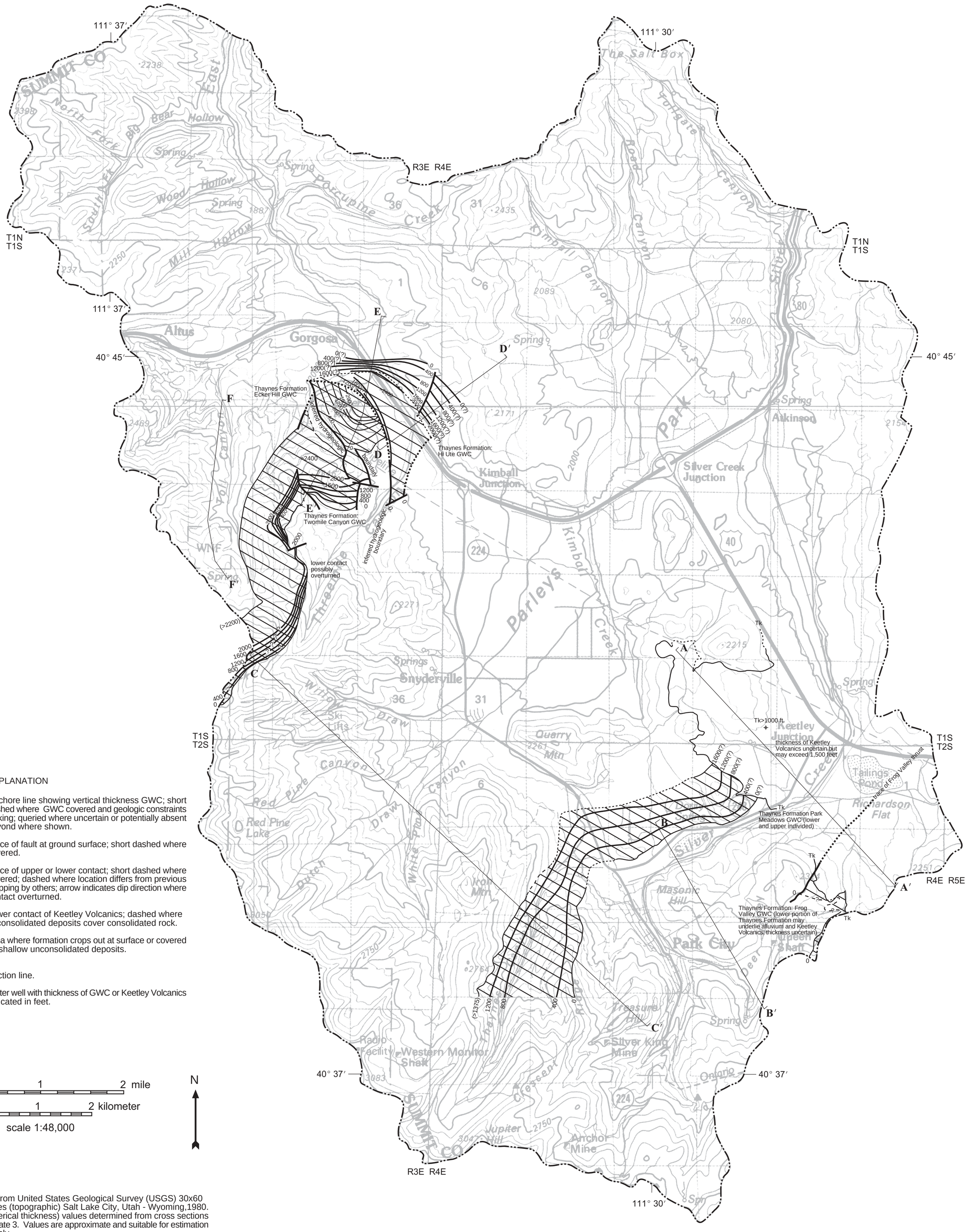

EXPLANATION

- Isochore line showing vertical thickness GWC; short dashed where GWC covered and geologic constraints lacking; queried where uncertain or potentially absent beyond where shown.
- Trace of fault at ground surface; short dashed where covered.
- Trace of upper or lower contact; short dashed where covered; dashed where location differs from previous mapping by others; arrow indicates dip direction where contact overturned.
- Lower contact of Keetley Volcanics; dashed where unconsolidated deposits cover consolidated rock.
- Area where formation crops out at surface or covered by shallow unconsolidated deposits.
- A A′ Section line.
- Water well with thickness of GWC or Keetley Volcanics indicated in feet.

0 1 2 mile
0 1 2 kilometer
scale 1:48,000

N

NOTES

1. Base map from United States Geological Survey (USGS) 30x60 minute series (topographic) Salt Lake City, Utah - Wyoming,1980.
2. Isochore (verical thickness) values determined from cross sections shown on plate 3. Values are approximate and suitable for estimation purposes only.
3. GWC = Ground Water Compartment, SGWC = Stratigraphic Ground Water Compartment, NGVD = National Geodetic Vertical Datum

ISOCHORE MAP OF THE THAYNES FORMATION, SNYDERVILLE BASIN 2001

EXPLANATION

- Structure-contour line of upper contact of GWC; short dashed where GWC covered by Keetley Volcanics, thick unconsolidated deposits, or glacial deposits and geologic constraints lacking; queried where uncertain or potentially absent beyond where shown; elevations are in feet (NGVD); contour interval is 400 feet.
- Trace of fault; short dashed where covered; teeth on upthrown side.
- Trace of upper or lower contact; short dashed where covered; dashed where location differs from previous mapping by others.
- Lower contact of Keetley Volcanics; dashed where unconsolidated deposits cover consolidated rock.
- Inferred subsurface trace of upper contact with inclined fault surface (not shown where attitude of fault unknown).
- Area where formation crops out at surface or covered by shallow unconsolidated deposits.
- A — A′ Section line.
- Water well with thickness of GWC or Keetley Volcanics in feet.

0 1 2 mile
0 1 2 kilometer
scale 1:48,000

N

NOTES

1. Base map from United States Geological Survey (USGS) 30x60 minute series (topographic) Salt Lake City, Utah - Wyoming,1980.
2. Structure contours determined from cross sections (some are shown on plate 3) and published map data using descriptive geometry techniques. Values are approximate and suitable for estimating purposes only.
3. GWC = Ground Water Compartment, SGWC = Stratigraphic Ground Water Compartment, NGVD = National Geodetic Vertical Datum.

STRUCTURE-CONTOUR MAP OF THE WEBER QUARTZITE, SNYDERVILLE BASIN
2001

EXPLANATION

- Isochore line showing vertical thickness GWC; short dashed where GWC covered and geologic constraints lacking; queried where uncertain or potentially absent beyond where shown.
- Trace of fault at ground surface; short dashed where covered.
- Trace of upper or lower contact; short dashed where covered; dashed where location differs from previous mapping by others; arrow indicates dip direction where contact overturned.
- Lower contact of Keetley Volcanics; dashed where unconsolidated deposits cover consolidated rock.
- Area where formation crops out at surface or covered by shallow unconsolidated deposits.
- A A′ Section line.
- Water well with thickness of GWC indicated in feet.

0 1 2 mile
0 1 2 kilometer
scale 1:48,000

N

NOTES

1. Base map from United States Geological Survey (USGS) 30x60 minute series (topographic) Salt Lake City, Utah - Wyoming,1980.
2. Isochore (verical thickness) values determined from cross sections shown on plate 3. Values are approximate and suitable for estimation purposes only.
3. GWC = Ground Water Compartment, SGWC = Stratigraphic Ground Water Compartment, NGVD = National Geodetic Vertical Datum

ISOCHORE MAP OF THE WEBER QUARTZITE, SNYDERVILLE BASIN
2001

MESOSCOPIC JOINT DOMAIN MAP OF THE SNYDERVILLE BASIN, WITH ROSE DIAGRAMS

Summary of mesoscopic joint domains

Domain	Predominant and (1, 2) Secondary Trend(s)	Number (m) of Stations	Number (n) of Joints (3)	Hydraulic Conductivity: Isotropic vs Aniso-tropic (4, 5)	Hydraulic Conductivity: Trend (6)	
Parleys Canyon syncline						
1	SSE,NS*,NNE	13	126	A	175	NS
2	NS,ENE*	1	5	sl. A	065	ENE
3	NE*,ENE,ESE	1	6	A	035	NE
Ecker Hill - Hi Ute Ranch						
4	NNE*,ESE	2	19	A	015	NNE
5	ENE*	1	8	A	065	ENE
6	NE,EW*	2	30	A	095	EW
Willow Draw anticline						
7	NS,NE*,ESE*,SE	6	30	I		
8	NNE,SE*	1	5	A	135	SE
9	NE,EW,ESE,SE,SSE*	1	2	u		
10	NS*,NE*	3	8	A	030	NNE
11	NE,SSE*	1	6	A	165	SSE
12	ESE*	1	5	A	115	ESE
13	NS*,ESE*	1	4	I	na	
14	NS,NNE,NE,SE*	1	13	sl. A	135	SE
Atkinson area - Keetley Volcanics						
15	NNE,EW*	3	27	sl. A or I	085	EW
16	ENE*,SE*	1	13	I		
17	NS, NE-EW,ESE*,SE	3	25	sl. A	110	ESE
18	NNE*,SE	2	31	sl. A or I	025	NNE
19	NS*,ESE,SE	4	31	A	005	NS
Quarry Mountain - Round Valley area						
20	NS*,NNE,EW	2	18	A	005	NS
21	NE*,EW,SE	2	16	A	035	NE
22	NNE*-NE*,ESE	2	25	A	047.5	NE
23	NE,SE,SSE	11	120	A	155	SSE
Park City mining district - East						
24	NS*,SE	6	50	A	005	NS
25	NNE,NE*	4	40	sl. A or I	055	NE
26	NE*,SSE*,NS*	1	5	A	005	NS
27	NE*,SE*	1	12	I	na	
28	EW*,SE*,SSE*	1	5	A	133	SE
29	NNE*,EW	2	18	sl. A	025	NNE
Park City mining district - West						
30	EW*,SE	1	7	A	090	EW
31	NE,ENE*	4	47	A	070	ENE
32	NE*,EW,ESE	1	14	sl. A	035	NE
33	ENE,ESE*,SE	2	8	A	105	ESE
34	NS*,SE*	1	11	A	150	SSE
35	NNE,ENE,SE*	1	17	sl. A	125	SE
36	NNE*,ENE,SE	1	9	A	030	NNE
37	ENE*	2	20	A	070	ENE
	Subtotal	93	836			

1. Asterisk (*) indicates predominant trend(s).
2. Bias due to trend of outcrop may obscure secondary trend(s) in some domains. The tendency for such a bias decreases with an increase in the value of m.
3. Confidence in the estimate of the predominant trend being within a 30 degree window of the actual value is low for domains where n is less than 15; moderate where n is between 16 and 35; and high where n exceeds 35; and where m exceeds 1.
4. Degree of anisotrophy estimated from the shape of rose diagram.
5. I = isotropic; A = anisotropic; u = uncertain; sl. = slightly.
6. Use of four significant digits (i.e., 047.5) is made without implying a greater level of precision than in other domains.

EXPLANATION

Equal area rose diagram (histogram) showing relative frequency of joint trends. Minimum circle size ranges between 35 and 50 percent. See table for information on number of measurements (n), predominant trend(s), and inferred anisotropy of fractured-rock ground-water compartments. Dashed line(s) show(s) scan-line direction(s) where domain is established on the basis of only one outcrop station, and scan-line survey technique was used. Bias inherent in directional sampling may be present wherever scan-line direction is at an acute angle greater than forty-five degrees to the predominant joint trend. Elsewhere, relative frequency distribution as shown in rose diagram is considered to lack significant inherent bias. Excludes bedding joints.

Equal area rose diagram (histogram) showing inferred hydraulic conductivity ellipse (not shown on map). The maximum hydraulic conductivity is inferred to be parallel to the long axis of the ellipse. Hydraulic conductivity in each domain is defined as either isotropic or anisotropic on the basis of the shape of the relative frequency distribution on the rose diagrams or the ellipse. Ratio of ellipticity (long axis/short axis) is indicative of degree of anisotropy. Isotropic hydraulic conductivity is inferred where ellipse is circular. Bedding joints, especially in the Twin Creek Limestone and Thaynes Formation, and differences in fracture-set permeability may influence the shape of hydraulic conductivity ellipse.

Domain boundaries are approximate as shown. Domains represent areas of distinct joint patterns. Major geologic structures or formational contacts typically define boundaries. Elsewhere, boundaries are poorly constrained and may be transitional.

NOTES

1. Base map from United States Geological Survey (USGS) 30x60 minute series (topographic) Salt Lake City, Utah - Wyoming,1980.
2. Rose diagrams show trends of mesoscopic joints as measured from outcrops using scan-line survey techniques or standard field mapping.
3. Use of map is applicable where ground-water flow is predominantly along joints (i.e., in joint-dominated areas).

0 1 2 miles
0 1 2 kilometers
scale 1:48,000

MESOSCOPIC FAULT DOMAIN MAP OF THE SNYDERVILLE BASIN, WITH ROSE DIAGRAMS

Summary of mesoscopic fault domains

Domain	Predominant and (1, 2) Secondary Trend(s)	Number (m) of Stations	Number (n) of Faults (3)	Hydraulic Conductivity: Isotropic vs Aniso-tropic (4, 5)	Hydraulic Conductivity: Trend (6)	
Park City mining district						
1	NNE*,NE,ENE*	8	45	A	040	NE
2	NNE*,NE*,EW*,ESE*,SSE*	1	5	I		
3	ENE*,EW*	2	12	A	075	ENE
4	ENE*,ESE*,SE*	1	5	A	102.5	EW
5	NE*,EW,ESE	1	5	A	055	NE
6	NS,NE,ESE*	3	13	sl. A	115	ESE
Willow Draw anticline - Mt. Raymond thrust						
7	NNE,NE,SE*	4	30	sl. A	135	SE
8	NE*,EW,SE*	2	25	I		
9	NNE,NE,ESE*,SE	2	8	A	120	ESE
10	NE*	1	4	A	035	NE
11	NS*,EW,SE	1	11	A	175	NS
12	NNE,NE,ENE*,EW	1	8	A	075	ENE
13	NS*,ESE*	1	8	sl. A	150	SSE
14	EW*,ESE*	1	9	A	105	ESE
15	ENE*,EW	2	24	A	065	NE
Jeremy Ranch - Ecker Hill - Hi Ute Ranch						
16	NE,EW*	1	7	sl. A	095	EW
17	NNE*	1	8	A	015	NNE
18	SE*,EW	1	18	A	140	SE
19	NE*,ENE*,EW*	1	4	A	060	ENE
20	NS,SE*	1	8	A	135	SE
21	NNE*,ENE,SSE	2	21	A	015	NNE
22	NE*,SE*	1	9	I		
23	NS,NNE,NE*,EW	2	18	sl. A or I	055	NE
24	NNE*,NE*,EW*,SE*	1	6	I		
25	NNE,SE*,SSE*	2	23	A	142.5	SE
26	NNE,ENE,EW*	1	7	A	085	EW
27	NE*	1	7	A	055	NE
28	SE*,ENE*	1	9	A	102.5	EW
29	ESE*	2	5	A	105	ESE
	Subtotal	49	362			

1. Asterisk (*) indicates predominant trend(s).
2. Bias due to trend of outcrop may obscure secondary trends in some domains. The tendency for such a bias decreases with an increase in the value of m.
3. Confidence in the estimate of the predominant trend being within a 30 degree window of the actual value is low for domains where n is less than 15; moderate where n is between 16 and 35; and high where n exceeds 35; and where m exceeds 1.
4. Degree of anisotropy estimated from the shape of rose diagram.
5. I = isotropic; A = anisotropic; sl. = slightly.
6. Use of four significant digits (i.e., 102.5) is made without implying a greater level of precision than in other domains.

EXPLANATION

Equal area rose diagram (histogram) showing relative frequency of fault trends. Minimum circle size ranges between 35 and 50 percent. See table for information on number of measurements (n), predominant trend(s), and inferred anisotropy of fractured-rock ground-water compartments. Dashed line(s) show(s) scan-line direction(s) where domain is established on the basis of only one outcrop station, and scan-line survey technique was used. Bias inherent in directional sampling may be present wherever scan-line direction is at an acute angle greater than forty-five degrees to the predominant joint trend. Elsewhere, relative frequency distribution as shown in rose diagram is considered to lack significant inherent bias. Excludes bedding joints.

Equal area rose diagram (histogram) showing inferred hydraulic conductivity ellipse (not shown on map). The maximum hydraulic conductivity is inferred to be parallel to the long axis of the ellipse. Hydraulic conductivity in each domain is defined as either isotropic or anisotropic on the basis of the shape of the relative frequency distribution on the rose diagrams or the ellipse. Ratio of ellipticity (long axis/short axis) is indicative of degree of anisotropy. Isotropic hydraulic conductivity is inferred where ellipse is circular. Bedding joints, especially in the Twin Creek Limestone and Thaynes Formation, and differences in fracture-set permeability may influence the shape of hydraulic conductivity ellipse.

Domain boundaries are approximate as shown. Domains represent areas of distinct fault patterns. Major geologic structures typically define boundaries. Elsewhere, boundaries are poorly constrained and may be transitional.

NOTES

1. Base map from United States Geological Survey (USGS) 30x60 minute series (topographic) Salt Lake City, Utah - Wyoming,1980.
2. Rose diagrams show trends of mesoscopic faults as measured from outcrops using scan-line survey techniques or standard field mapping.
3. Use of map is applicable where ground-water flow is predominantly along faults (i.e., in fault-dominated areas).

0 1 2 miles

0 1 2 kilometers

scale 1:48,000

MACROSCOPIC FAULT DOMAIN MAP OF THE PARK CITY MINING DISTRICT, WITH ROSE DIAGRAMS

Summary of macroscopic fault domains, Park City mining district

Fault Domain	Predom. (1) Trend	Range	Second-ary Trend	Notes	n	Hydraulic Conductivity Isotropic vs. Aniso-tropic (2, 3)	Trend
Ia	035	020-060	075		19	A	035 NE
Ib	025	010-040			9	A	025 NNE
Ic	015	010-020	075	minor set	8	A	015 NNE
IIa	075	060-110			51	A	075 ENE
IIb	095	050-110	005	minor set	19	A	095 EW
			Subtotal		106		

1. Confidence in the estimate of the predominant trend being within a 30 degree window of the actual value is low for domains where n is less than 15; moderate where n is between 16 and 35; and high where n exceeds 35.
2. Degree of anisotropy estimated from the shape of rose diagram.
3. A = anisotropic.

EXPLANATION

Domain IIa

Equal area rose diagram (histogram) showing relative frequency of fault trends. Minimum circle size ranges between 35 and 50 percent. See table for information on number of measurements (n), predominant trend(s), and inferred anisotropy of fractured-rock ground-water compartments. Dashed line(s) show(s) scan-line direction(s) where domain is established on the basis of only one outcrop station, and scan-line survey technique was used. Bias inherent in directional sampling may be present wherever scan-line direction is at an acute angle greater than forty-five degrees to the predominant joint trend. Elsewhere, relative frequency distribution as shown in rose diagram is considered to lack significant inherent bias. See plate 13 for explanation of hydraulic conductivity ellipse.

Domain boundaries are approximate as shown. Domains represent areas of distinct fault patterns. Major geologic structures or formational contacts typically define boundaries. Elsewhere, boundaries are poorly constrained and may be transitional.

NOTES

1. Base map from United States Geological Survey (USGS) 30x60 minute series (topographic) Salt Lake City, Utah - Wyoming,1980.
2. Rose diagrams show trends of macroscopic faults as measured from previously published maps of the Park City mining district.
3. Use of map is applicable where wells intercept macroscopic faults or their subsidiary fracture zones. For well sites midway between macroscopic fault traces, see also plate 13.

0 1 2 miles

0 1 2 kilometers

scale 1:48,000

UNDIFFERENTIATED FRACTURE DOMAIN MAP OF THE SNYDERVILLE BASIN, WITH ROSE DIAGRAMS

Summary of mesoscopic undifferentiated fracture domains

Domain	Predominant and (1, 2) Secondary Trend(s)	Number (m) of Stations	Number (n) of Fractures (3)	Hydraulic Conductivity: Isotropic vs Aniso-tropic (4, 5)	Trend (6)	
Parleys Canyon syncline						
1	SSE*-NS*,NE-ENE*	1	20	I		
2	SSE-NS*-NNE,ENE	12	93	A	175	NS
3	NS,ENE*,SE	2	55	sl. A	055	NE
Summit Park - Jeremy Ranch - Ecker Hill - Kimball Junction						
4	NS-NNE*,ENE-EW	3	41	sl. A	015	NNE
5	NS*-NNE,SE-SSE*	3	53	A	355	NS
6	NNE,NE*,EW,SE-NS	3	24	sl. A	055	NE
7	NNE-NE,ENE,EW-SE*	2	18	sl. A	145	SE
8	NNE-ENE	1	7	A	047.5	NE
9	NNE,ENE*-EW,ESE	2	17	A	060	ENE
10	NE,EW*,SE	2	55	A	095	EW
Willow Draw anticline						
11	NNE-NE*,ESE,SE*	3	41	A	082.5	EW
12	NS-ENE*,EW*-ESE,SSE	5	60	I		
13	NS*,NE,EW,SE*	4	35	sl. A	145	SE
14	NE,EW*-ESE*,SE	2	22	A	105	ESE
15	SSE-NS,ESE*	3	17	A	105	ESE
16	NS,NNE,NE*,SE	1	18	sl. A	035	NE
Atkinson area - Keetley Volcanics						
17	NS,NNE,NE-EW*,SE	2	25	A	085	EW
18	ENE*,SE*	1	13	sl. A	100	EW
19	NE*,ENE*	1	11	A	055	NE
20	NNE*-EW,ESE,SE*	4	54	I		
21	NS*,ENE,SE-SSE	4	34	sl. A	360	NS
Quarry Mountain - Round Valley area						
22	NE*-EW,ESE,SE	5	53	sl. A	035	NE
23	SSE-NS*,NNE,NE,EW	2	18	sl. A	355	NS
24	NS,NE-ENE,EW,SE*,SSE	13	152	sl. A	145	SE
Park City mining district - East						
25	NNE-ENE,ESE-SE,SSE*	9	108	sl. A	155	SSE
26	NS*,NE-EW,SE	2	27	sl. A	360	NS
27	NNE*,NE,ENE,EW*,SE	2	26	sl. A	060	NE
Park City mining district - West						
28	NS-NE*,ENE*,EW*,SE	2	28	sl. A	065	ENE
29	NE,ENE*,ESE-SE	7	77	A	075	ENE
30	NE*,EW*-ESE	1	16	sl. A	055	NE
31	NS,NNE-NE,ENE-SE*	4	51	I		
	Subtotal	108	1269			

1. Asterisk (*) indicates predominant trend(s).
2. Bias due to trend of outcrop may obscure secondary trend(s) in some domains. The tendency for such a bias decreases with an increase in the value of m.
3. Confidence in the estimate of the predominant trend being within a 30 degree window of the actual value is low for domains where n is less than 15; moderate where n is between 16 and 35; and high where n exceeds 35; and where m exceeds 1.
4. Degree of anisotrophy estimated from the shape of rose diagram.
5. I = isotropic; A = anisotropic; sl. = slightly.
6. Use of four significant digits (i.e., 047.5) is made without implying a greater level of precision than in other domains.

EXPLANATION

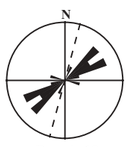

Equal area rose diagram (histogram) showing relative frequency of fracture trends. Minimum circle size ranges between 35 and 50 percent. See table for information on number of measurements (n), predominant trend(s), and inferred anisotropy of fractured-rock ground-water compartments. Dashed line(s) show(s) scan-line direction(s) where domain is established on the basis of only one outcrop station, and scan-line survey technique was used. Bias inherent in directional sampling may be present wherever scan-line direction is at an acute angle greater than forty-five degrees to the predominant joint trend. Elsewhere, relative frequency distribution as shown in rose diagram is considered to lack significant inherent bias. Excludes bedding joints.

Equal area rose diagram (histogram) showing inferred hydraulic conductivity ellipse (not shown on map). The maximum hydraulic conductivity is inferred to be parallel to the long axis of the ellipse. Hydraulic conductivity in each domain is defined as either isotropic or anisotropic on the basis of the shape of the relative frequency distribution on the rose diagrams or the ellipse. Ratio of ellipticity (long axis/short axis) is indicative of degree of anisotropy. Isotropic hydraulic conductivity is inferred where ellipse is circular. Bedding joints, especially in the Twin Creek Limestone and Thaynes Formation, and differences in fracture-set permeability may influence the shape of hydraulic conductivity ellipse.

Domain boundaries are approximate as shown. Domains represent areas of distinct fracture patterns. Major geologic structures typically define boundaries. Elsewhere, boundaries are poorly constrained and may be transitional.

NOTES

1. Base map from United States Geological Survey (USGS) 30x60 minute series (topographic) Salt Lake City, Utah - Wyoming,1980.
2. Rose diagrams show trends of mesoscopic fractures (joints, faults and veins) as measured from outcrops using scan-line survey techniques or standard field mapping.
3. Use of map is most applicable where neither joints nor faults predominate.

0 1 2 miles
0 1 2 kilometers
scale 1:48,000